

Some pages of this thesis may have been removed for copyright restrictions.

If you have discovered material in AURA which is unlawful e.g. breaches copyright, (either yours or that of a third party) or any other law, including but not limited to those relating to patent, trademark, confidentiality, data protection, obscenity, defamation, libel, then please read our [Takedown Policy](#) and [contact the service](#) immediately

**NOVEL HYDROGEL COPOLYMERS AND
SEMI-INTERPENETRATING POLYMER
NETWORKS**

FIONA JANE LYDON

Doctor of Philosophy

THE UNIVERSITY OF ASTON IN BIRMINGHAM

September 1994

This copy of the thesis has been supplied on condition that anyone who consults it is understood to recognise that its copyright rests with its author and that no quotation from the thesis and no information derived from it may be published without proper acknowledgement.

NOVEL HYDROGEL COPOLYMERS AND SEMI-INTERPENETRATING
POLYMER NETWORKS

FIONA JANE LYDON

Submitted for the Degree
of Doctor of Philosophy

September 1994

Summary

Interpenetrating polymer networks (IPN's), have been defined as a combination of two polymers each in network form, at least one of which has been synthesised and / or crosslinked in the presence of the other. A semi-IPN, is formed when only one of the polymers in the system is crosslinked, the other being linear. IPN's have potential advantages over homogeneous materials presently used in biomedical applications, in that their composite nature gives them a useful combination of properties. Such materials have potential uses in the biomedical field, specifically for use in hard tissue replacements, rigid gas permeable contact lenses and dental materials. Work on simply two or three component systems in both low water containing IPN's supplemented by the study of hydrogels (water swollen hydrophilic polymers) can provide information useful in the future development of more complex systems. A range of copolymers have been synthesised using a variety of methacrylates and acrylates. Hydrogels were obtained by the addition of N-vinyl pyrrolidone to these copolymers. A selection of interpenetrants were incorporated into the samples and their effect on the copolymer properties was investigated. By studying glass transition temperatures, mechanical, surface, water binding and oxygen permeability properties samples were assessed for their suitability for use as biomaterials.

In addition copolymers containing tris-(trimethylsiloxy)- γ -methacryloxypropyl silane, commonly abbreviated to 'TRIS', have been investigated. This material has been shown to enhance oxygen permeability, a desirable property when considering the design of contact lenses. However, 'TRIS' has a low polar component of surface free energy and hence low wettability. Copolymerisation with a range of methacrylates has shown that significant increases in surface wettability can be obtained without a detrimental effect on oxygen permeability. To further enhance to surface wettability 4-methacryloxyethyl trimellitic anhydride was incorporated into a range of promising samples. This study has shown that by careful choice of monomers it is possible to synthesise polymers that possess a range of properties desirable in biomedical applications.

Keywords: hydrogel, interpenetrating polymer networks, surface properties, oxygen permeability, mechanical properties

To my family

ACKNOWLEDGEMENTS

I would like to take this opportunity to express my thanks to the following:

Firstly, to my supervisor Professor Brian Tighe for his advice, encouragement and enthusiasm throughout the course of this work.

To Phil Corkhill for his help during the first two years of my time at Aston.

To all the members of the group and division, past and present, who have made my time at Aston so enjoyable. Particularly Karen French and Mark Eccleston who have gone beyond the call of duty to help with both academic issues and otherwise.

To my house 'mates' for having to put up with me whilst 'writing up'.

To EPSRC and Pilkington who have partly funded this project under the CASE award Scheme.

LIST OF CONTENTS

	<u>Page</u>
TITLE PAGE	1
SUMMARY	2
DEDICATION	3
ACKNOWLEDGEMENTS	4
LIST OF CONTENTS	5
LIST OF TABLES	9
LIST OF FIGURES	11
LIST OF ABBREVIATIONS	22
<u>CHAPTER 1</u>	
INTRODUCTION	24
1.1 Hydrogels	25
1.1.1 Articular Cartilage	25
1.1.2 The Cornea	26
1.1.3 Synthetic Hydrogels	27
1.2 Interpenetrating Polymer Networks	29
1.3 Interpenetrants	34
1.4 Methacrylates in Medicine	34
1.5 4-Methacryloxyethyl Trimellitic Anhydride	37
1.6 Contact Angle Measurement	39
1.6.1 Dehydrated Surfaces	39
1.6.2 Hydrated Surfaces	42
1.7 Mechanical Testing	45
1.8 Oxygen Permeabilities	46
1.9 Scope and Objectives	48
<u>CHAPTER 2</u>	
MATERIALS AND EXPERIMENTAL TECHNIQUES	50
2.1 Reagents	51
2.2 Polymer Synthesis	57
2.2.1 Preparation of Membranes	57

2.3	Equilibrium Water Content	59
2.4	Tensile Testing	59
2.5	Differential Scanning Calorimetry	60
2.5.1	Freezing Water Content	62
2.5.2	Glass Transition Temperatures using DSC	63
2.5.3	Glass Transition Temperatures using Thermal Mechanical Analysis	63
2.6	Surface Properties	64
2.6.1	Hamiltons Method	65
2.6.2	Captive Air Bubble Technique	65
2.6.3	Sessile Drop Technique	65
2.7	Oxygen Permeability	66
<u>CHAPTER 3</u>	HYDROGELS	68
3.1	Introduction	69
3.2	Mechanical Properties of Hydrogels	75
3.2.1	Mechanical Properties of Hydrogel Copolymers	75
3.2.2	Mechanical Properties of Hydrogel Semi-IPN's using CAB as an Interpenetrant	83
3.3	Water Binding Properties of Hydrogels	99
3.4	Surface Properties of Hydrogels	101
3.4.1	Dehydrated Surface Properties	101
3.4.2	Hydrated Surface Properties	110
3.5	Oxygen Permeabilities	116
3.6	General Conclusions	121
3.6.1	Effect of Monomer Structure on Properties of NVP Containing Hydrogels	121
3.6.2	Effect of CAB as an Interpenetrant on Properties of NVP:Methacrylate/Acrylate Copolymer Matricies	122

<u>CHAPTER 4</u>	HYDROGEL SEMI-INTERPENETRATING	124
	POLYMER NETWORKS	
4.1	Introduction	125
4.2	A Comparison of the Mechanical Properties of Ester and Ether Polyurethanes	129
4.2.1	Mechanical Properties of Semi-IPN's Preparedwith Tetrahydrofurfuryl Methacrylate	130
4.2.2	Mechanical Properties of Semi-IPN's Preparedwith Tetrahydrofurfuryl Acrylate	133
4.2.3	Mechanical Properties of Semi-IPN's Preparedwith Iso-bornyl Methacrylate	135
4.2.4	Mechanical Properties of Semi-IPN's Preparedwith Iso-butyl Methacrylate	139
4.2.5	Mechanical Properties of Semi-IPN's Preparedwith Tetrbutyl Methacrylate	142
4.3	Surface Properties	147
4.4	General Conclusions	153
<u>CHAPTER 5</u>	LOW WATER CONTENT	155
	SEMI-INTERPENETRATING	
	POLYMER NETWORKS	
5.1	Introduction	156
5.2	Effect of Interpenetrant Concentration on the Surface Free Energy	158
5.2.1	Effect of Interpenetrant on Polar Component of Surface Free Energy	160
5.3	Relationship between Interpenetrant Concentration and Oxygen Permeability	162
5.4	Relationship between Oxygen Permeability polar Component of Surface Free Energy	164
5.5	Thermal Mechanical Analysis	165

5.6	General Conclusions	167
<u>CHAPTER 6</u>	OXYGEN PERMEABLE MATERIALS	168
6.1	Introduction	169
6.2	Effect of 'TRIS' on Methacrylate Copolymers and Terpolymers	171
6.2.1	Relationship between Surface Polarity and Oxygen Permeability	173
6.3	Effect of 4-META on the Surface Properties and the Oxygen Permeability of Methacrylate Copolymers	175
6.4	Thermal Mechanical Analysis	179
6.5	General Conclusions	182
<u>CHAPTER 7</u>	CONCLUSIONS AND SUGGESTIONS FOR FURTHER WORK	183
7.1	Conclusions	184
7.2	Suggestions for Further Work	188
	LIST OF REFERENCES	190
	APPENDICES	199

LIST OF TABLES

		<u>Page</u>
Table 1. 1	The Chemical Composition of the Cornea	26
Table 1. 2	Surface Energies of wetting Liquids	41
Table 2. 1	Suppliers and Reagents Used	51
Table 3. 1	Tetrahydrofurfuryl Methacrylate Copolymers and Semi-IPN's Compositions and Associated EWC	70
Table 3. 2	Tetrahydrofurfuryl Acrylate Copolymers and Semi-IPN's Compositions and Associated EWC	71
Table 3. 3	Iso-bornyl Methacrylate Copolymers and Semi-IPN's Compositions and Associated EWC	72
Table 3. 4	Iso-butyl Methacrylate Copolymers and Semi-IPN's Compositions and Associated EWC	72
Table 3. 5	Tert-butyl Methacrylate Copolymers and Semi-IPN's Compositions and Associated EWC	73
Table 4. 1	Compatibility of Interpenetrants with Methacrylate / Acrylate :NVP Copolymers	126
Table 4. 2	Tetrahydrofurfuryl Methacrylate : Polyurethane semi-IPN's	127
Table 4. 3	Tetrahydrofurfuryl Acrylate : Polyurethane semi-IPN's	127
Table 4. 4	Iso-bornyl Methacrylate : Polyurethane semi-IPN's	128
Table 4. 5	Iso-butyl Methacrylate : Polyurethane semi-IPN's	128
Table 4. 6	Tert-butyl Methacrylate : Polyurethane semi-IPN's	129
Table 5. 1	Rigid Semi-IPN Compositions	157
Table 5.2	Compatibility of Semi-IPN Systems	157
Table 5. 3	'Onset' Temperature of THFFMA : CAB Semi-IPN's	165

Table 5. 4	'Onset' Temperature of Iso-butyl MA : CAB Semi-IPN's	166
Table 5. 5	'Onset' Temperature of Tert-butyl MA : CAB Semi-IPN's	166
Table 6. 1	Thermal Mechanical Analysis Data for 'TRIS' : MA Copolymers	180
Table 6. 2	Thermal Mechanical Analysis Data for 'TRIS' : HFIPMA : THFFMA Terpolymers	181
Table 6. 3	Multicomponent Systems with High Onset Temperatures	181

LIST OF FIGURES

	<u>Page</u>
Figure 1.1 Poly(2-hydroxyethyl methacrylate)	27
Figure 1.2 A Semi-Interpenetrating Polymer Network	29
Figure 1.3 4-Methacryloxyethyl Trimellitic Anhydride	38
Figure 1.4 Interfacial Energies of a Sessile Drop in a Solid Surface	40
Figure 1.5 Components of Surface Energy for Hamiltons Method	43
Figure 1.6 Components of Surface Energy for the Captive air Bubble Technique	44
Figure 2.1 Ethylene glycol dimethacrylate	52
Figure 2.2 Azo-Bis-Isobutyronitrile	52
Figure 2.3 N-Vinyl Pyrrolidone	52
Figure 2.4 Cellulose Acetate Butyrate	53
Figure 2.5 Ether Polyurethane	53
Figure 2.6 Tetrahydrofurfuryl Acrylate	53
Figure 2.7 Tetrahydrofurfuryl Methacrylate	53
Figure 2.8 Iso-bornyl Methacrylate	52
Figure 2.9 Iso-butyl Methacrylate	54
Figure 2.10 Tert-butyl Methacrylate	54
Figure 2.11 Methyl Methacrylate	54
Figure 2.12 Lauryl Methacrylate	55
Figure 2.13 Hexafluoro-iso-propyl Methacrylate	55
Figure 2.14 Tris-(trimethylsiloxy)- γ -Methacryloxypropyl Silane	55
Figure 2.15 4-Methacryloyloxyethyl Trimellitic Anhydride	56
Figure 2.16 Membrane Mould	58
Figure 2.17 Differential Scanning Calorimeter	61
Figure 2.18 T.M.A.	64
Figure 2.19 Model 201T Permiometer	66
Figure 3.1 Methacrylate Structures	73
Figure 3.2 Cellulose Acetate Butyrate	74

Figure 3.3	Relative Initial Young's Moduli of Copolymers of Iso-bornyl Methacrylate with NVP and Methyl Methacrylate	76
Figure 3.4	Relative Tensile Strengths of Copolymers of Iso-bornyl Methacrylate and Methyl Methacrylate with NVP	76
Figure 3.5	Relative Elongations at Break of Copolymers of Methyl Methacrylate and Iso-bornyl Methacrylate with NVP	77
Figure 3.6	Relative Mechanical Properties of Linear and Cyclic Methacrylates Copolymerised with NVP	77
Figure 3.7	A Comparison of the Tensile Properties Obtained with the use of Cyclic and Linear Monomers Copolymerised with NVP	78
Figure 3.8	A Comparison of the Elongation Properties Obtained with the use of Cyclic and Linear Monomers Copolymerised with NVP	78
Figure.3.9	Initial Modulus Variations Obtained with the use of Different Methacrylates Copolymerised with NVP	79
Figure 3.10	Strength Increases Obtained with the use of Cyclic Methacrylates Copolymerised with NVP	79
Figure 3.11	Effect of Water Content on the Initial Young's Modulus of 40 : 60 NVP : THFFMA / THFFA with CAB Semi-IPN'S	83
Figure 3.12	Effect of Interpenetrant on the Young's Modulus of 40 : 60 NVP : THFFMA / THFFA Semi-IPN's Prepared with CAB	84
Figure 3.13	Effect of Water Content on the Young's Modulus of 60 : 40 NVP : THFFMA / THFFA with CAB Semi-IPN'S	85

Figure 3.14	Effect of Interpenetrant on the Young's Modulus of 60 : 40 NVP : THFFMA / THFFA with CAB Semi-IPN'S	85
Figure 3.15	Effect of Water Content on the Tensile Strength of 40 : 60 NVP : THFFMA / THFFA with CAB Semi-IPN'S	86
Figure 3.16	Effect of Interpenetrant on the Tensile Strength of 40 : 60 NVP : THFFMA / THFFA with CAB Semi-IPN's	87
Figure 3.17	Effect of Water Content on the Tensile Strength of 60 : 40 NVP : THFFMA / THFFA with CAB Semi-IPN'S	87
Figure 3.18	Effect of Interpenetrant on the Tensile Strength of 60 : 40 NVP : THFFMA / THFFA with CAB Semi-IPN'S	88
Figure 3.19	Effect of Water Content on the Elongation at Break of 40 : 60 NVP : THFFMA / THFFA with CAB Semi-IPN'S	88
Figure 3.20	Effect of Interpenetrant on the Elongation at Break of 40 : 60 NVP : THFFMA / THFFA with CAB Semi-IPN'S	89
Figure 3.21	Effect of Water Content on the Elongation at Break of 60 : 40 NVP : THFFMA / THFFA with CAB Semi-IPN'S	89
Figure 3.22	Effect of Water Content on the Initial Modulus of 60 : 40 NVP : Iso-bornyl MA with CAB Semi-IPN's	90
Figure 3.23	Effect of CAB Content on the Initial Modulus of 60 : 40 NVP : Iso-bornyl MA with CAB Semi-IPN's	90
Figure 3.24	Effect of Water Content on the Tensile Strength of 60 : 40 NVP : Iso-bornyl MA with CAB Semi-IPN's	91

Figure 3.25	Effect of CAB Content on the Tensile Strength of 60 : 40 NVP : Iso-bornyl MA with CAB Semi-IPN's	91
Figure 3.26	Effect of Water Content on the Elongation at Break of NVP : Iso-bornyl MA : CAB 60 : 40 Semi-IPN's	92
Figure 3.27	Effect of Water Content on the Initial Modulus of 40 : 60 NVP : Iso-butyl MA / TBMA with CAB Semi-IPN's	93
Figure 3.28	Effect of % Interpenetrant on the Initial Modulus of 40 : 60 NVP : Iso-butyl MA / TBMA with CAB Semi-IPN's	93
Figure 3.29	Effect of Water Content on the Initial Modulus of 40 : 60 NVP : Iso-butyl MA / TBMA with CAB Semi-IPN's	94
Figure 3.30	Effect of % Interpenetrant on the Initial Modulus of 40 : 60 NVP : Iso-butyl MA / TBMA with CAB Semi-IPN's	94
Figure 3.31	Effect of Water Content on the Tensile Strength of 40 : 60 NVP : Iso-butyl MA / TBMA with CAB Semi-IPN's	95
Figure 3.32	Effect of % Interpenetrant on the Tensile Strength of 40 : 60 NVP : Iso-butyl MA / TBMA with CAB Semi-IPN's	96
Figure 3.33	Effect of Water Content on the Tensile Strength of 60 : 40 NVP : Iso-butyl MA / TBMA with CAB Semi-IPN's	97
Figure 3.34	Effect of % Interpenetrant on the Tensile Strength of 60 : 40 NVP : Iso-butyl MA / TBMA with CAB Semi-IPN's	97
Figure 3.35	Effect of Water Content on the Elongation at Break of 40 : 60 NVP : Iso-butyl MA / TBMA with CAB Semi-IPN's	98
Figure 3.36	Effect of Water Content on the Elongation at Break of 60 : 40 NVP : Iso-butyl MA / TBMA with CAB Semi-IPN's	98
Figure 3.37	Water Binding Properties of NVP : Methacrylate Hydrogel Copolymers	100
Figure 3.38	Freezing Water Content for NVP : Methacrylate :CAB Semi-IPN's	101

Figure 3.39	Effect of Methacrylate Content on the Surface Free Energy in Dehydrated NVP : Tetrahydrofurfuryl Methacrylate Copolymers	102
Figure 3.40	Effect of Methacrylate Content on the Surface Free Energy in Dehydrated NVP : Tetrahydrofurfuryl Acrylate Copolymers	103
Figure 3.41	Effect of Methacrylate Content on the Surface Free Energy in Dehydrated NVP : Iso-bornyl Methacrylate Copolymers	103
Figure 3.42	Effect of Equilibrium Water Content on the Polar Component of Surface Free Energy for Dehydrated Hydrogel Copolymers	104
Figure 3.43	Effect of Methacrylate Content on the Polar Component of Surface Free Energy for Dehydrated Hydrogel Copolymers	104
Figure 3.44	Effect of CAB Content on the Surface Free Energy in 40 : 60 Dehydrated NVP : Tetrahydrofurfuryl Methacrylate with CAB Semi-IPN's	105
Figure 3.45	Effect of CAB Content on the Surface Free Energy in 40 : 60 Dehydrated NVP : Tetrahydrofurfuryl Acrylate with CAB Semi-IPN's	106
Figure 3.46	Effect of CAB Content on the Surface Free Energy in 40 : 60 Dehydrated NVP : Tert-butyl Methacrylate with CAB Semi-IPN's	106
Figure 3.47	Effect of CAB Content on the Surface Free Energy in 40 : 60 Dehydrated NVP : Iso-butyl Methacrylate with CAB Semi-IPN's	107
Figure 3.48	Effect of CAB Content on the Surface Free Energy in Dehydrated 60 : 40 NVP : THFFMA with CAB Semi-IPN's	108

Figure 3.49	Effect of CAB Content on the Surface Free Energy in Dehydrated 60 : 40 NVP : THFFA with CAB Semi-IPN's	108
Figure 3.50	Effect of CAB Content on the Surface Free Energy in Dehydrated 60 : 40 NVP : TBMA with CAB Semi-IPN's	109
Figure 3.51	Effect of CAB Content on the Surface Free Energy in Dehydrated 60 : 40 NVP : IBUTMA with CAB Semi-IPN's	109
Figure 3.52	Effect of CAB Content on the Surface Free Energy in Dehydrated 60 : 40 NVP : IBMA with CAB Semi-IPN's	110
Figure 3.53	Effect of Water Content on the Surface Free Energy in Hydrated NVP : Tetrahydrofurfuryl Methacrylate Copolymers	111
Figure 3.54	Effect of Water Content on the Surface Free Energy in Hydrated NVP : Tetrahydrofurfuryl Acrylate Copolymers	112
Figure 3.55	Effect of Water Content on the Surface Free Energy in Hydrated NVP : Iso-bornyl Methacrylate Copolymers	112
Figure 3.56	Effect of Water Content on the Polar Component of Surface Free Energy in Hydrated NVP : Methacrylate Copolymers	113
Figure 3.57	Effect of Water Content on the Surface Free Energy in Hydrated 40 : 60 NVP : Tetrahydrofurfuryl Methacrylate with CAB Semi-IPN's	114
Figure 3.58	Effect of Water Content on the Surface Free Energy in Hydrated 40 : 60 NVP : Tetrahydrofurfuryl Acrylate with CAB Semi-IPN's	115

Figure 3.59	Effect of Water Content on the Surface Free Energy in Hydrated 40 : 60 NVP : Tert-butyl Methacrylate with CAB Semi-IPN's	115
Figure 3.60	Effect of Water Content on the Surface Free Energy in Hydrated 40 : 60 NVP : Iso-butyl Methacrylate with CAB Semi-IPN's	116
Figure 3.61	Relationship Between Oxygen Permeability and EWC in THFFMA / THFFA : NVP Hydrogels	117
Figure 3.62	Relationship Between Oxygen Permeability and EWC in Iso-bornyl MA : NVP Hydrogels	118
Figure 3.63	Relationship Between Oxygen Permeability and EWC in 60 : 40 THFFMA : NVP with CAB Semi-IPN's	119
Figure 3.65	Relationship Between Oxygen Permeability and EWC in 60 : 40 THFFA : NVP with CAB Semi-IPN's	119
Figure 3.66	Relationship Between Oxygen Permeability and EWC in 60 : 40 Iso-butyl / Tert-butyl MA : NVP with CAB Semi-IPN's	120
Figure 4.1	A Comparison of Initial Young's Modulus with EWC in 60 : 40 NVP : THFFMA SIPN's Prepared with PU1 and PU2	130
Figure 4.2	A Comparison of Initial Young's Modulus with Interpenetrant Concentration in 60 : 40 NVP : THFFMA SIPN's Prepared with PU1 and PU2	130
Figure 4.3	A Comparison of Tensile Strength with EWC in 60 : 40 NVP : THFFMA SIPN's Prepared with PU1 and PU2	131
Figure 4.4	A Comparison of Tensile Strength with Interpenetrant Concentration in 60 : 40 NVP : THFFMA SIPN's Prepared with PU1 and PU2	131

Figure 4.5	A Comparison of Elongation at Break with EWC in 60 : 40 NVP : THFFMA SIPN's Prepared with PU1 and PU2	132
Figure 4.6	A Comparison of Young's Modulus with EWC in 60 : 40 NVP : THFFA SIPN's Prepared with PU1 and PU2	133
Figure 4.7	A Comparison of Tensile Strength with EWC in 60 : 40 NVP : THFFA SIPN's Prepared with PU1 and PU2	133
Figure 4.8	A Comparison of Elongation at Break with EWC in 60 : 40 NVP : THFFMA :SIPN's Prepared with PU1 and PU2	134
Figure 4.9	A Comparison of Initial Modulus with EWC in 60 : 40 NVP : Iso-bornyl MA SIPN's Prepared with PU1 and PU2	135
Figure 4.10	A Comparison of Initial Modulus with % PU in 60 : 40 NVP : Iso-bornyl MA Prepared with PU1 and PU2	135
Figure 4.11	A Comparison of Tensile Strength with EWC in 60 : 40 NVP : Iso-bornyl MA Prepared with PU1 and PU2	136
Figure 4.12	A Comparison of Tensile Strength with % PU in 60 : 40 NVP : Iso-bornyl MA Prepared with PU1 and PU2	136
Figure 4.13	A Comparison of Elongation at Break with EWC in 60 : 40 NVP : Iso-bornyl MA Prepared with PU1 and PU2	137
Figure 4.14	A Comparison of Initial Modulus with EWC in 60 : 40 NVP : Iso-butyl MA Prepared with PU1 and PU2	139
Figure 4.15	A Comparison of Initial Modulus with % PU in 60 : 40 NVP : Iso-butyl MA Prepared with PU1 and PU2	139
Figure 4.16	A Comparison of Tensile Strength with EWC in 60 : 40 NVP : Iso-butyl MA Prepared with PU1 and PU2	140
Figure 4.17	A Comparison of Tensile Strength with % PU in 60 : 40 NVP : Iso-butyl MA Prepared with PU1 and PU2	140

Figure 4.18	A Comparison of Elongation at Break with EWC in 60 : 40 NVP : Iso-butyl MA Prepared with PU1 and PU2	141
Figure 4.19	A Comparison of Initial Modulus with EWC in 60 : 40 NVP : Tert-butyl MA Prepared with PU1 and PU2	142
Figure 4.20	A Comparison of Initial Modulus with % PU in 60 : 40 NVP : Tert-butyl MA Prepared with PU1 and PU2	143
Figure 4.21	A Comparison of Tensile Strength with EWC in 60 : 40 NVP : Tert-butyl MA Prepared with PU1 and PU2	143
Figure 4.22	A Comparison of Tensile Strength with % PU in 60 : 40 NVP : Tert-butyl MA Prepared with PU1 and PU2	144
Figure 4.23	A Comparison of Elongation at Break with EWC in 60 : 40 NVP : Tert-butyl MA Prepared with PU1 and PU2	144
Figure 4.24	Effect of PU1 Content on the Surface Free Energy in Dehydrated 60 : 40 NVP : THFFMA Semi-IPN's	147
Figure 4.25	Effect of PU2 Content on the Surface Free Energy in Dehydrated 60 : 40 NVP : THFFMA Semi-IPN's	148
Figure 4.26	Effect of PU1 Content on the Surface Free Energy in Dehydrated 60 : 40 NVP : THFFMA Semi-IPN's	148
Figure 4.27	Effect of PU2 Content on the Surface Free Energy in Dehydrated 60 : 40 NVP : THFFMA Semi-IPN's	149
Figure 4.28	Effect of PU1 Content on the Surface Free Energy in Dehydrated 60 : 40 NVP : IBMA Semi-IPN's	149
Figure 4.29	Effect of PU2 Content on the Surface Free Energy in Dehydrated 60 : 40 NVP : IBMA Semi-IPN's	150
Figure 4.30	Effect of PU1 Content on the Surface Free Energy in Dehydrated 60 : 40 NVP : IBUTMA Semi-IPN's	150
Figure 4.31	Effect of PU2 Content on the Surface Free Energy in Dehydrated 60 : 40 NVP : IBUTMA Semi-IPN's	151
Figure 4.32	Effect of PU1 Content on the Surface Free Energy in Dehydrated 60 : 40 NVP : TBMA Semi-IPN's	151

Figure 4.33	Effect of PU2 Content on the Surface Free Energy in Dehydrated 60 : 40 NVP : TBMA Semi-IPN's	152
Figure 5.1	Effect of CAB Concentration on Surface Free Energy in THFFMA Samples	159
Figure 5.2	Effect of CAB Concentration on Surface Free Energy in Tert-butyl Methacrylate Samples	159
Figure 5.3	Effect of CAB Concentration on Surface Free Energy in Iso-butyl Methacrylate Samples	160
Figure 5.4	Effect of CAB Concentration on the Polar Component of Surface Free Energy	161
Figure 5.5	Effect of CAB Content on the Oxygen Permeability of Methacrylate Semi-IPN's	162
Figure 5.6	Effect of CAB Content on the Oxygen Permeability of Tetrahydrofurfuryl Acrylate	163
Figure 5.7	Relationship of Polar Component of Surface Free Energy and Oxygen Permeability in Methacrylate / Acrylate : CAB Semi-IPN's	164
Figure 6.1	Tris-(trimethylsiloxy)- γ -methacryloxypropyl Silane	170
Figure 6.2	Effect of Polar Component of Surface Free Energy on Oxygen Permeability for a Range of TRIS : Methacrylate Copolymers	172
Figure 6.3	Polymers Increasing the Polar Component of Surface Free Energy whilst Retaining a High Oxygen Permeability	174
Figure 6.4	4-methacryloyloxyethyl trimellitic anhydride	175
Figure 6.5	Effect of 4-META on the Polar Component of Surface Free Energy in TRIS : MA Copolymers	175
Figure 6.6	Relationship between the Polar Component of Surface Free Energy and Oxygen Permeability with Increasing Amounts of 4-META in TRIS 50 : THFFMA 50 Copolymers	176

Figure 6.7	Relationship between the Polar Component of Surface Free Energy and Oxygen Permeability with Increasing Amounts of 4-META in TRIS 50 : THFFA 50 Copolymers	177
Figure 6.8	Relationship between the Polar Component of Surface Free Energy and Oxygen Permeability with Increasing Amounts of 4-META in TRIS 50 : Iso-bornyl MA 50 Copolymers	177
Figure 6.9	Relationship between the Polar Component of Surface Free Energy and Oxygen Permeability with Increasing Amounts of 4-META in TRIS 50 : Iso-butyl MA 50 Copolymers	178
Figure 6.10	Relationship between the Polar Component of Surface Free Energy and Oxygen Permeability with Increasing Amounts of 4-META in TRIS 50 : Tert-butyl MA 50 Copolymers	178

LIST OF ABBREVIATIONS

AZBN	Azo-bis-isobutyronitrile	CAB	Cellulose acetate butyrate
E	Initial Young's modulus	ϵ_b	Elongation at break
EGDM	Ethylene glycol dimethacrylate	EWC	Equilibrium water content
γ^d	Dispersive component of surface free energy	γ^p	Polar component of surface free energy
γ^t	Total component of surface free energy	HFIPMA	Hexafluoro-iso-propyl methacrylate
HEMA	2-Hydroxyethyl methacrylate	IPN	Interpenetrating polymer network
IBMA	Iso-bornyl methacrylate	IBUTMA	Iso-butyl methacrylate
LMA	Lauryl methacrylate	MAA	Methacrylic acid
4-META	4-Methacryloyloxyethyl trimellitic anhydride	MMA	Methyl methacrylate
NVP	N-Vinyl pyrrolidone	PC	Poly(carbonate)
PU1	Ether polyurethane	PU2	Ester polyurethane

PMMA	Poly(methyl methacrylate)	SIPN	Semi-interpenetrating polymer network
σ_b	Tensile strength	Tg	Glass transition temperature
TBMA	Tert-butyl methacrylate	THFFA	Tetrahydrofurfuryl acrylate
THFFMA	Tetrahydrofurfuryl methacrylate	TRIS	Tris-(trimethylsiloxy)- γ -methacryloxypropyl silane

CHAPTER 1

Introduction

1. 1 Hydrogels

This thesis is concerned with the development of a class of water containing synthetic materials for biomedical applications. The materials in question are hydrogel semi-interpenetrating polymer networks for use in the replacement of natural water swollen structures. The introduction deals with both natural and synthetic hydrogels.

Hydrogels have been defined as hydrophilic polymers which swell but do not dissolve in water. Typically hydrogels contain 20-98% water, this water influences the transport, surface and mechanical properties of the gel¹. The water in hydrogels is expressed as the equilibrium water content, (EWC), and is defined as;

$$\text{EWC (\%)} = \frac{\text{weight of the water in the gel}}{\text{total weight of hydrated gel}} \times 100 \quad (1. 1)$$

Naturally occurring hydrogel composites include articular cartilage and the cornea. By understanding the structure of these materials it may be possible to overcome some of the problems associated with high water content synthetic materials.

1. 1. 1 Articular Cartilage

Articular cartilage is a 1-2mm thick covering on opposite bony faces^{2,3,4}. Its purpose is to aid force absorption and provide the low friction bearing surfaces of the joint. Natural cartilage when saturated, contains 70-85% water. It is an insoluble gel suspended in a pool of liquid and acts as a small pored sponge to absorb force and lubricate. It is composed mainly of collagen, between 47% and 60% of dehydrated cartilage, but also contains chondroitin sulphate and other polysaccharides. The collagen is present as a woven fibrous network in a polysaccharide matrix and provides the majority of the strength in the system. The polysaccharide matrix contains hyaluronic acid, chondroitin sulphate, keratin sulphate and stabilising proteins. The chondroitin and keratin sulphate are anionic muco-saccharides with many hydrophilic groups which bind water, and cations which help to stabilise and strengthen the system. Cartilage is anisotropic with an increase in the proteoglycan concentration occurring from the articular surface to the bone. The collagen network

is also anisotropic, with the collagen fibrils aligned parallel to the articular surface at the surface, being randomly oriented in the middle zone and present in oriented bundles nearest the bone. This is apparent when mechanical properties of various sections through cartilage are examined moving from the articular surface to bone. The tensile strength of articular cartilage ranges from 30-10 MPa, anisotropy helps to explain the wide range of results quoted here.

1. 1. 2 The Cornea

The cornea is a transparent tissue which readily transmits light, it is avascular, viscoelastic and quite resistant to deformation. Forming a protective layer enclosing ocular tissues it is a most important part of the ocular system⁵. The chemical composition of the cornea was defined by Haurice and Riley in 1968⁵ and is shown in table 1.1 :-

Table 1.1 The Chemical Composition of the Cornea

WATER	78.0%
COLLAGEN	15.0%
PROTEINS	5.0%
SALTS	1.0%
KERATIN SULPHATE	0.7%
CHONDROITIN SULPHATE	0.3%

The cornea is composed of five layers, the epithelium, the stroma, Bowmans layer, Descemets layer and the endothelium. The stroma is the bulk of the cornea, consisting of collagen lamellae which run parallel to the surface of the cornea, it is this section that gives the cornea its rigidity. Little data on the mechanical properties of the cornea are available, however Jue and Maurice compared the mechanical properties of the human cornea with rabbit cornea, and an estimated value for tensile modulus was quoted to be 5MPa. This is similar to the value quoted by Nyquist, 4.86MPa, for the equilibrium modulus¹⁶.

1. 1. 3 Synthetic Hydrogels

Hydrogels were first suggested for medical use by Wichterle and Lim in 1960⁶, in particular for use in contact lenses. Poly(2-hydroxyethyl methacrylate), {poly(HEMA)}, was suggested as a potential lens material, and indeed is still used in conjunction with other materials today.

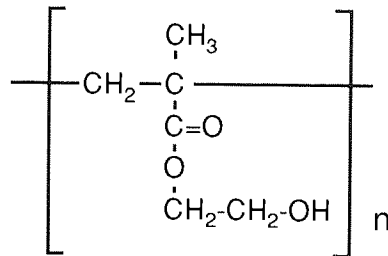


Figure 1. 1 Poly(2-hydroxyethyl methacrylate)

When dehydrated, poly(HEMA) is brittle and glassy with properties similar to those of poly(methyl methacrylate), however when hydrated it becomes soft and compliant. This is due to water interacting with the polymer which acts as a plasticiser giving the polymer its flexibility. This water also effects all other polymer properties.

In many hydrogel polymers at low temperatures only part of the water in the network freezes, this phenomenon can be observed using calorimetric techniques. The differential scanning calorimeter, (DSC.), was developed by Perkin-Elmer in 1964. It works on the principle that a measured energy input is required to keep the reference holder and the sample holder at the same temperature. If the temperature is varied and a transition occurs, energy will have to be supplied to either the sample or reference holder to keep them at the same temperature. If energy needs to be input into the sample holder the transition is endothermic and if energy is input into the reference holder the transition is exothermic. This energy input is the transition energy and is measured directly as the area under a recorded peak. Water binding states are elucidated from the peak shape¹. It has been shown that the heat of fusion of water in polymers is equal to that of pure water^{7,8}. Hence, using a calibration

graph and by measuring the area under melting endotherms of pure water, a quantitative determination of the amounts of freezing and non-freezing water in the polymer can be obtained.

In general water bound to the backbone by hydrogen bonding will not freeze, whilst freezing water is more mobile and unaffected by the polymeric environment. If the amount of freezing water is very low the mechanical properties of the hydrated sample have been found to be similar to those in the dehydrated state⁹. Low freezing water content has been proved to be useful in reverse osmosis applications, as it affects permselectivity and permeability¹.

Hydrogels to date have been used for a variety of medical applications these include; artificial articular cartilage^{10,11} drug delivery systems¹², artificial muscles and tendons¹³, wound or burn dressings¹⁴ and, their main commercial application, as soft contact lenses¹⁵.

Hydrogels in theory are ideal as contact lens materials having good tolerance in the eye, optical clarity and high permeability permitting diffusion of molecular species, specifically dissolved oxygen, essential to maintain a healthy cornea. The oxygen permeability is controlled by the equilibrium water content and is approximately proportional to the exponential of the equilibrium water content¹⁵. However, the intrinsic nature of the chemical constituents, chain flexibility, water binding and pore size distribution, must also be taken into account. It has been reported that the minimum oxygen tension for an open eye must be 11-19 mmHg at the anterior surface of the corneal epithelium to prevent corneal swelling¹⁵. On average 15mmHg behind the lens in an open or closed eye would be considered critical. Under normal conditions the eye is exposed to an oxygen tension of 155 mmHg when open and 55mmHg when closed. The oxygen flux through a lens can be calculated and is found to be inversely proportional to the thickness of the lens. This principle may be of great use in the design of new lens materials. The wettability of

the lens by tear fluid is also of great importance, tear fluid is needed both behind and in front of the lens to prevent adhesion to the cornea.

Mechanical properties are often a limiting factor with hydrogels. For a material to be successful in contact lens applications suitable mechanical properties must be achieved. Strength to prevent deformation by the eyelid, which has a deforming force of $2.5 \times 10^3 \text{Nm}^{-2}$, and to withstand daily handling is essential. By increasing the equilibrium water content of a lens, the mechanical strength is reduced, while the linear and volume swell of the material will increase, hence increasing the permeability. A balance must be found to produce the best combination of properties possible.

Several methods have been suggested for changing and controlling the mechanical properties of hydrogels; copolymerisation¹, fibre reinforcement¹⁶, formation of interpenetrating polymer networks and of particular interest the development of semi-interpenetrating polymer networks².

1. 2 Interpenetrating Polymer Networks

Interpenetrating polymer networks, commonly abbreviated to IPN's, have been defined as a combination of two polymers each in network form, at least one of which is synthesised and/or cross-linked in the immediate presence of the other¹⁷. Because of dual cross-links, both networks affect the physical and mechanical properties. A semi-IPN, is formed when only one of the polymers in the system is cross-linked, the other being linear. This is shown in figure 1. 2.

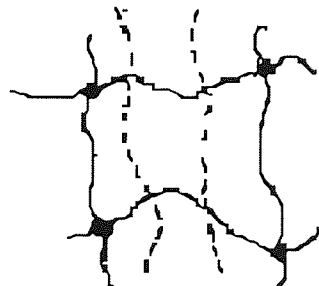


Figure 1. 2 A Semi- Interpenetrating Polymer Network

Thermoset IPN's can be subdivided into four types¹⁸; simultaneous IPN's, semi-IPN's, homo-IPN's and sequential IPN's. A simultaneous IPN is produced by homogeneous mixing of monomers, prepolymers, linear polymers, initiators and cross-linkers. The monomers and prepolymers are simultaneously polymerised by independent reactions that differ enough to avoid interfering with each other. As previously mentioned semi-IPN's have one linear and one cross-linked polymer. Homo-IPN's are made up of polymers that have the same chemical constituents but retain their specific characteristics. The final type of IPN's, sequential IPN's, are formed with one of the polymers already cross-linked. This polymer is then swollen, and a monomer, initiator and a cross-linking agent are added and then polymerised. There are however problems associated with sequential IPN's morphology, centred around the shapes and sizes of phases, and aspects of phase continuity^{19,20}. This may be due to the way in which sequential IPN's are formed: network I being fully formed before network II is introduced, thus chains are extended by the swelling action of monomer II reducing the phase domain size. This problem does not arise with simultaneous IPN's as both monomers, (or prepolymers), are introduced together.

Thermoplastic IPN's can be made by two methods, mechanical blending or chemically by sequential polymerisation. These IPN's can be processed in standard extrusion and moulding equipment. Exxon Chemicals was one of the companies to pioneer this technique¹⁸, by melt blending ethylene-propylene copolymer in the presence of a peroxide cross-linker. More recently Shell Chemicals have started to market Kraton IPN, a mechanical polyblend of styrene-ethylene/butadiene-styrene block copolymer with poly(butylene terephthalate)¹⁹. A material of this type has two types of physical crosslinks, one network crosslinked by glassy block copolymer segments, and the other polymer crosslinked by crystalline regions. This polymer remains flexible down to the glass transition temperature of the elastomer centre block, and remains serviceable up to the melting temperature of the crystalline polymer.

Millar first named and prepared interpenetrating polymer networks in the early 1960's but it was not until the late 1960's and early 1970's that major research programmes were launched on these materials¹⁷. Before this time multipolymer combinations were recognised to be grafts, blocks, blends and statistical and alternating copolymers, all of which contain components which are covalently bound to each other. These polymer hybrids or alloys have many properties that cannot be achieved with conventional homopolymers. IPN's differ from conventional blends in that they are linked with no covalent bonds present. In addition they will swell but do not dissolve in solvents and are characterised by their suppression of creep and flow. True IPN's exhibit only one glass transition temperature, when total compatibility of the two components occurs, however, this is often not the case. Although, Frisch *et. al.* have shown that the introduction of opposite charge groups in two-component IPN's lead to improved compatibility²¹. IPN's have potential advantages over homogeneous materials presently used in biomaterials, in that their composite nature gives them a useful combination of controllable properties.

It was first suggested by Bausch and Lomb that IPN's be used as contact lens materials²². The lenses were based on a cross-linkable siloxane compound in conjunction with hydroxyethyl methacrylate or N-vinyl pyrrolidone and ethylene glycol dimethacrylate. These compositions were oxygen permeable and transparent, however no commercial success was achieved.

Since this date interpenetrating polymer networks and semi-interpenetrating polymer networks have been researched for use in a range of biomedical applications. In the late 1970's Dror *et. al.* attempted to enhance the biocompatibility of surfaces with the synthesis of sequential IPN's²³. A poly(ether-urethane) thermoplastic elastomer and a hydrogel were chosen, samples absorbed in the manner of hydrogels, but had superior mechanical properties.

In the early 1980's Mueller *et. al.* used sequential IPN's in controlled drug delivery systems²⁴. Once again one of the components in this system was a hydrogel, 2-

hydroxyethyl methacrylate and / or N-vinyl pyrrolidone, in conjunction with a polyurethane containing IPN layer whose thickness and compositional gradient are a function of reaction rate and diffusion time. These gradient IPN's, as they have been named were synthesised by a process termed diffusion polycondensation, in which two initially separate reactants diffuse against each other within a polymer matrix and react in a mixing zone. This forms a sequential IPN bonded to the original polymer through a compositional gradient zone. If a water soluble drug was imbibed into such a material, release of this drug would be diffusion-controlled and dependent on the polymer concentration and water solubility of the drug. Further work on drug delivery systems was carried out by You Han Bae *et. al.* in the early 1990's²⁵. As with the system used by Mueller *et. al.* the networks used were based on a hydrophobic polyurethane component, in conjunction with a hydrophilic / hydrophobic balanced vinyl network. By varying the crosslinking density of the polyurethane network and the hydrophilicity of the vinyl network, the desired kinetics for drug release can be achieved. In the case of water soluble drugs the release mechanism is dominated by the magnitude of the net force in the monolithic device and by osmotic expansion forces. The latter are caused by dissolved solutes, the hydrophilicity of the vinyl network, and the elastic contraction force generated by both networks. When an optimum net force between the osmotic and the contractive forces occurs, zero order release can be obtained. Microcapsule techniques similar to those used in drug delivery systems are utilised in other commercial applications. These include carbonless copy paper where ink is released upon pressure, food flavourings which are contained until chewed and artificial blood cells containing sheel hemolysate which requires diffusion in both directions⁷⁵.

Studies performed more recently by Nair *et. al.* investigated the effect of degree of hydrophilicity on tissue response of polyurethane interpenetrating polymer networks²⁶. Increases in hydrophilicity, hydrophobicity and a balance of both hydrophilicity and hydrophobicity were made by forming IPN's with suitable materials. The histological response was then correlated to the morphological aspects of the IPN. This paper was somewhat inconclusive only appearing to prove that

factors other than hydrophilic and hydrophobic sites at the surface are involved in producing biocompatible materials.

Surface physical interpenetrating networks of poly(ethylene terephthalate), PET, and poly(ethylene oxide), PEO, were prepared by Desai *et. al.* This was done by diffusing PEO on to the surface of PET which is swollen in a mutual solvent²⁷. This is followed by deswelling in a nonsolvent for PET resulting in the PEO entrapped within the surface of the PET. This surface is actually a blend but the name of surface physical interpenetrating network is used due to its synthesis being similar to those for semi-IPN's. Materials of this type have extraordinary resistance to cellular adhesion. Unfortunately PEO leaching occurred upon incubation in water at temperatures near the PET glass transition temperature as well as upon swelling of the PET with organic solvents at room temperature.

The most relevant application to this work, however, is synthetic articular cartilage. This work has been pioneered by Corkhill *et. al.*². Although materials with a similar equilibrium water content to articular cartilage and low coefficients of friction can be fabricated²⁸, because of the poor mechanical properties of conventional synthetic hydrogels, these materials are not yet suitable as a replacement material. By using the composite structure of natural materials as a model, a new family of hydrogels based on interpenetrating polymer network technology was developed. The semi-IPN's formed were stiffer and stronger than hydrogel copolymers of similar water content. These materials are better at mimicking the properties of biological hydrogels, and thus, have exciting potential for demanding *in vivo* applications.

1. 3 Interpenetrants

Several interpenetrants for use in biomedical applications have been used to date. Polyurethane has been a popular choice for many years, now having an excellent range of physical and mechanical properties and relatively good biocompatibility²⁹. Polyurethane elastomers are the reaction products of organic isocyanates, high molecular weight polyols and low molecular weight chain extenders. Other popular choices of interpenetrants and combinations of materials for biomedical applications are cellulose acetate butyrate, gelatin - sodium carboxymethylcellulose³⁰ and N-acryloylpyrrolidine - poly(oxyethylene)³¹. The gelatin - sodium carboxymethylcellulose system was developed in an attempt to mimic true biological hydrogels, in particular cartilage. However, it is not only for biomedical use that IPN's and semi-IPN's have been investigated. General studies of these materials have shown that many combinations of properties can be achieved, as with all IPN's, by changing any one of a range of parameters. These include; changing the initiator³², polymerisation pressure³³, crosslinking density²⁰ and mixing temperature¹⁹, as well as the obvious changing of components in the IPN's and the relative interpenetrant concentrations. Functional groups can be incorporated into side chains which may be sensitive to changing environments, such as pH, temperature, electric current and chemicals³¹.

1. 4 Methacrylates in Medicine

Other than poly(2-hydroxyethyl methacrylate), or poly(HEMA), which has been mentioned previously, one of the principal materials used to date in dentistry and other clinical applications is poly(methyl methacrylate), PMMA. When poly(HEMA) is dehydrated it has similar physical and mechanical properties to PMMA, both being stiff and having glass transition temperatures in the 105-110°C range. However, once placed in contact with water unlike poly(HEMA), PMMA retains its rigidity. Poly(methyl methacrylate) is easy to handle in the 'dough' technique developed by the Kulzeer Company and later modified by Braden *et. al.* ^{34, 35}. However, it has a

high polymerisation shrinkage, (approximately 20%), is brittle, barely strong enough as a dental material and has doubtful biological properties. The monomer displays irritant properties; a danger if polymerisation is incomplete. Polymerisation is highly exothermic with temperatures of greater than 90°C being recorded, which has caused problems in bone cement applications³⁶. This has led to the investigation of other poly(alkyl methacrylate)'s, of which n-butyl methacrylate was found to be the least irritant monomer^{35,37}. In most cases samples were found to follow the simple statistical theory of rubber - like elasticity and giving approximately equal calculated and experimental values of Young's modulus, with the strength of these materials decreasing drastically as the homologous series is ascended³⁸. Work on monofunctional methacrylates showed a net shrinkage with molar volume and with the size of the substituent side group³⁵. The change in molar volume on polymerisation is approximately constant, 22cm³.mol⁻¹, irrespective of the geometry of substituent group. Hence, for low shrinkage glassy polymers, there is a need to use methacrylate esters of large molar volume, with a side group geometry that gives a high glass transition temperature. This principle can be used to calculate the conversion of polymerisation and is also utilised in the production of cast lenses and dental fillings, where prediction and controlling shrinkage is of importance. Cast polymerisation is potentially the most convenient way to mass produce lenses, since, providing that the shrinkage can be controlled, the monomer mix is cast directly into moulds having the exact form that is required for the finished lens³⁹. Bailey has studied the influences of ring opening polymerisation on shrinkage, basing his work on spirocarbonates, and has achieved polymers with low shrinkage and even some polymers which expand.

Cyclic and heterocyclic methacrylates have been used in dental applications for some time^{35,36,41,42,43,44} most of the pioneering work being done by Braden *et. al.* Therefore, basic biocompatibility studies have been performed on a number of these materials with some satisfactory results. Cyclic methacrylates, especially iso-bornyl methacrylate, offer a relatively high glass transition temperature, T_g, whilst still retaining a relatively low density. This allows for high gas permeability in a glassy

rigid polymer, which would be needed if this polymer were to be used as a lens material. Cyclic and heterocyclic materials have proved useful in low shrinkage applications having attributes such as high Tg's and high molar volume^{35,41,45,46}. High Tg's are desirable as they give a minimised distortion at higher temperatures, in addition the Young's modulus is also usually enhanced⁴⁷. The mechanical properties of cyclic and heterocyclic homopolymers used by Braden in dental applications have Young's moduli ranging from 1.38 - 2.19 GN/m². Although lower than the Young's moduli of poly(methyl methacrylate), it is still a useful set of results when looking for potential biomaterials. Heterocyclic dental resins have previously been stiffened by Kevlar fibres which also increases the glass transition temperature⁴².

The water absorption of polymers is of clinical importance and has been shown to cause many problems in the heterocyclic polymers of interest⁴⁸. High water absorption leads to a reduction in mechanical strength and to ingress of micro-organisms which can cause residual monomer and other possibly toxic materials to be released. Poly(tetrahydrofurfuryl methacrylate) and poly(tetrahydropyranyl methacrylate) homopolymers have been found to not have reached an equilibrium water content after 33 months⁴³. It was found that the water absorption decreased with an increase in the size of the ring in a limited study of these materials⁴³ and that the position of the oxygen and the neighbouring groups was also found to affect the water uptake⁴⁵. Non-polar samples, such as poly(iso-bornyl methacrylate), which have lower water contents cause less concern. Copolymerisation of the problem materials restrained water uptake but a linear uptake was still not observed. Samples may go white and opaque during absorption due to light scattering from water droplets in the material which accumulate at either water soluble impurities or hydrophilic chemical groups⁴³. There would be an increased chance of creep and tensile failure occurring around these droplets⁴⁸. The discolouring of these materials would obviously need to be controlled if these materials were to be used in contact lens applications.

1. 5 4-Methacryloxyethyl Trimellitic Anhydride

4-Methacryloxyethyl trimellitic anhydride, also a methacrylate, is of particular interest in this work in improving the polar component of surface free energy or wettability in highly oxygen permeable materials. However, it has been more commonly studied in connection with dental applications which to date have used composite materials to restore teeth. Improvements in mechanical properties have been achieved with the addition of various silane coupling agents which serve to bond ceramic particles to the polymeric matrix. Presently work is being carried out to investigate whether similar improvements can be made by incorporating 4-methacryloxyethyl trimellitate into a polymer matrix⁴⁹. Much of this work was carried out by Nakabayashi in his attempts to connect artificial materials to natural tissues^{50,51,52}. Nakabayashi, was mainly concerned with dental materials, specifically concentrating on the bonding of polymers to dentin. Fixation of artificial materials is a major problem in orthopaedic and dental surgery; it is usual to use mechanical fixation which shaves off or drills tissues to fix the prosthesis, in conjunction with the *in situ* polymerisation of poly(methyl methacrylate), PMMA, to set the prosthesis. While this method gives fast fixation there is the disadvantage of polymerisation shrinkage which causes loosening of the prosthesis^{39,41,51,53,54,55}; by having an adhesive prosthesis this problem would be overcome. Nakabayashi proposed that if a chemical reaction between resin and tooth substrate occurred, good secure bonding would occur⁵⁰. However, aware that this would be difficult to achieve at room temperature and in short times, he tried new materials proposed to have good affinity to tissues, which would consequently result in good bonding. Methacrylates with hydrophobic and hydrophilic groups were prepared and combined with the most promising 4-methacryloxyethyl trimellitate⁵⁶, with the use of tri-*N*-butyl borane as an initiator. Figure 1. 3 illustrates the structure of 4-META. .

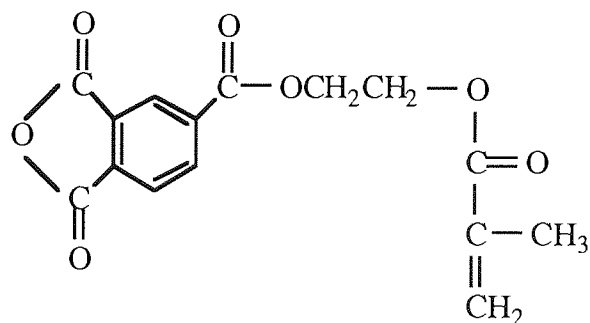


Figure 1. 3 4-Methacryloxyethyl Trimellitic Anhydride

The addition of 5 wt. % of 4-methacryloxyethyl trimellitate into composites made with silanated LiAlSiO_4 and methyl methacrylate was found to give an increase in the Knoop hardness number, Young's modulus, and transverse strength⁴⁹. 4-methacryloxyethyl trimellitate has been shown to be biotolerant and succeeds in promoting interpenetration of monomers into enamel and dentin^{40,50,52,56}. When failure surfaces were examined by scanning electron microscopy cohesive failure predominated. The interpenetrating zone that resulted was found to be a hybrid of natural tissue and artificial material. Further tests showed 4-methacryloxyethyl trimellitate to adhere strongly to bone, tooth and metal. Thus, it was concluded that a 4-META / methacrylate mixture would be useful as a bone cement. More recently work on acrylic bone cement, using hydroxyapatite as a filler in conjunction with 4-META, showed that with 4-META present the strength of this system increased with increasing hydroxyapatite, whilst if it was absent the mechanical strength decreased⁷⁴. It was therefore found that hydroxyapatite particles could be contained in 4-META / methyl methacrylate bone cement with no adverse effect on the mechanical properties. Moreover, the surface of the cement possesses an adhesion ability to bone and direct bonding of hydroxyapatite particles in the cement to bone would be expected.

Findings of this kind, although not utilised in this study, where 4-META was used simply because of its polarity and its expected effect upon surface properties, may be useful in many biomaterials where secure fixation to bone or tissue is required.

1. 6 Contact Angle Measurements

Contact angle measurements provide information about the interfacial properties of polymer systems. Forces are resolved at a three phase interface of a drop of wetting liquid or vapour on a solid surface, the sessile drop and captive bubble methods^{1,57,58,59}. Results from these measurements enable the surface free energy of solids in both the hydrated and dehydrated states to be determined. The data can be split into polar (γ_s^p) and dispersive (γ_s^d) components of surface free energy. The magnitude of the polar and dispersive components along with the total surface free energy influence blood compatibility and the biotolerance of the material. The polar component is of particular interest, being a determining factor in the wettability of a material, and a controlling factor when determining the suitability of a material in the design of a contact lens.

Surface energies are difficult to measure particularly in the dehydrated state where hydrophilic samples absorb water rapidly, changing true readings. Contact angle hysteresis has been attributed to several inaccuracies which may occur^{1,60}. These are surface rugosity, heterogeneity, contamination of the liquid, the extent to which the drop is vibrated and reorientation of polymer chains at the surface. However, difficult though it may be to obtain accurate and consistent results, surface properties are of great importance in determining the interaction of polymers in a biological environment.

1. 6. 1 Dehydrated Surfaces

In 1805 Young resolved forces at the point of contact of a sessile drop and a solid surface^{61,62}, fig 1. 4, and derived equation 1. 2

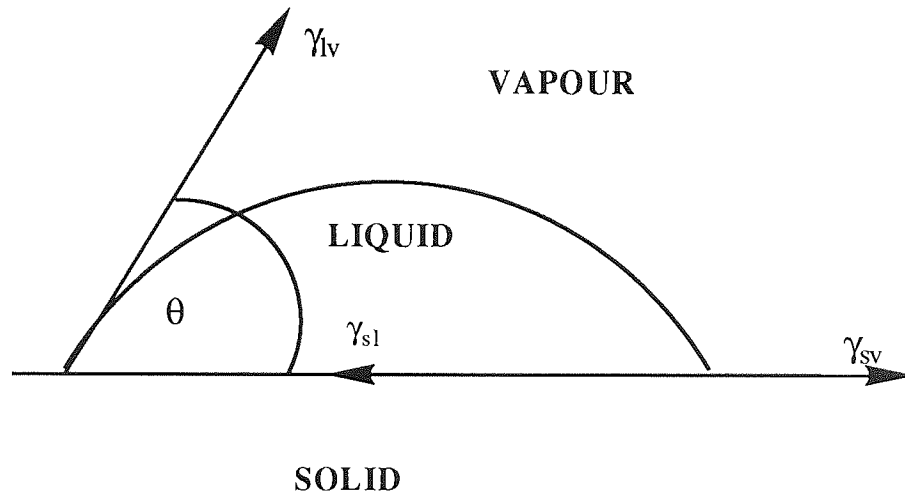


Figure 1. 4 Interfacial Energies of a Sessile Drop in a Solid Surface

$$\gamma_{sv} = \gamma_{sl} + \gamma_{lv} \cos \theta \quad (1. 2)$$

Dupre followed Young's work and in 1865 deduced that the reversible work of adhesion of a liquid and a solid was :-

$$W_a = \gamma_s + \gamma_{lv} - \gamma_{sl} \quad (1. 3)$$

where

γ_{sv} - the solid / vapour interfacial free energy

γ_{sl} - the solid / liquid interfacial free energy

γ_{lv} - the liquid / vapour interfacial free energy

γ_{sv} - the solid / vapour interfacial free energy $\sim \gamma_s =$ surface free energy

W_a - the work of adhesion

Combining equations 1. 2 and 1. 3 gives the Young - Dupre equation :-

$$W_a = (\gamma_s - \gamma_{sv}) + \gamma_{lv} (1 + \cos \theta) \quad (1. 4)$$

For solid surfaces in contact with the saturated vapour of a wetting liquid, some adsorption of liquid onto the surface occurs, thus reducing the surface free energy.

The difference between the surface free energy of the solid and the solid / vapour interfacial free energy is called the spreading pressure. This, however, is negligible for low energy solids which form a finite contact angle with a solid^{1,62}.

When $\cos \theta = 1$, extrapolating a graph of $\cos \theta$ versus surface tension of a hypothetical liquid allows the critical surface tension i. e. when a liquid completely wets a surface, to be obtained. A maximum is obtained with non-polar liquids while a minimum with polar liquids is obtained.

The Owens and Wendt equation is the most used equation for obtaining surface energies on dehydrated surfaces^{57,59,62} :-

$$1 + \cos \theta = 2/\gamma_{lv} [(\gamma_{lv}^d \cdot \gamma_s^d)^{0.5} + (\gamma_{lv}^p \cdot \gamma_s^p)^{0.5}] \quad (1. 5)$$

where

γ_{lv}^d is the dispersive component of the liquid and γ_{lv}^p is the polar component. This relates the contact angle to the polar and dispersive forces of the solid. Therefore, if the polar and dispersive forces of the liquid are known, the polar and dispersive components of the solid can be calculated.

The total surface free energy γ_s^t , can be obtained by adding the values of the polar and dispersive forces :-

$$\gamma_s^t = \gamma_s^d + \gamma_s^p \quad (1. 6)$$

The wetting liquids generally used are distilled water and methylene iodide. They were chosen because of their high surface free energies and their balance in dispersive and polar components as can be seen in table 1. ^{259,62,63}

Table 1. 2 Surface Energies of Wetting Liquids

LIQUID	γ^d (mN/m)	γ^p (mN/m)	γ^t (mN/m)
Water	21.8	51.0	72.8
Methylene Iodide	48.1	2.3	50.4

In general an increase in hydrophilicity decreases the interfacial free energy between the polymer and water. One suggested requirement for blood compatibility is that the interfacial free energy should be low when the water content is high⁵⁷.

1. 6. 2 Hydrated Surfaces

With hydrated surfaces, problems arose in measuring contact angles in air as there was no reproducible way of removing surface water from the sample, thus, dehydration occurred. Two methods commonly used to measure contact angles under water are Hamilton's method and the captive air bubble technique.

Hamilton's method involved measuring contact angles of n-octane drops under water. Assuming that gravity is negligible, the polar component of the surface energy may be determined. The Dupre equation for the work of adhesion of liquid to solid is given by :-

$$W_a = 2 (\gamma_{lv} \cdot \gamma_s)^{0.5} \quad (1. 7)$$

The equation developed by Fowkes for the work of adhesion at the solid-liquid interface⁶³, assuming that no polar interactions act across the interface, is given by :-

$$\gamma_{sl} = \gamma_s + \gamma_{lv} - 2 (\gamma_{lv}^d \gamma_s^d)^{0.5} \quad (1. 8)$$

This equation involves terms for the stabilisation from dispersive forces. Tamai *et al.* derived an equation which took into account the non-dispersive (polar) forces :-

$$\gamma_{sv} = \gamma_s + \gamma_{lv} - 2 (\gamma_{lv}^d \gamma_s^d)^{0.5} - I_{sl} \quad (1. 9)$$

where ;

$$I_{sl} = (\gamma_{lv}^p \gamma_s^p)^{0.5} \quad (1. 10)$$

As n-octane has no polar component and $\gamma_{lv}^d \text{ octane} = \gamma_{lv}^d \text{ water}$, both being 21.8 mN/m, combining equations 1. 2 and 1. 9 gives the polar stabilisation energy between water and the solid :-

$$I_{sw} = \gamma_{wv} - \gamma_{ov} - \gamma_{ow} \cdot \cos \theta \quad (1. 11)$$

where γ_{wv} is the surface tension of n-octane saturated water and γ_{ov} and γ_{ow} are found experimentally, as seen in Figure 1. 5 :

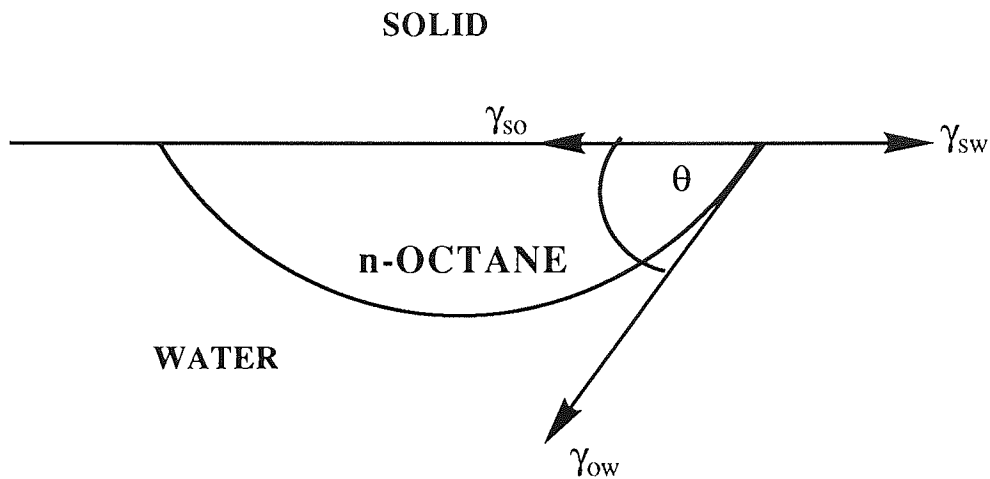


Figure 1. 5 Components of Surface Energy for Hamilton's Method

where:

γ_{sw} = solid-water interfacial free energy

γ_{so} = solid-octane interfacial free energy

γ_{ow} = octane-water interfacial free energy

From this γ_s^p , the polar component of surface free energy can be calculated using equation 1. 10.

By constructing a calibration curve showing the relationship between γ_s^p and the contact angle, results show that an increase in contact angle results in an increase in γ_s^p .

By using data from Hamilton's method and the captive air bubble technique, it is possible to find values for γ_{sv} , γ_{sv}^p , γ_{sv}^d , and γ_{sw} for the hydrogel water interface.

Applying Young's equation to the situation :-

$$\gamma_{sv} - \gamma_{sw} = \gamma_{wv} \cos \theta \quad (1. 12)$$

Knowing $\gamma_{wv} = 72.8 \text{ mN/m}$, and θ' measured by the captive air bubble technique shown in Figure 1. 6, allows $\gamma_{sv} - \gamma_{sw}$ to be calculated

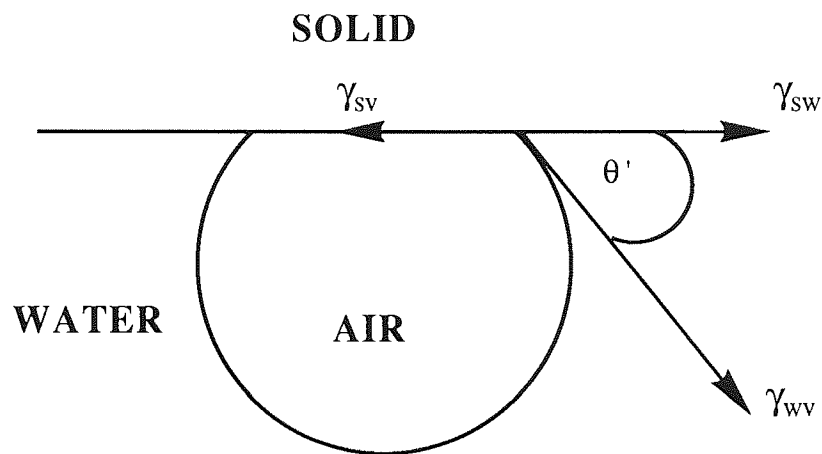


Figure 1. 6 Components of Surface Free Energy for the Captive air Bubble Technique

Where

γ_{sw} = solid-water interfacial free energy

γ_{wv} = water-vapour interfacial free energy (surface tension of water)

γ_{sv} = solid-vapour interfacial free energy or approximately γ_s the solid surface free energy

The polar stabilisation parameter (I_{sw}) shown to be :-

$$I_{sw} = \gamma_{wv} - \gamma_{ov} - \gamma_{ow} \cos \theta' \quad (1. 13)$$

equation 1. 13 can be rewritten as :-

$$I_{sw} = 51.0 (1 - \cos \theta') \quad (1.14)$$

Knowing $\gamma_{ov} = 21.8$ mN/m and $\gamma_{ow} = 51.0$ mN/m, then by combining equations 1.9 and 1.12 and rearranging, the dispersive component of the hydrogel can be obtained :-

$$\gamma_{sv}^d = [\{ (\gamma_{sv} - \gamma_{sw}) - I_{sw} + \gamma_{wv} \} / 2 (\gamma_{wv}^d)^{0.5}]^2 \quad (1.15)$$

or

$$\gamma_{sv}^d = I_{sw}^2 / (4 \gamma_{wv}^d) \quad (1.16)$$

By using Macintosh TM works, programmed with appropriate equations ($\gamma_{sv} - \gamma_{sw}$), I_{sw} , γ_{sv}^d , γ_{sv}^p , γ_{sv} and γ_{sw} can be calculated.

The dispersive component can also be found by using the Owen and Wendt equation (1.5) for hydrated gels. By using Hamilton's method, the polar component is obtained and using the water / air contact angle and substituting into the Owen and Wendt equation the dispersive component can be calculated, results have shown the two values to be within 0.2 mN/m of each other³.

1.7 Mechanical Testing

Mechanical testing particularly in tension is a useful test in that it is relatively straight forward and sensitive to small changes in composition. This method allows the tensile strength, elasticity and the Young's modulus to be obtained. However, with the viscoelastic nature of polymers, mechanical response is a function of time, temperature and previous loading history, therefore, standard conditions must be set up to enable relative comparisons of samples to be observed. Standards set up by Trevett and Tighe include the use of standard specimen geometry, cross head speed and the initial modulus to be used⁶⁴. When applying this to the testing of lens materials an indication of clinical performance can be obtained.

1. 8 Oxygen Permeabilities

In this work a permeometer model 201 T was used to calculate the oxygen permeability of membranes. This method measures the permeability between gas and liquid. Samples were contact lenses or flat material of equivalent size. With most methods of oxygen permeability measurement used to date, either gravimetric (change in sample weight), barometric (change in ambient gas pressure), or volumetric (change in ambient gas volume) measurements are used. These methods quantify gas sorption into, or desorption out of, a polymer sample or gas permeation through a polymer membrane. Current commercial instruments often rely on modern thermal conductivity, coulometric, or ionisation based detectors.

Yuanping *et. al.* developed a new technique to quantify oxygen diffusion in polymer films⁶⁵. It was suggested that pin-holes in samples, if traditional methods were used, could lead to inaccuracies in permeability readings. A spectroscopic technique was developed in which oxygen diffusion coefficients can be quickly obtained for readily prepared polymer films of small area. This technique depends on the oxygen sorption into the polymer and not at detecting the oxygen that permeates through the material. This eliminates the errors that may occur due to pinholes.

Another method of oxygen permeability measurement has been developed by Alexander *et. al.*⁶⁶. A chemical technique was used in which the volume of oxygen crossing the membrane was measured volumetrically. This was said to be a simple technique that could be easily set up in any laboratory without expensive specialist equipment.

Studies by Compan *et. al.*⁶⁷ have shown, by testing a selection of contact lenses, that there are differences in true and apparent oxygen permeabilities. Using a time-lag method, oxygen diffusion coefficients were obtained. The permeability measurements were obtained with a potentiostatic cell. Assuming that all the oxygen

reaching the cathode is instantly reduced, measurements are related to the system composed of the lens and the two boundary layers and are therefore called apparent permeabilities. If the effect of boundary layers is taken into account the true permeability can be determined. Tear layers at the anterior and posterior surfaces of the lens may reduce the flow of oxygen to the cornea. It was found that the apparent transmissibility decreased with increasing lens thickness. This effect was more apparent for lenses with low water content. In addition, in Compan's work, oxygen permeability was found to be exponentially dependent on water content rather than on the chemical composition of the hydrogel.

Kumaki *et. al.* investigated the antithrombogenicity and oxygen permeability of block and graft copolymers of polydimethylsiloxane and poly(α -amino acid)⁶⁸. When copolymers are made that contain chains which are dissimilar, phase separation in the casting process from a solution will form a film, the surface of which is heterogeneous. It is suggested that heterogeneous morphology of the film surface is related to a selective absorption of blood proteins and their conformational change, the adhesion and deformation of platelets, and ultimately the thrombus formation. This would make such materials suitable for biomedical use. In addition, due to the regular structure of the polymers, a selective permeation of oxygen will occur.

Common methods of enhancing the oxygen permeability of materials are to incorporate silicon or fluorine containing materials; this will be discussed in more detail in Chapter 6. Another method to enhance oxygen permeability of polymers for use in biomedical applications has been developed by Ulubayram *et. al.*⁶⁹. The materials chosen were bio- and haemo-compatible polyurethane elastomers with unique physical and mechanical properties which result from having hard segment / soft segment microphase segregation. Materials were synthesised using toluene-2, 4-diisocyanate and polypropylene glycol. These materials have high flexibility, high strength and inherent non-thrombogenic characteristics. Factors which determine the performance in biomedical applications are both chemical and physical. These will alter the structure and morphology of phase separation in the bulk or at the surface.

Chemical factors are the molecular weight of soft segments, length of hard segments and addition of chain extender. One physical factor is the fabrication method. Samples with higher toluene-2, 4-diisocyanate to polypropylene glycol ratios, a chain extender incorporated or higher molecular weight polypropylene glycol had higher tensile strength, lower ultimate elongation and lower oxygen permeability.

Ng *et. al.* studied the 'dissolved' oxygen permeability in poly(2-hydroxyethyl methacrylate) hydrogels used in contact lens applications¹⁵. The oxygen permeability through this lens material was shown to be insufficient alone to preserve corneal transparency and a fresh tear fluid layer behind the lens was necessary for the lens to be suitable to be used for daily wear. Poly(2-hydroxyethyl methacrylate) lenses were also shown to be unsuitable for use in continuous wear applications. It was found that the permeability of 'dissolved' oxygen through hydrogels is approximately an exponential function of the equilibrium water content over a wide range of water contents. However, chain flexibility, water-binding ability and pore size distribution, particularly at low water contents also effect oxygen permeability.

1. 9 Scope and Objectives

There has been increasing interest in hydrogels for use in medical applications, specifically where they replace or mimic natural hydrogels such as the cornea or cartilage. Earlier studies have shown the potential of semi-interpenetrating polymer networks in such applications². The formation and properties of semi-interpenetrating polymer networks are dependent on the choice of interpenetrant and the monomer or comonomer matrix in which the interpenetrant is dissolved. Given such a range of possible systems only a very small number of combinations have been examined to date.

This thesis is concerned with the two interlinking aspects of this; the formation of semi-IPN's and the use of monomers that are novel, in that they have not been used previously in hydrogels of this sort. Monomers were chosen which may have

advantageous solubility properties and that would hopefully contribute to increasing the mechanical properties of the polymer matrix. The extension of work on semi-interpenetrating polymer networks, firstly incorporating interpenetrants that had been previously used with some success into novel polymer matrices and the use of new interpenetrants, were explored.

It is hard to predict from the nature of the monomers and interpenetrants how semi-IPN's would behave. This work is aimed at providing an additional information base which would make it easier to predict and control the properties that these materials may exhibit. Properties such as; mechanical, surface, EWC, water binding, oxygen permeability and glass transition temperature, are of particular interest.

In an attempt to synthesise potential contact lens materials copolymers containing tris-(trimethylsiloxy)- γ -methacryloxypropyl silane, commonly abbreviated to 'TRIS', have been investigated. This material has been shown to greatly enhance oxygen permeability, however, 'TRIS' has a low polar component of surface free energy and hence low wettability. By copolymerising with a range of methacrylates, attempts to increase surface wettability were made. In a further attempt to enhance surface wettability 4-methacryloxyethyl trimellitate was incorporated into a range of samples in the hope that this material would significantly increase the polar component of surface free energy with little effect on other desirable properties that samples exhibited.

CHAPTER 2

Materials and Experimental Techniques

2.1 Reagents

A list of reagents and suppliers are given below in table 2. 1, structures of these chemicals can be seen in figures 2. 1 - 2. 15

<u>Reagent</u>	<u>Abbreviation</u>	<u>Supplier</u>
Ethylene glycol dimethacrylate	EGDM	B.D.H.
Azo-bis-isobutyronitrile	AZBN	Aldrich
N-Vinyl pyrrolidone	NVP	Vista Optics
Cellulose acetate butyrate Mwt 70,000	CAB	Eastman chemicals
Cellulose acetate butyrate Mwt 40,000	CAB	Eastman chemicals
Ether-polyurethane	PU1 (Pellethane)	Upjohn
Ester-Polyurethane	PU2 (5706P)	Goodrich
Poly(carbonate)	PC	Monomer and Polymer Dajac
Tetrahydrofurfuryl acrylate	THFFA	Monomer and Polymer Dajac
Tetrahydrofurfuryl methacrylate	THFFMA	Monomer and Polymer Dajac
Iso-bornyl methacrylate	IBMA	Monomer and Polymer Dajac
Iso-butyl methacrylate	IBUTMA	Monomer and Polymer Dajac
Tert-butyl methacrylate	TBMA	Monomer and Polymer Dajac
Methyl methacrylate	MMA	B.D.H.

<u>Reagent</u>	<u>Abbreviation</u>	<u>Supplier</u>
Lauryl methacrylate	LMA	B.D.H.
Hexafluoro-iso-propyl methacrylate	HFIPMA	Vickers Laboratories Ltd
Tris-(trimethylsiloxy)- γ -methacryloxypropyl silane	TRIS	Polysciences
4-Methacryloxyethyl trimellitic anhydride	4-META	Monomer and Polymer Dajac

Table 2.1 Suppliers and Reagents used

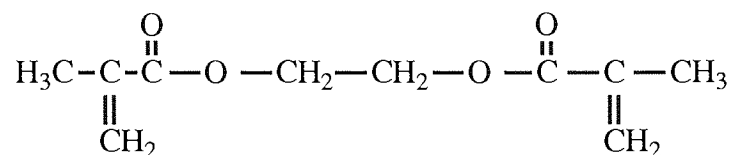


Figure 2.1 Ethylene Glycol Dimethacrylate

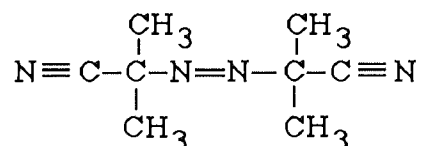


Figure 2.2 Azo-Bis-Isobutyronitrile

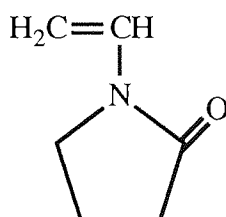


Figure 2.3 N-Vinyl Pyrrolidone

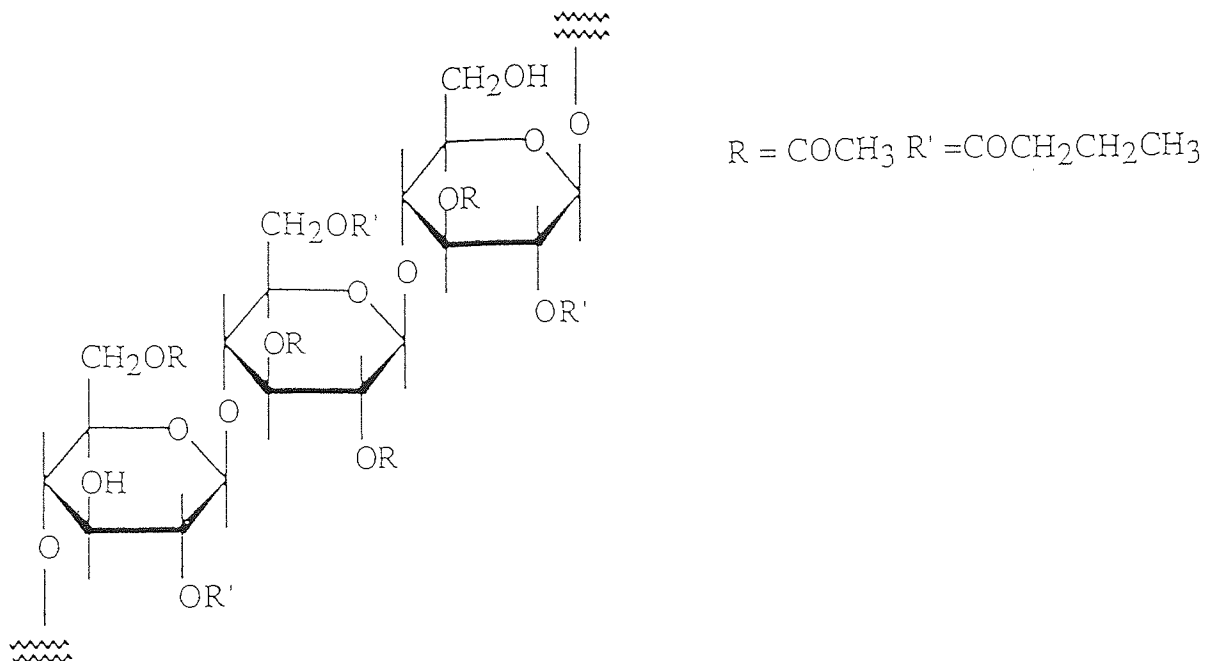


Figure 2.4 Cellulose Acetate Butyrate

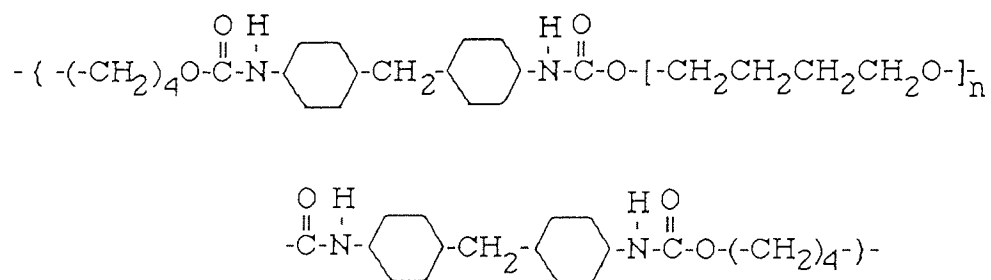


Figure 2.5 Ether Polyurethane

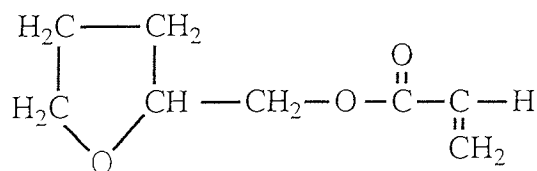


Figure 2.6 Tetrahydrofurfuryl Acrylate

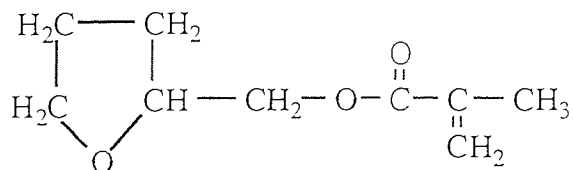


Figure 2.7 Tetrahydrofurfuryl Methacrylate

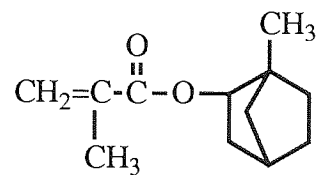


Figure 2.8 Iso-bornyl Methacrylate

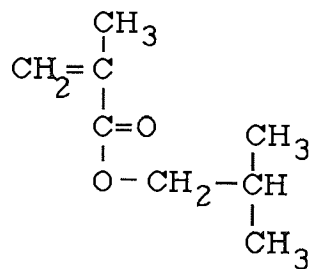


Figure 2.9 Iso-butyl Methacrylate

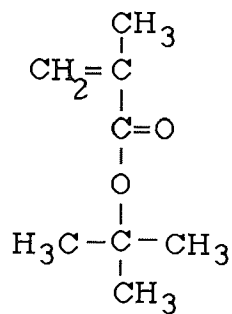


Figure 2.10 Tert-butyl Methacrylate

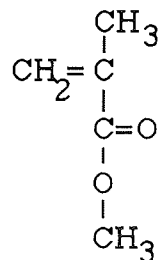


Figure 2. 11 Methyl Methacrylate

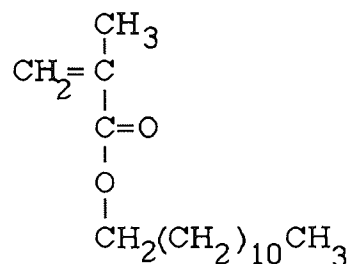


Figure 2. 12 Lauryl Methacrylate

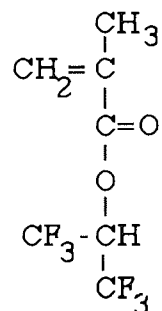


Figure 2. 13 Hexafluoro-iso Propyl Methacrylate

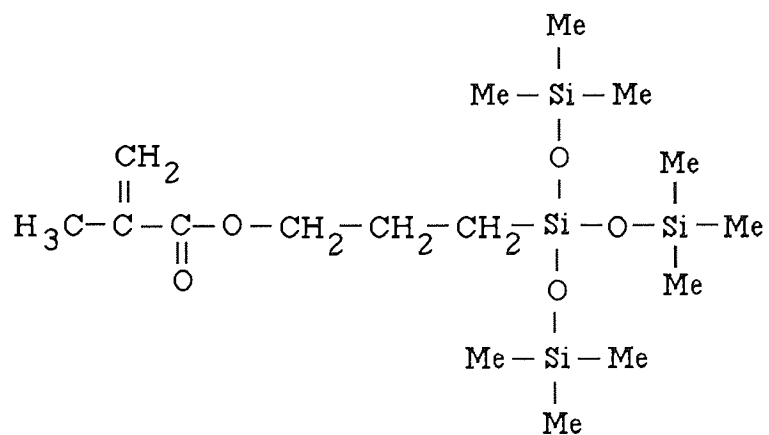


Figure 2. 14 Tris-(trimethylsiloxy)- γ -Methacryloxypropyl Silane

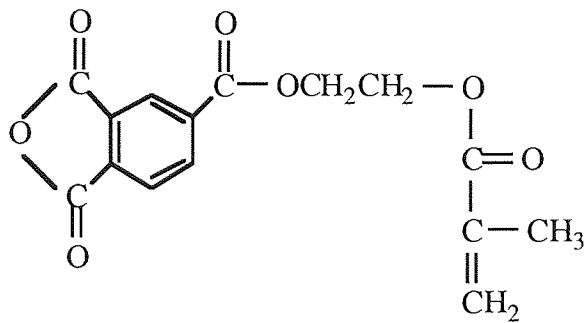


Figure 2. 15 4-Methacryloyloxyethyl Trimellitic Anhydride

2.2 Polymer Synthesis

2.2.1 Preparation of Membranes

Polymers were produced in the form of membrane sheets which were produced by free radical polymerisation in a glass mould. To make the mould two glass plates, 15cm x 10cm, were covered with melinex sheets, which were secured with spray mount. This allowed for easy removal of the finished membrane from the mould. The plates were placed together with two polyethylene gaskets, each 0.2mm thick, separating the melinex sheets. The whole assembly was held together using sprung clips. The monomer was injected into the mould cavity using a syringe and syringe needle, see figure 2. 17.

Polymers and copolymers were made using a standard 1% (w/w) cross-linker of ethylene glycol dimethacrylate (EDMA) and 0.5% (w/w) of initiator, azo-bis-isobutyronitrile (AZBN). For semi-interpenetrating polymer network (SIPN) membranes, the linear or interpenetrating polymer was dissolved in the monomer or comonomer. Tetrahydrofuran, THF, was used as a solvent in these systems, with a maximum of 15% (w/w) being added at this stage if necessary. Once a homogeneous mixture was obtained, in both the copolymers and the semi-IPN's, the cross-linker and initiator were added. It should be noted that tetrahydrofuran was used as a solvent for both CAB and the polyurethanes. For samples which contained 4-META, the 4-META was dissolved in no more than 15% (w/w) of THF, prior to the addition of other monomers to be used in the system. A total of 5 grams of mixture was required. Nitrogen gas was bubbled through the mixture for ten minutes before injection into the mould to ensure that all oxygen was removed from the mixture. Semi-IPN samples containing 10-15% of polymer were poured directly into the mould as the mixture was too viscous to inject into the mould. The mould was then placed in an oven at 60°C for three days to cure and at 90°C for a further three hours to post cure.

On removal from the oven the clips were removed and the polymer sheet was placed in distilled water and hydrated for at least one week. The water in which the membrane sheets were placed was changed daily.

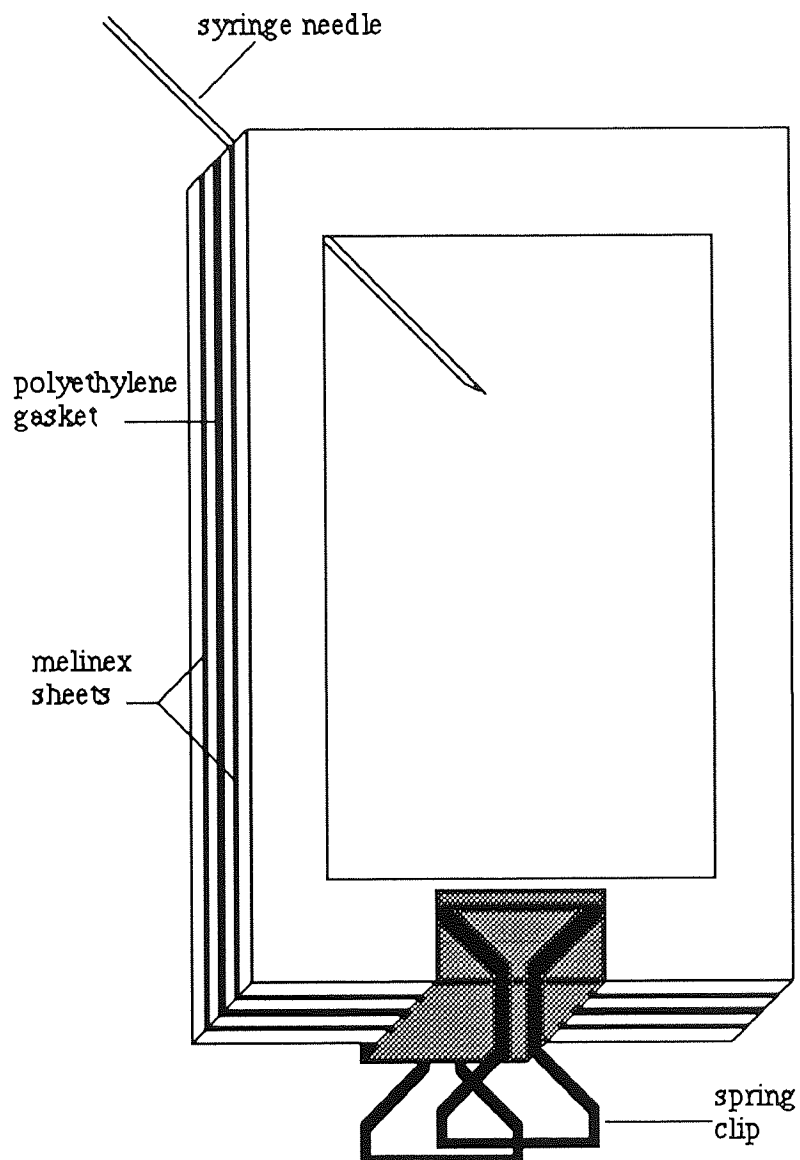


Figure 2. 16 Membrane Mould

2. 3 Equilibrium Water Content

Several samples of polymer were cut from a membrane sheet using a size seven cork borer. Surface water was removed using filter paper, care was taken not to squeeze water from within the structure. Samples were weighed using a five place balance and then dehydrated in a microwave oven for ten minutes and then reweighed. Using the following equation the equilibrium water content was calculated.

$$\text{EWC (\%)} = \frac{\text{weight of the water in the gel}}{\text{total weight of hydrated gel}} \times 100 \quad (2. 1)$$

The final value is an average of the results from at least three determinations.

2.4 Tensile Testing

A Houndsfield HK 10KN universal testing machine in conjunction with an IBM 55SX computer were used to test all of the samples. This equipment calculated the Young's modulus (E), tensile strength at break (σ_b), and elongation to break (ϵ_b), after dimensional values of the polymers length (8.0mm), width (5.0mm), and thickness, were input. Throughout this study the initial value for Young's modulus has been quoted. The following equations were used to calculate mechanical properties :-

$$E = \sigma / \epsilon \quad (2. 2)$$

where:-

$$\text{stress } (\sigma) = \text{load} / \text{cross-sectional area} \quad (2. 3)$$

and

$$\text{strain } (\epsilon) = \text{extension of gauge length} / \text{original gauge length} \quad (2. 4)$$

$$\text{stress at break } (\sigma_b) = \text{load at break} / \text{cross-sectional area} \quad (2. 5)$$

$$\text{elongation at break } (\epsilon_b) (\%) = \text{extension of gauge length} / \text{original gage length} \times 100$$

(2. 6)

Samples of polymer from a membrane sheet were cut using a 'dog bone' cutting jig giving constant length and width. The thickness of each sample was measured using a micrometer. For hydrogel samples firm pressure was sufficient to cut a shape. A test speed of 20 mm/min was selected for the testing of hydrogels. Throughout the testing the hydrogel samples were sprayed with water, which enabled 100% humidity to be maintained throughout the test. All samples were tested at room temperature and pressure. An average from at least five sets of results was obtained for each sample.

2.5 Differential Scanning Calorimetry (DSC)

A schematic diagram of this apparatus is shown in figure 2. 18. The DSC was used to determine the glass transition temperatures and percentage of freezing water present in hydrogel samples.

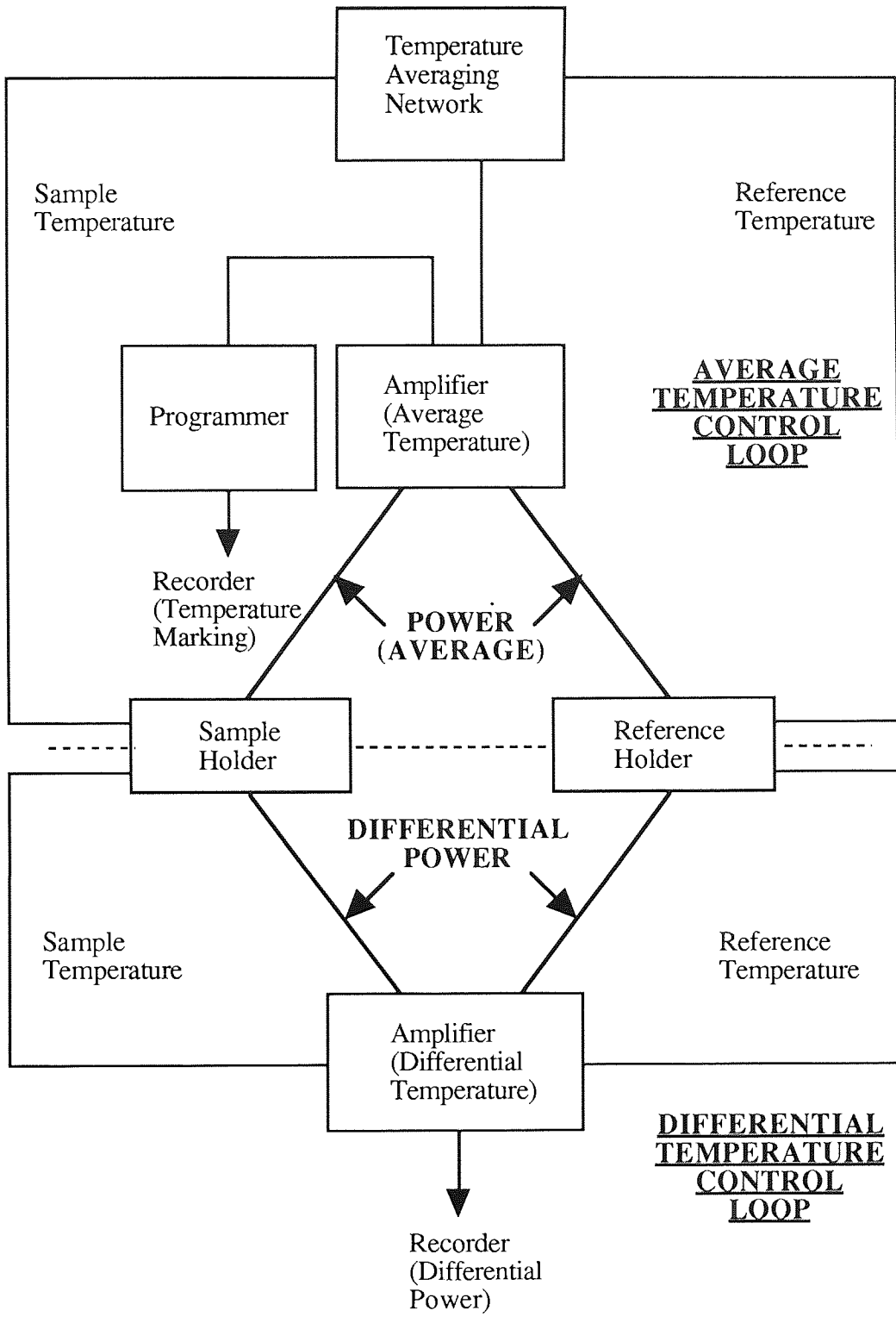


Figure 2. 17 Differential Scanning Calorimeter

2.5.1 Freezing Water Content

Thermograms were obtained using a Perkin Elmer differential scanning calorimeter, (DSC), DSC7, in conjunction with a 7500 professional computer and liquid nitrogen accessory. Samples were cut from a hydrated sheet of hydrogel using a size one cork borer and the surface water was removed using filter paper. The samples were weighed and sealed in aluminium pans.

Samples were cooled to 223K which ensured that any supercooled water was frozen and then allowed to reach equilibrium. Samples were heated to 253K and subsequently heated to ambient temperature at a rate of 5K/min.

The area under the peaks, in the form of mountain ranges, of hydrogel samples was measured and the amount of freezing water in the sample was calculated. ΔH for the sample is given and the percent of freezing water in the sample is obtained using equation 2. 7:-

$$\text{Freezing Water (\%)} = \Delta H \text{ calculated} / \Delta H \text{ for pure water} \times 10 \quad (2. 7)$$

where:-

$$\Delta H = \text{area under the peak} / \text{weight of the sample} \quad (2. 8)$$

and

$$\Delta H \text{ for pure water} = 333.77 \text{ J/g}$$

The process was repeated three times for each specimen and three samples of each composition were used.

2.5.2 Glass Transition Temperatures using the DSC

When determining glass transition temperatures, samples were cut to size using a size 1 cork borer, dehydrated in the microwave oven for a period of ten minutes, and placed in an aluminium pan which was then sealed. This was then placed into the sample holder of the thermal analyser unit. To quench the sample it was heated rapidly to above an estimated glass transition temperature, usually to 200°C, then cooled below 0°C, followed by controlled heating at a rate of 10 K/min. A positive change in the resulting endothermic was considered to be the glass transition temperature. This was repeated at least five times for each sample.

2.5.3 Glass Transition Temperatures using the Thermal Mechanical Analysis

Thermal mechanical analysis or TMA was used in addition to the DSC to determine glass transition temperatures. It was found that inaccurate results which spanned over a broad temperature range were obtained using the DSC. This led to the use of the TMA in an attempt to increase the accuracy of glass transition temperatures. A diagram of this apparatus is shown in figure 2. 19.

Once again samples were cut to size using a size one cork borer and dehydrated in a microwave oven for 5 minutes. Once the sample was in place on the platform, a quartz probe with a constant force was applied to the sample and heated at a rate of 10K/min. Probe force was controlled and altered when necessary, for different samples. This technique was again repeated at least five times for each sample.

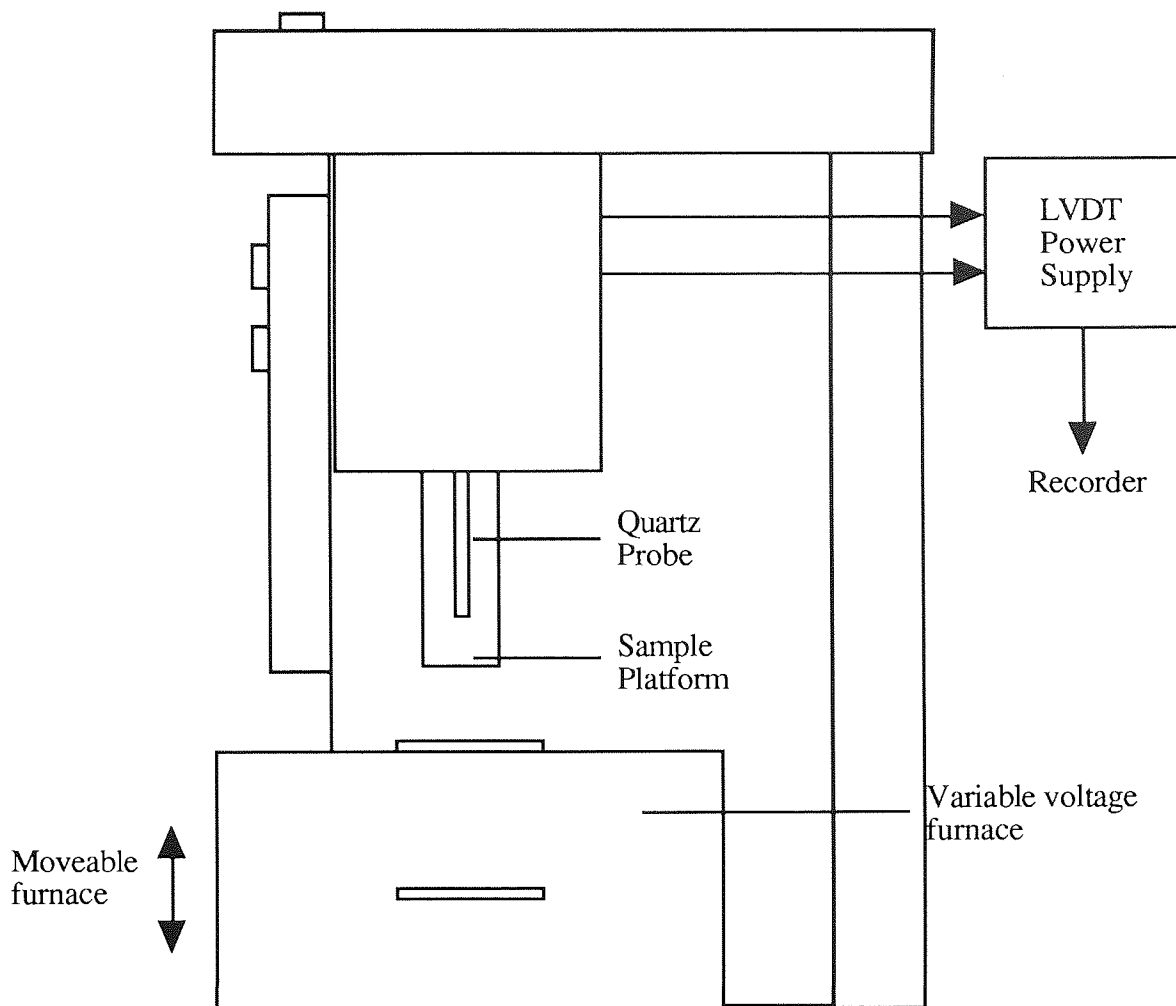


Figure 2. 18 Thermal Mechanical Analyser

2. 6 Surface Properties

Surface energies were studied in the hydrated state using Hamilton's method and the captive air bubble technique, and in the dehydrated state using the sessile drop technique. Samples were cut from a hydrated sheet using a size seven cork borer. In each case the samples were cleaned using Teepol 'L' and rinsed thoroughly in distilled water. They were then left to soak in distilled water for several days before testing and this ensured that any remaining traces of detergent were removed.

Using a Rame Hart goniometer with a calibrated eye piece the contact angle at the three phase interface was measured and an average at each side of the bubble/drop

was measured. Once the contact angle results were obtained, polar, dispersive and total surface free energies were calculated using Macintosh WorksTM, which had been programmed with relevant equations, seen in Chapter 1.

2. 6. 1 Hamiltons Method

Surface water was removed from a sample using filter paper and was then glued to an electron microscope stub using super glue. The sample was suspended inverted in an optical cell which was then filled with distilled water. A small drop of n-octane was placed on the surface of the sample using a G25 syringe needle. This was repeated at least three times on three samples this was to reduce any errors arising from surface topology irregularities and experimental errors.

2. 6. 2 Captive Air Bubble Technique

Samples were mounted as described above for Hamilton's method, however, air bubbles instead of n-octane, were released onto the surface using a specially curved G35 needle. This set-up allowed for accurate control of the bubble volume onto the surface of the samples. Once again at least nine readings were taken to reduce errors.

2. 6. 3 Sessile Drop Technique

Samples were dehydrated for ten minutes in a microwave oven and placed on a microscope slide which was in turn placed on the support of the goniometer. The wetting liquids used were water and diiodomethane. A small drop of liquid was placed onto the surface of the sample using a G25 hypodermic needle. Using the calibrated eye piece contact angle readings were taken. A number of samples were tested to give a more accurate comprehensive set of results.

2. 7 Oxygen Permeability

Oxygen permeability measurements were obtained using a model 201T Permiometer in conjunction with a chart plotter, as seen in figure 2. 19.

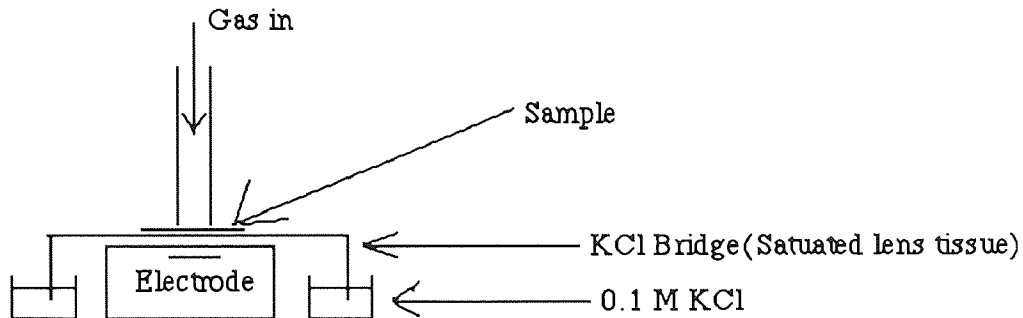


Figure 2. 19 Model 201T Permiometer

Polymer samples were cut to size using a size eight cork borer and the thickness was measured using a micrometer. Samples were placed over an electrode and a lens tissue, saturated in 0.1 molar potassium chloride was used as an electrode bridge situated in between the sample and the electrode. A column was placed over the sample and a slow flow of gas, either nitrogen or oxygen, was passed through the sample, as seen in figure 2.19. A constant stream of gas was passed through the sample until a steady current was obtained, which was then noted. The steady current obtained when passing nitrogen gas through the sample was denoted as i_0 . In all cases in this study i_0 was found to be zero. The steady current reading obtained when oxygen was passed through the sample was denoted as i . Oxygen permeability readings were calculated using equation 2. 9, and are given in the form of Dk , the diffusivity of oxygen through a material and the solubility of oxygen in a given material.

$$Dk = L(i - i_0) V / n F A P_s \quad (2. 9)$$

Where:

L - thickness (cm)

i_o - current obtained for nitrogen - zero in all cases in this work

i - current obtained for oxygen passing through the sample

F - Faraday constant = $96490 \times 10^6 \mu\text{A s mol}^{-1}$

A - area of gold (electrode) = 0.1278 cm^2

P_s - oxygen tension = 760 mm Hg S.T.P.

n - No. of electrons involved = 4

V - Standard gas molar volume = $22.415 \times 10^3 \text{ ml}$

If a constant is calculated the equation becomes:

$$Dk = i (\mu\text{A}) \times L (\text{cm}) \times (6 \times 10^{-9}) \quad \text{units cc cm} / \text{cm}^2 \text{ s cmHg} \quad (2. 9)$$

CHAPTER 3

Hydrogels

3.1 Introduction

One of the main limiting factors with hydrogels is their poor mechanical properties. When setting about improving the mechanical properties of hydrogels, care must be taken in order that the desirable properties that these materials exhibit are not lost. Two methods of improving mechanical properties were employed, the first was by the incorporation of bulky side chain monomers, see figure 3. 1. This technique had possibilities of increasing the glass transition temperature of the resulting dehydrated polymer, which would hopefully lead to an increase in the initial Young's modulus.

Corkhill and Trevett showed useful effects with the use of methacrylates with bulky side chains in copolymers, i.e. higher moduli. However, this strength increase usually has the effect of lowering the EWC, therefore monomers with more polar groups were chosen as comonomers to be polymerised with N-vinyl pyrrolidone. It has also been shown that bulky side chain methacrylate polymers have lower densities than straight chain polymers of similar molecular weight, which lead to an increase in the permeability of the material, another desirable feature when considering materials in the design of contact lenses. N-vinyl pyrrolidone, commonly abbreviated to NVP, was chosen as the hydrophilic component in the systems used throughout this study, which is one of the most widely commercially used hydrophilic monomers to produce hydrogels with equilibrium water contents greater than 40%. The formation of semi-interpenetrating polymer networks was the second way used to increase the mechanical properties of hydrogel materials. This was one of the successful techniques used by P.Corkhill *et. al.* ^{1, 2} and information obtained from his work was utilised and built upon. In general this work attempts to show that by the careful choice of monomers to copolymerise with N-vinyl pyrrolidone, improvements in the restricting mechanical properties of hydrogels can be made.

This chapter contains information on a range of compositions which were made, using novel methacrylate monomers in conjunction with N-vinyl pyrrolidone, into which polymers used previously and successfully by P.Corkhill *et. al.* were

incorporated. Tables 3. 1 - 3. 5 shows a list of compositions of copolymers and semi-interpenetrating networks that were made. Copolymers and semi-IPN's were synthesised using the method described in section 2. 2. Subsequent chapters will investigate other polymers for use as interpenetrants.

Chapter 3 and Chapter 4 which both deal with hydrogel systems can be conveniently broken down into several experimental sections, these are:

- a Novel methacrylate monomers used in conjunction with NVP
- b Novel methacrylate - NVP copolymers as matrices for an established interpenetrant, CAB
- c Novel methacrylate - NVP copolymers as matrices for novel interpenetrants (Chapter 4)

Properties of these hydrogel compositions were assessed using the range of experimental techniques described in Chapter 2.

<u>Polymer Composition</u>	<u>Equilibrium Water Content</u> (%)
NVP: THFFMA 80:20	82
NVP: THFFMA 75:25	78
NVP: THFFMA 70:30	74
NVP: THFFMA 60: 40	64
NVP: THFFMA: CAB 60: 40: 5	60
NVP: THFFMA: CAB 60: 40 10	57
NVP: THFFMA: CAB 60: 40: 15	53
NVP: THFFMA 40: 60	49
NVP: THFFMA: CAB 40: 60: 5	45
NVP: THFFMA: CAB 40: 60: 10	41
NVP: THFFMA: CAB 40: 60: 15	40

Table 3. 1 Tetrahydrofurfuryl Methacrylate Copolymers and Semi-IPN's Compositions and Associated EWC

The compositions quoted throughout this study, as previously mentioned in Chapter 2, are weight/weight values.

As expected with increasing percentages of methacrylate or acrylate in the system, the equilibrium water content decreased. Similarly with the incorporation of the more hydrophobic cellulose acetate butyrate molecule into the composition the EWC is once again reduced.

<u>Polymer Composition</u>	<u>Equilibrium Water Content</u> (%)
NVP: THFFA 80:20	86
NVP: THFFA 75:25	83
NVP: THFFA 70:30	82
NVP: THFFA 60:40	81
NVP: THFFA: CAB 60:40:5	74
NVP: THFFA: CAB 60:40:10	68
NVP: THFFA: CAB 60:40:15	62
NVP: THFFA 40:60	72
NVP: THFFA: CAB 40:60:5	64
NVP: THFFA: CAB 40:60:10	58
NVP: THFFA: CAB 40:60:15	57

Table 3.2 Tetrahydrofurfuryl Acrylate Copolymers and Semi-IPN's Compositions and Associated EWC

<u>Polymer Composition</u>	<u>Equilibrium Water Content</u> (%)
NVP: ISOBORNYL MA 80:20	56
NVP: ISOBORNYL MA 75:25	46
NVP: ISOBORNYL MA 70:30	40
NVP: ISOBORNYL MA:CAB 60: 40	59
NVP: ISOBORNYL MA:CAB 60: 40: 5	57
NVP: ISOBORNYL MA:CAB 60: 40:10	55
NVP: ISOBORNYL MA:CAB 60: 40:15	53

Table 3. 3 Iso-bornyl Methacrylate Copolymers and Semi-IPN's
Compositions and Associated EWC

<u>Polymer Composition</u>	<u>Equilibrium Water Content</u> (%)
NVP: ISOBUTYLMA 60: 40	43
NVP: ISOBUTYLMA: CAB 60: 40: 5	39
NVP: ISOBUTYLMA: CAB 60: 40: 10	38
NVP: ISOBUTYLMA: CAB 60: 40 15	36
NVP: ISOBUTYLMA 40: 60	22
NVP: ISOBUTYLMA: CAB 40: 60: 5	21
NVP: ISOBUTYLMA: CAB 40: 60: 10	19
NVP: ISOBUTYLMA: CAB 40: 60: 15	18

Table 3. 4 Iso-butyl Methacrylate Copolymers and Semi-IPN's
Compositions and Associated EWC

<u>Polymer Composition</u>	<u>Equilibrium Water Content</u> (%)
NVP: TERTBUTYLMA 60: 40	36
NVP: TERTBUTYLMA: CAB 60: 40: 5	33
NVP: TERTBUTYLMA: CAB 60:40:10	31
NVP: TERTBUTYLMA: CAB 60:40:15	30
NVP: TERTBUTYLMA 40: 60	18
NVP: TERTBUTYLMA: CAB 40: 60: 5	17
NVP: TERTBUTYLMA: CAB 40:60:10	14
NVP: TERTBUTYLMA: CAB 40:60:15	12

Table 3. 5 Compositions and Associated EWC Tert-butyl Methacrylate Copolymers and Semi-IPN's

Data for lauryl methacrylate and methyl methacrylate with NVP copolymers is given in Appendix 1.

The methacrylate unit is shown in figure 3. 1

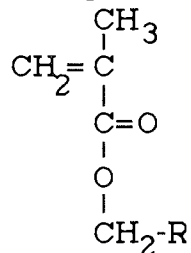
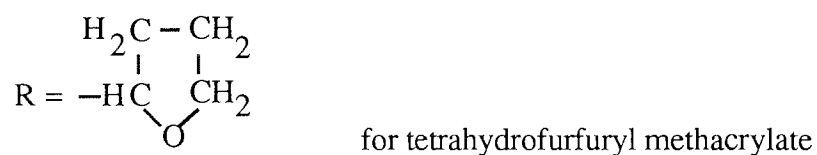


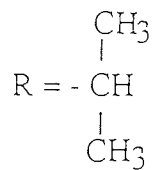
Figure 3. 1 Methacrylate Structures

Where R changes as follows in the differing methacrylates:

R = - H for methyl methacrylate

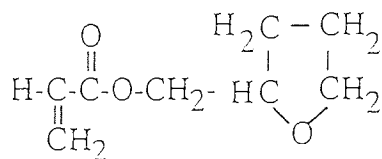
R = - (CH₂)₁₀CH₃ for lauryl methacrylate



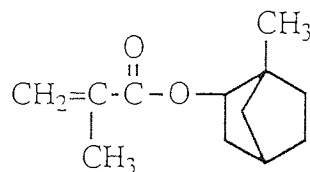


for iso-butyl methacrylate

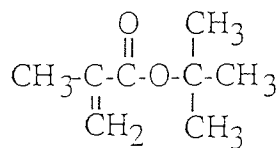
Other structures are as follows :



tetrahydrofurfuryl acrylate



iso-bornyl methacrylate



tert-butyl methacrylate

The CAB used throughout the production of hydrogels had a molecular weight of 70,000, and its structure is shown in figure 3. 2.

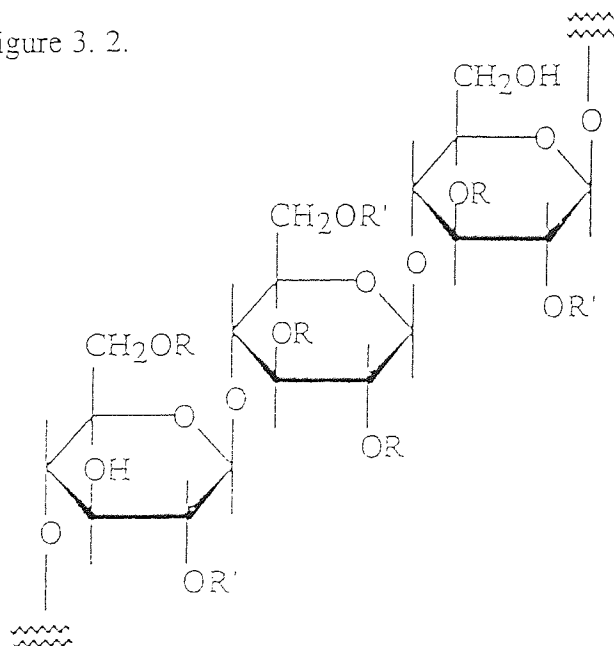
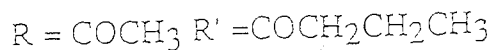


Figure 3. 2 Cellulose Acetate Butyrate

3. 2 Mechanical Properties of Non-Reinforced Hydrogels

The effect of polymer structure and the equilibrium water content on the mechanical properties of a series of hydrogels was studied. Results are presented as the Young's modulus, tensile strength and elongation at break relative to the percentage of methacrylate in the sample or the equilibrium water content. If mechanical properties are plotted with EWC, the structural effects of different methacrylates can be directly compared.

3.2.1 Mechanical Properties of Hydrogel copolymers

Figures 3. 3 - 3. 10 illustrate the mechanical properties of hydrogel copolymers. It is noted that the crosshead displacement measured throughout this work, used to calculate strain, is a measurement of the extension in the parallel and the tapered portion of the sample, hence a true value for strain is not obtained. However, alternative methods for obtaining values of strain involving the use of conventional extensometry equipment is not a viable alternative when testing hydrogels (other methods involve the use of clips which would tear or break the sample). An alternative method would be to use non-contact extensometry by marking the samples in some way. This would also involve problems in that the throughput of samples tested would be greatly reduced and the small size and fragile nature of the samples would make a marking system hard to operate. However, it is of greater interest to compare actual values rather than absolute values of strain for a variety of samples. Provided that a suitable shaped sample is used and the strain is small, extensions should be almost confined to the parallel portion of the sample and the results should not be greatly affected⁵⁰. It is noted that at high strains some extension in the tapered region would occur and that this would be reflected in the elongation at break. As previously mentioned, in Chapter 2, the initial value for Young's modulus is quoted throughout this work.

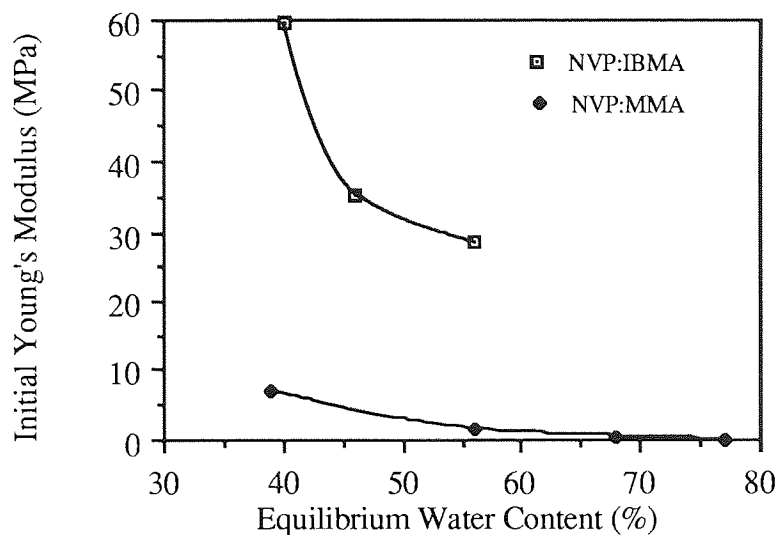


Figure 3. 3 Relative Initial Young's Moduli of Copolymers of Iso-bornyl Methacrylate and Methyl Methacrylate with NVP

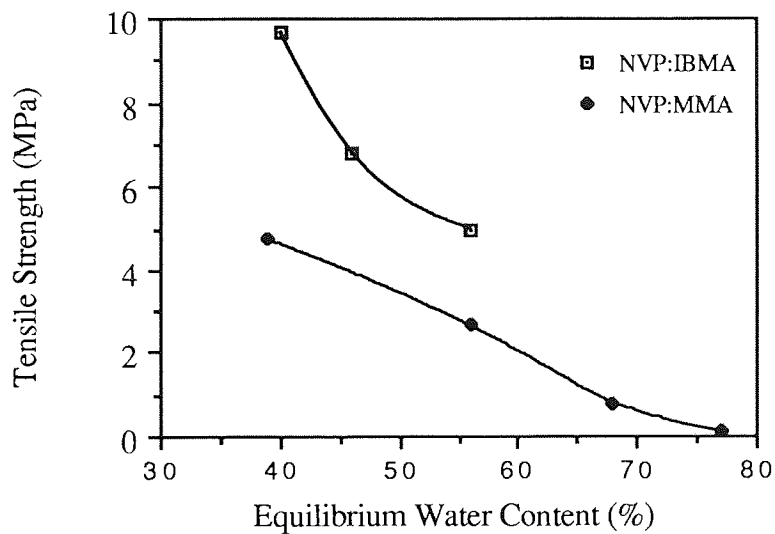


Figure 3. 4 Relative Tensile Strengths of Copolymers of Iso-bornyl Methacrylate and Methyl Methacrylate with NVP

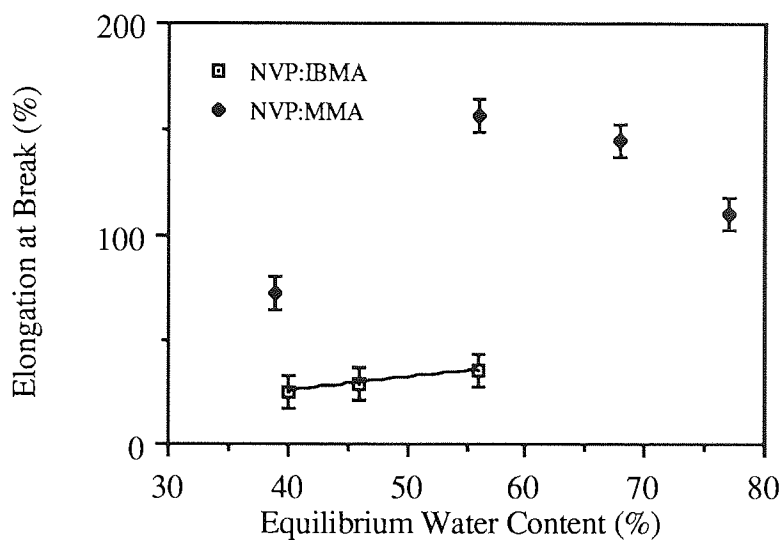


Figure 3.5 The Relative Elongations at Break of Copolymers of Methyl Methacrylate and Iso-bornyl Methacrylate with NVP

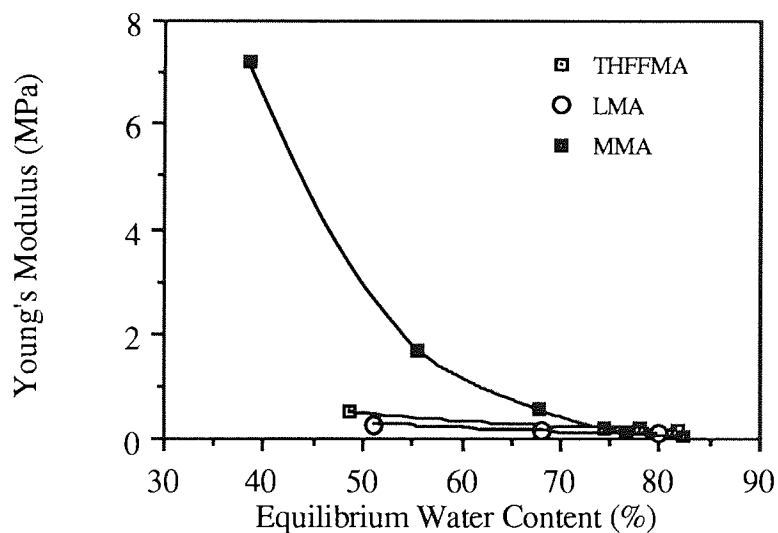


Figure 3.6 Relative Mechanical Properties of Linear and Cyclic Methacrylates Copolymerised with NVP

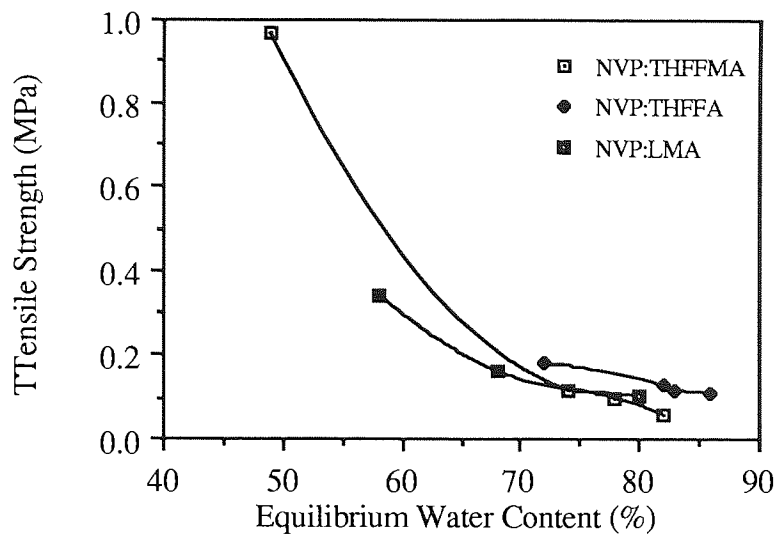


Figure 3. 7 A Comparison of the Tensile Properties Obtained with the use of Cyclic and Linear Monomers Copolymerised with NVP

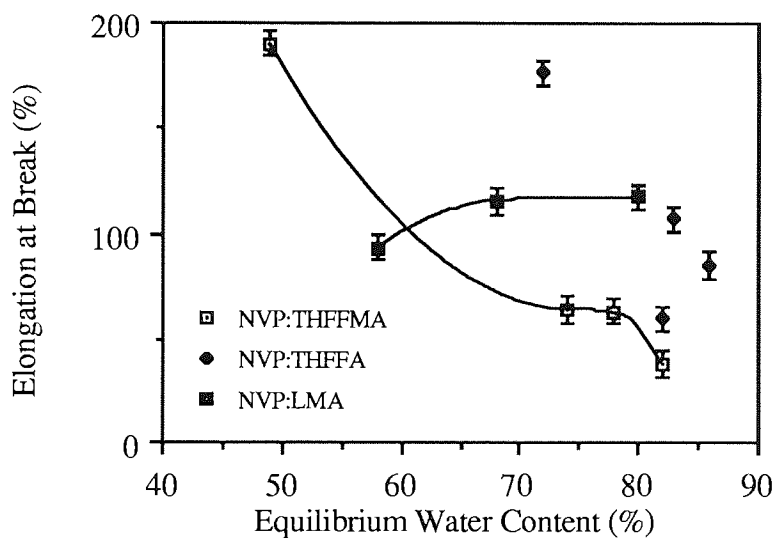


Figure 3. 8 A Comparison of the Elongation Properties Obtained with the use of Cyclic and Linear Monomers Copolymerised with NVP

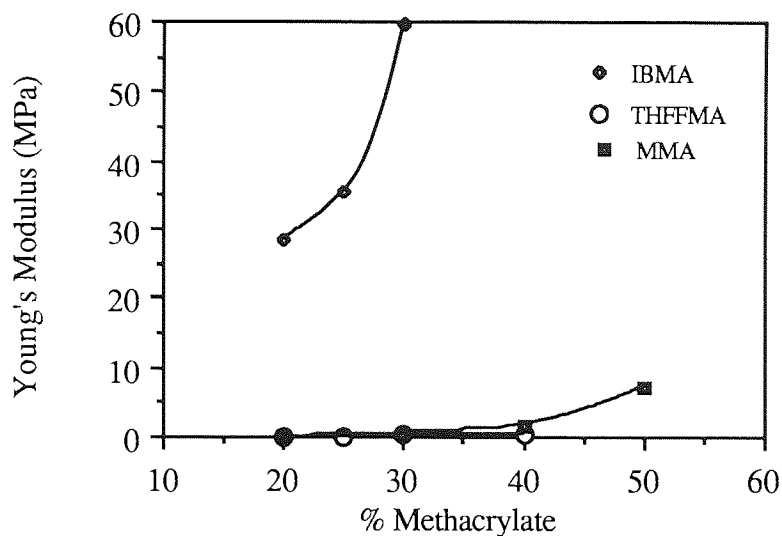


Figure 3.9 Initial Modulus Variations Obtained with the use of Different Methacrylates Copolymerised with NVP

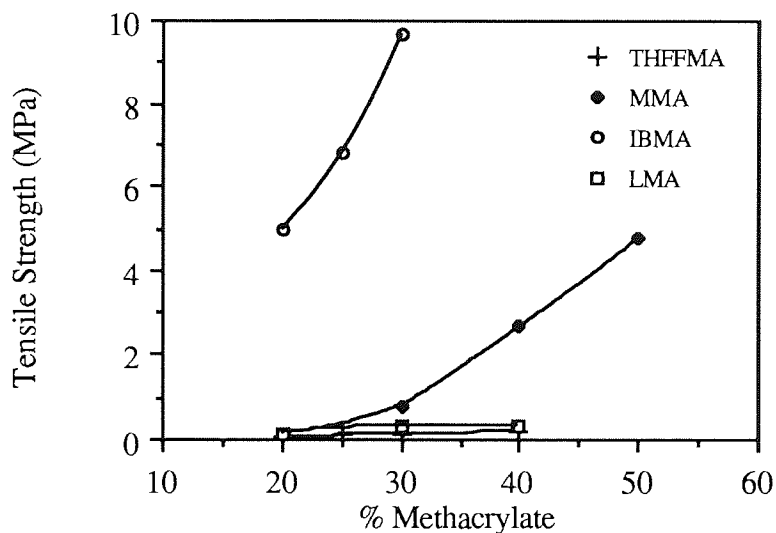


Figure 3.10 Tensile Strength Variations Obtained with the use of Different Methacrylates Copolymerised with NVP

As can be seen in figures 3.3 - 3.10, the mechanical properties of hydrogels differ greatly. They appear to follow traditional trends, increases in initial modulus and tensile strength occur with an increase in the percentage of the more hydrophobic methacrylate component, or a reduction in EWC. The elongation at break and the

tensile strength are usually dependent on each other. Hence, in general, for materials that increase in tensile strength with a decrease in EWC, the elongation at break also increases. However, this is not always the case, the way the water is structured will also affect the mechanical properties. Figure 3. 5 illustrates this phenomenon. In methyl methacrylate copolymers, the elongation at break increases with a reduction in water content, but only to a certain point where it then reduces. At this point the sample contains very little freezing or plasticising water. This makes the sample less flexible and somewhat brittle. This phenomenon is also observed with samples containing iso-bornyl methacrylate, where in all samples the freezing water content is low, 28.6%, 15.6 % and 8.4 %, in samples containing 20 %, 25 % and 30 % of methacrylate respectively. As the EWC in these samples increases, the elongations at break also increase. However, in samples with high equilibrium water contents, and consequently high freezing water contents see (figure 3. 37 showing the relationship between equilibrium water content and freezing water content), the plasticising water is high, maintaining flexibility in such samples. Hence, the elongation at break for the NVP with THFFMA or THFFA increases with an increase in tensile strength and a reduction in equilibrium water content, see figures 3.7 and 3.8.

In the past, poly(methyl methacrylate) has been considered a very important biomaterial, used in many applications ranging from contact lenses to bone cement. However this material is less than ideal and although it has a high Young's modulus and has often been used to strengthen weaker hydrogel materials, other cyclic materials have been shown to enhance mechanical properties considerably more². In compositions of 70 : 30 NVP : MMA, Young's moduli of 0.8 MPa have been reported with the addition of methyl methacrylate, whereas a modulus of 59 MPa can be achieved by simply replacing the methyl methacrylate with iso-bornyl methacrylate.

It is apparent that the increase and decrease in equilibrium water content is directly related to a decrease and increase in mechanical properties in a specific series of materials. This is observed in figures 3. 9-3. 10, where the addition of the more

hydrophobic component results in an increase in Young's modulus and tensile strength. However, the overriding factor that controls mechanical properties is the chemical structure of the monomers used. This is illustrated in figures 3. 3-3. 8, which show the range of properties that can be achieved at the same equilibrium water content by changing one of the chemicals in the system. It has been shown by Corkhill *et.al.*² that the addition of cyclic methacrylates into N-vinyl pyrrolidone gave a significant increase in initial Young's moduli and tensile strength, compared to linear methacrylates of similar molecular weight. This phenomenon is shown in figures 3. 3 and 3. 4 where iso-bornyl methacrylate : NVP copolymers have a considerably higher Young's moduli and tensile strengths than methyl methacrylate: NVP copolymers. However, this is not observed with the addition of THFFA to NVP. In these samples the modulus is less than the linear lauryl methacrylate, figure 3. 6. However, it is noted that this material lacks the hydrophobic α -methyl group present in methacrylates which has been shown to have a stiffening effect. Also, the THFFA has a glass transition temperature below room temperature, therefore it is expected that copolymers made with this monomer will be less stiff than copolymers made with higher glass transition temperature materials.

Results of copolymers of NVP : THFFMA, although better than the linear lauryl methacrylate with NVP copolymers, are somewhat disappointing. It was expected that the moduli and tensile strengths would be considerably higher than those observed, possibly in a similar region to benzyl methacrylate, both structures having the same HO-CH₂ linking group. This, however, is not the case. Benzyl methacrylate : NVP copolymers at approximately 55% equilibrium water content have an initial Young's modulus in the region of 80 MPa and a tensile strength of 6.5 MPa, whereas THFFMA copolymers at a similar water content have Young's moduli and tensile strengths less than 1 MPa. So why does THFFMA behave differently to the manner expected from first inspection of its structure? Initially it was thought that impurities may be present in the monomer. However, samples were remade after the monomer had been distilled and no appreciable change in polymer properties were observed. If glass transition temperatures of dehydrated samples are compared,

materials such as poly(2-hydroxyethyl methacrylate) and poly(methyl methacrylate) have similar Tg's approximately 105-110 °C. However, if both materials are hydrated the glass transition temperature of poly(methyl methacrylate) is unaffected, whilst that of poly(2-hydroxyethyl methacrylate) drops below room temperature. Hence, for samples copolymerised with NVP, materials containing PMMA are stiff and strong, whereas those incorporating poly(2-hydroxyethyl methacrylate) are weak. If when hydrated the glass transition temperature of THFFMA is lowered, this would explain why systems containing this material behave in an unexpected manner. Braden *et. al.* have previously reported that the THFFMA homopolymer does not reach an equilibrium water content after 33 months⁴³. It is therefore reasonable to assume that the hydrated glass transition temperature is lower than 47°C which is reported to be the dehydrated Tg. Therefore, if THFFMA were in a copolymer with NVP and could be isolated between the hydrophilic component and then hydrated, the Tg would drop considerably. Thus, energy to rotation would drop, and hence, stiffness or Young's modulus would be lower than expected by looking only at the properties the material would be expected to exhibit in the dehydrated state.

Results obtained with some of the higher equilibrium water content samples gave standard deviations that were quite considerable, see appendix 1. This was attributed to the very fragile nature of the samples, where handling of such samples may have caused small tears to develop, undetected by eye, but still enough to ensure that higher stress concentrations would be set up in these areas which would result in the premature breaking of those samples. Errors may also be associated with the difficulty of accurately measuring crosslinker in to the monomer mixtures, between two and three drops and in fragile samples this difference would be considerable.

Several of THFFA : NVP samples fracture by simply placing in the grips of the tensiometer and always if the grips were tightened. Therefore, for this range of samples, the grips were gently closed and never tightened. Although this technique was employed for THFFA : NVP high equilibrium water content samples, it was not

used for lower equilibrium water content and hence stronger samples, which had a tendency to 'slip' from the grips if not held securely in position.

3.2.2 Mechanical Properties of Hydrogel Semi-IPN's using CAB as an Interpenetrant

Having established that a range of mechanical properties can be achieved by changing the structure of the methacrylate monomer in a series of NVP : methacrylate/acrylate copolymers, these copolymers were used as matrices to examine the achievable mechanical properties in a series of hydrogel semi-interpenetrating polymer networks.

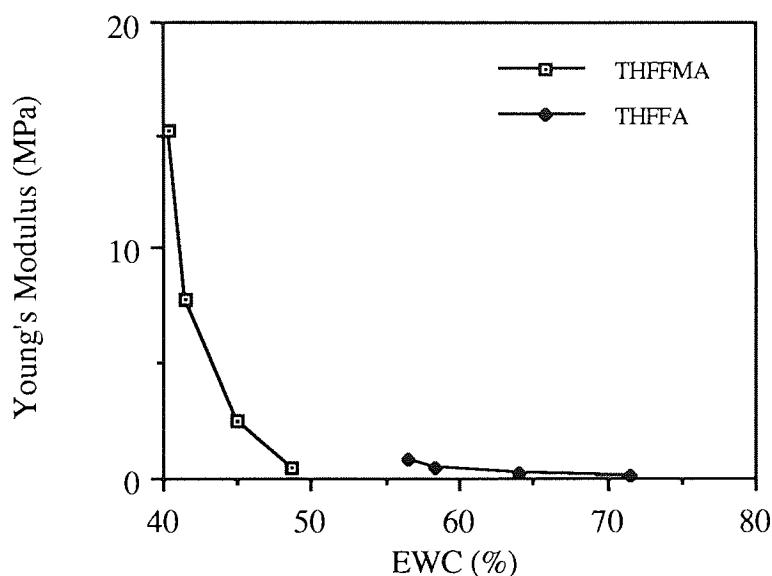


Figure 3.11 Effect of Water Content on the Initial Young's Modulus of 40 : 60 NVP : THFFMA / THFFA Semi-IPN'S Prepared with CAB

Proportions of CAB concentration are shown in figure 3.12.

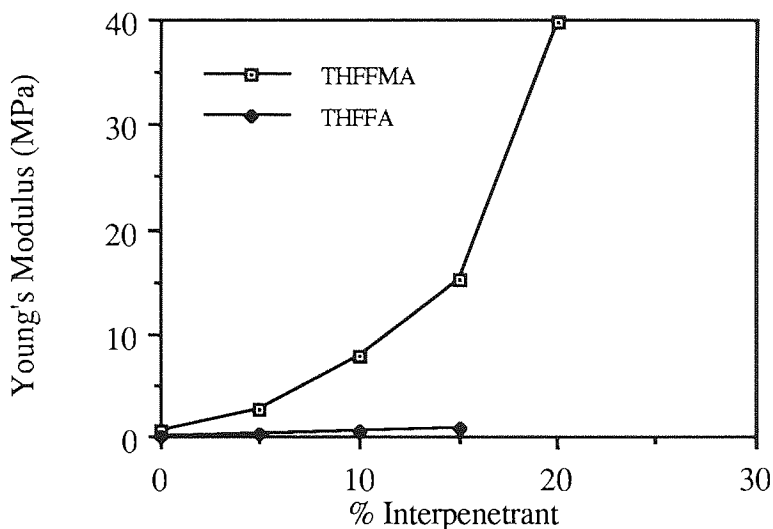


Figure 3.12 Effect of Interpenetrant on the Young's Modulus of 40 : 60
NVP : THFFMA / THFFA with CAB Semi-IPN'S

Figures 3. 11 and 3. 12 both show how the Young's modulus varies, the data being represented as a function of equilibrium water content and interpenetrant concentration respectively. The equilibrium water content reduces as the cellulose acetate butyrate content increases, and hence, by using the standard reasoning established for simple hydrogel copolymers, the Young's modulus and tensile strength increases with a reduction in EWC and an increase in CAB. The THFFA containing samples once again gave lower results than those containing THFFMA. Again this is due to the presence of the α -methyl group present in the THFFMA forming a stiffer copolymer with a higher glass transition temperature.

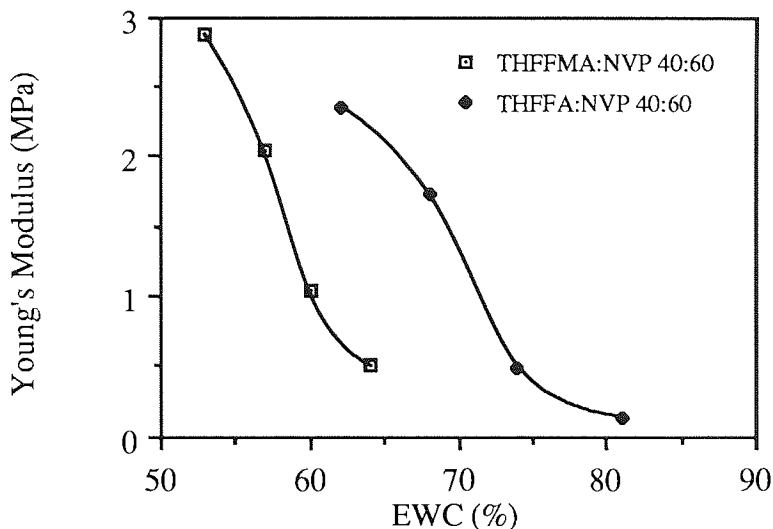


Figure 3.13 Effect of Water Content on the Young's Modulus of 60 : 40 NVP : THFFMA / THFFA with CAB Semi-IPN'S

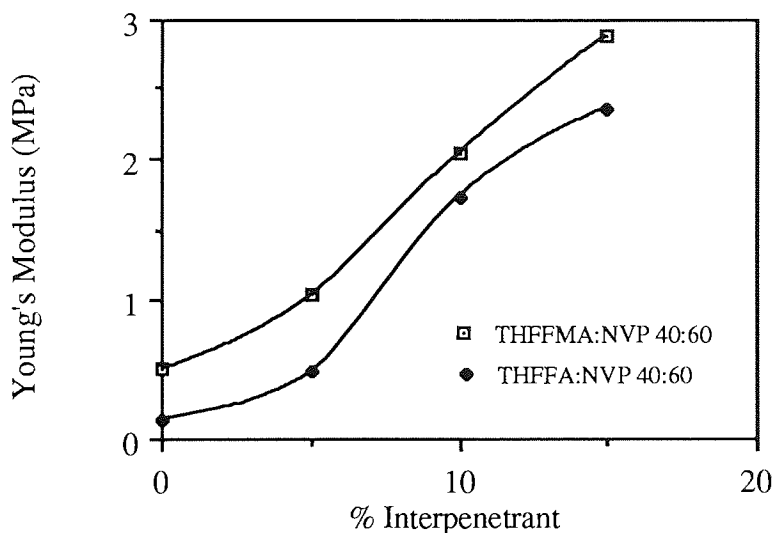


Figure 3.14 Effect of Interpenetrant on the Young's Modulus of 60 : 40 NVP : THFFMA / THFFA with CAB Semi-IPN'S

Figures 3. 13 and 3. 14 shows the effect of increasing the proportion of NVP from 40% to 60% in the THFFMA or THFFA systems. These samples, understandably, have a lower initial modulus than those containing 40% NVP. If figure 3. 13 is studied, showing the relationship between EWC and Young's modulus, results

appear to deviate from conventional theories. At a given EWC, the samples containing THFFA gave a higher value of initial modulus. It must be noted that these systems are semi-IPN's and at the points where both systems have a similar EWC, the samples containing THFFA have a greater concentration of CAB present than THFFMA samples. However, in figure 3. 14, showing the effect of interpenetrant concentration, a predicted pattern emerged. Increasing CAB concentration gave an increase in the initial Young's modulus, with the THFFMA containing samples having the higher values for initial modulus. This shows one of the advantages semi-IPN's have over conventional copolymers, i. e. the ability to form high water content polymers with superior mechanical properties.

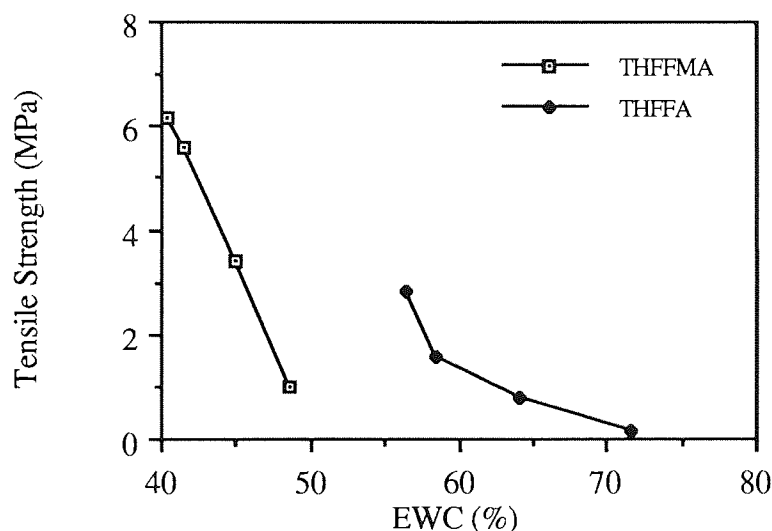


Figure 3.15 Effect of Water Content on the Tensile Strength of 40 : 60
NVP : THFFMA / THFFA with CAB Semi-IPN'S

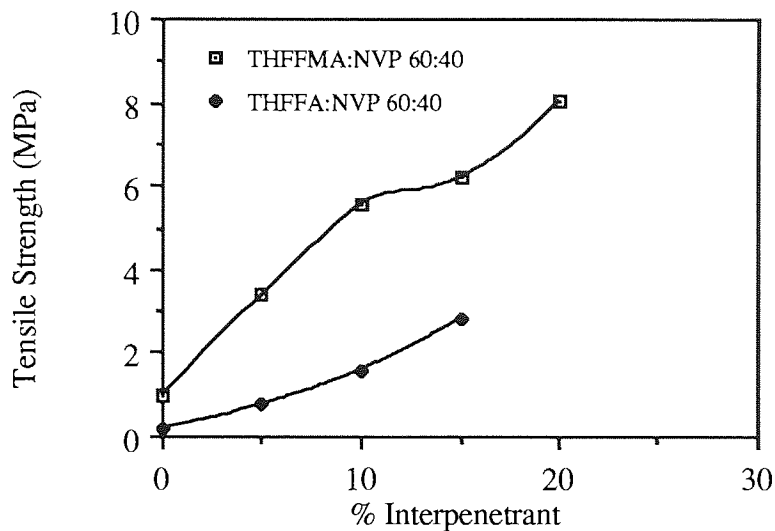


Figure 3.16 Effect of Interpenetrant on the Tensile Strength of 40 : 60
NVP : THFFMA / THFFA with CAB Semi-IPN'S

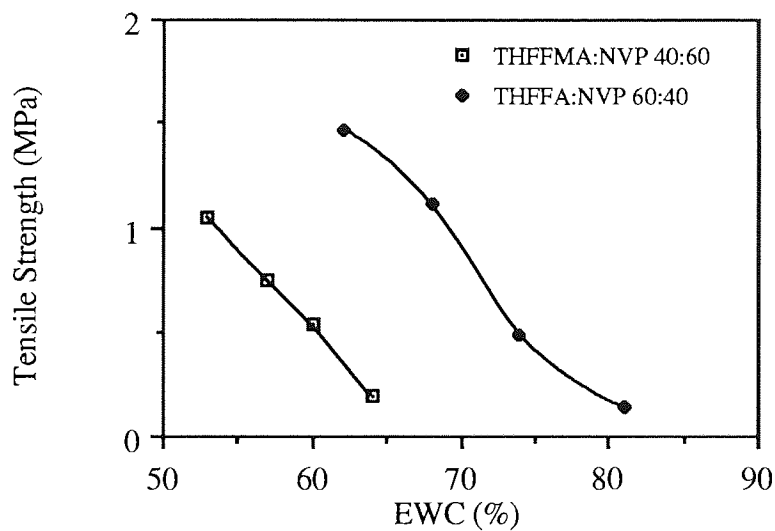


Figure 3.17 Effect of Water Content on the Tensile Strength of 60 : 40
NVP : THFFMA / THFFA with CAB Semi-IPN'S

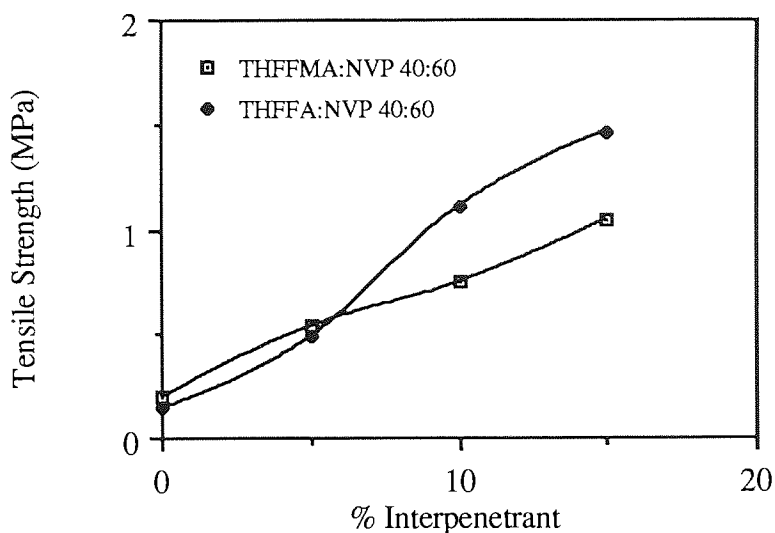


Figure 3.18 Effect of Interpenetrant on the Tensile Strength of 60 : 40
NVP : THFFMA / THFFA with CAB Semi-IPN'S

Tensile strengths of THFFMA and THFFA samples, shown in figures 3. 15 - 3. 18, show the same trends as with the initial modulus. THFFMA containing samples have higher values than THFFA containing samples, and with increasing amounts of interpenetrant in the samples, higher tensile strengths are obtained.

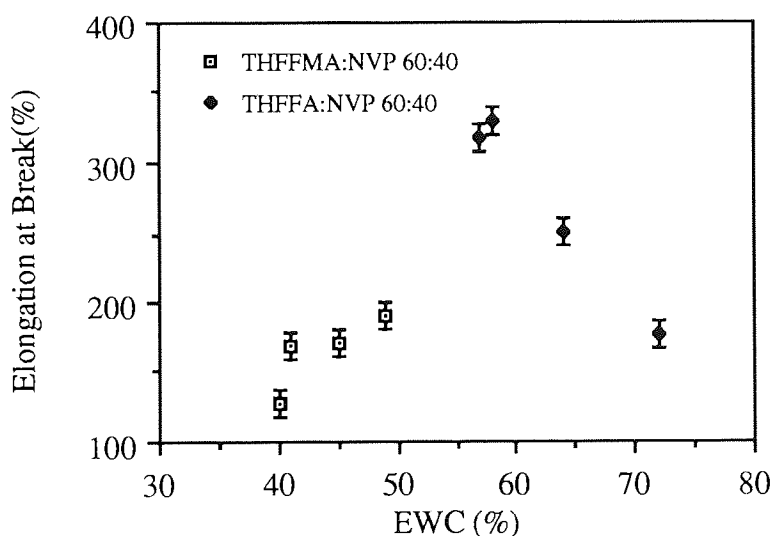


Figure 3.19 Effect of Water Content on the Elongation at Break 40 : 60
of NVP : THFFMA / THFFA with CAB Semi-IPN'S

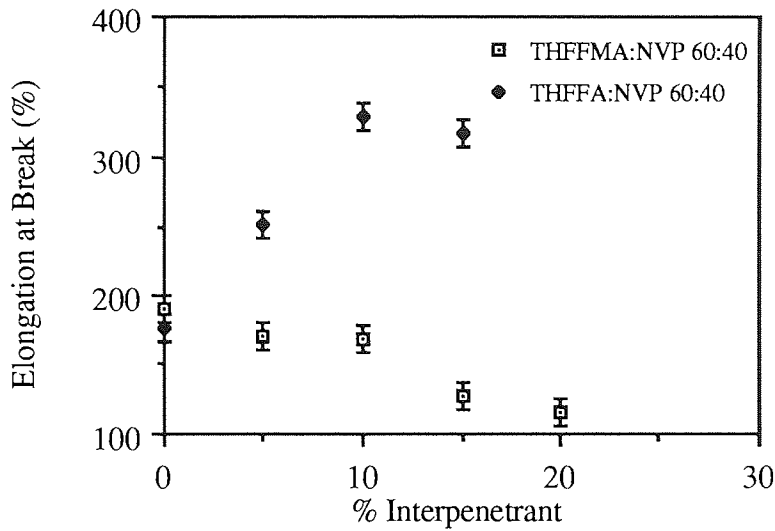


Figure 3.20 Effect of Interpenetrant on the Elongation at Break of 40 : 60
NVP : THFFMA / THFFA with CAB Semi-IPN'S

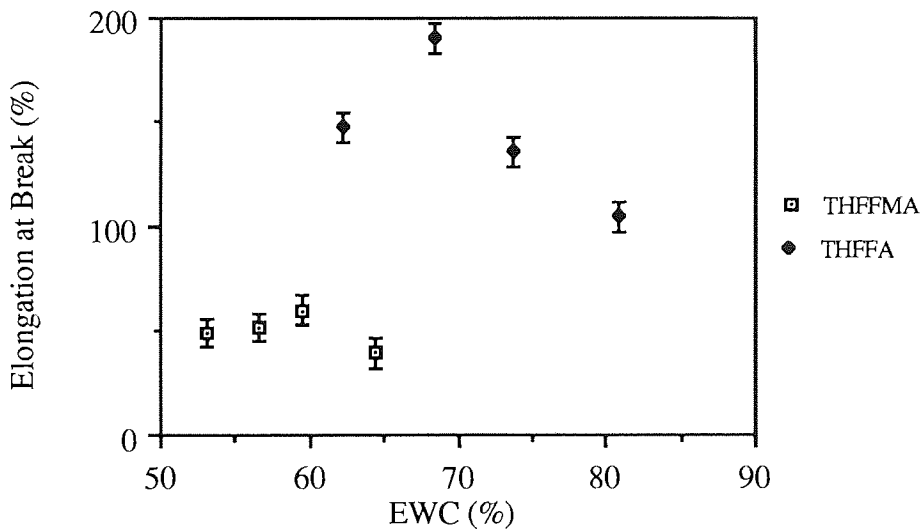


Figure 3.22 Effect of Water Content on the Elongation at Break
of 60 : 40 NVP : THFFMA / THFFA with CAB Semi-IPN'S

Elongations at break shown in figures 3. 19 - 3. 21 are somewhat difficult to interpret with samples giving a large spread of results. General trends show that THFFA containing samples showing superior elongations at break to those containing

THFFMA, this was observed in both sets of samples containing either 40% or 60% of NVP. The samples with a higher NVP concentration, (60%), showed lower elongations at break than samples with the lower concentration of NVP,(40%).

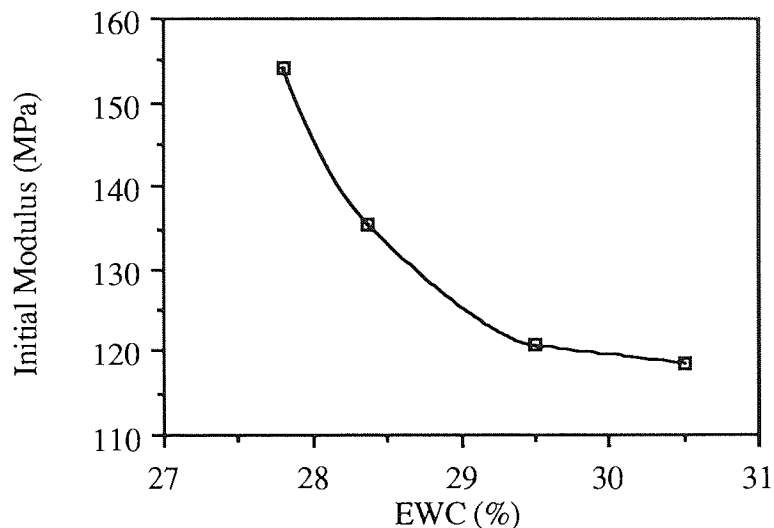


Figure 3.22 Effect of Water Content on the Initial Modulus of 60 : 40
NVP : Iso-bornyl MA with CAB Semi-IPN'S

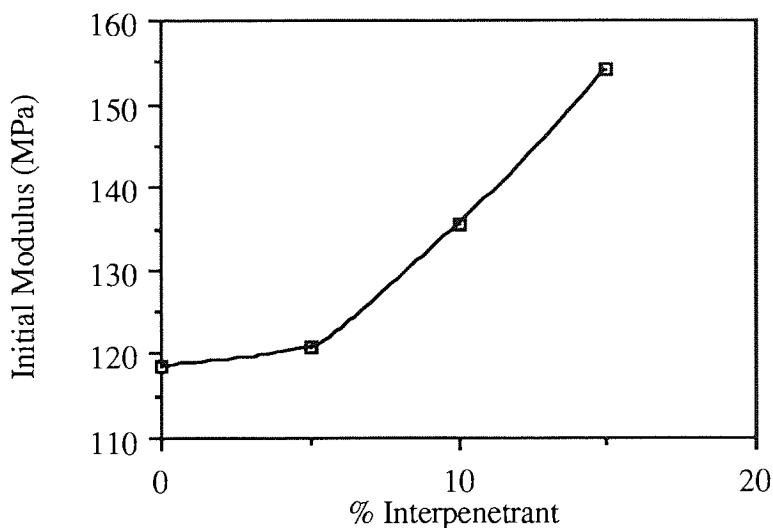


Figure 3.23 Effect of CAB Content on the Initial Modulus of 60 : 40
NVP : Iso-bornyl MA with CAB Semi-IPN'S

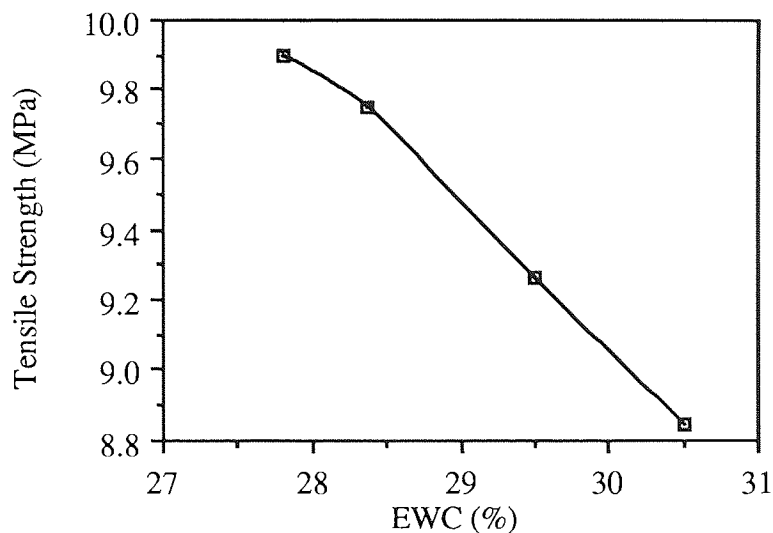


Figure 3.24 Effect of Water Content on the Tensile Strength of 60 : 40
NVP : Iso-bornyl MA with CAB Semi-IPN'S

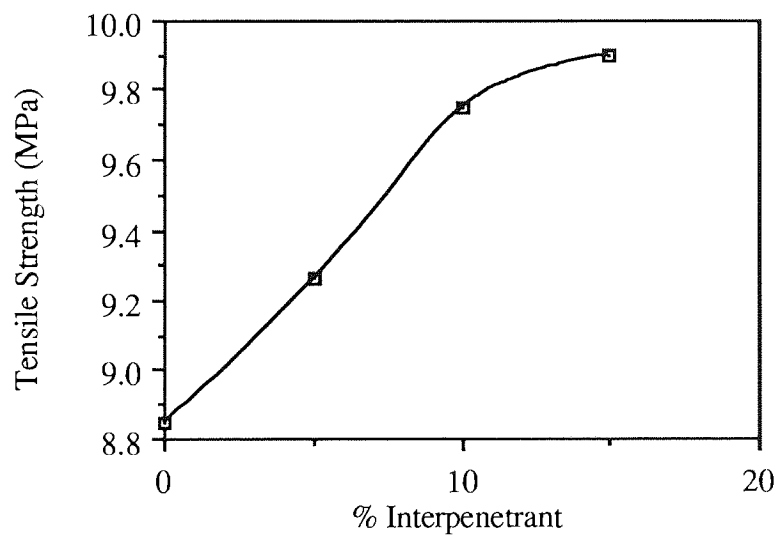


Figure 3.25 Effect of CAB Content on the Tensile Strength of 60 : 40
NVP : Iso-bornyl MA with CAB Semi-IPN'S

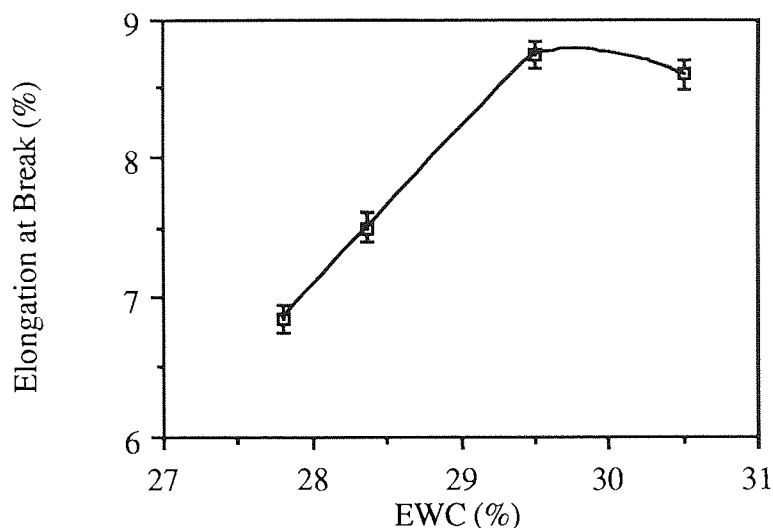


Figure 3.26 Effect of Water Content on the Elongation at Break of 60 : 40

NVP : Iso-bornyl MA with CAB Semi-IPN'S

Iso-bornyl methacrylate containing samples, shown in figures 3. 22 - 3. 26, show predicted patterns, increasing in initial modulus and tensile strength with a fall in EWC or an increase in CAB content. Elongation at break increased with increased EWC, however, the elongation at break is low with only a 3% span and differences could be attributed to experimental error. Alternatively as previously mentioned for simple copolymers with increased EWC, there is an increase in the amount of plasticising or non-freezing water, making the samples more flexible resulting in higher elongations.

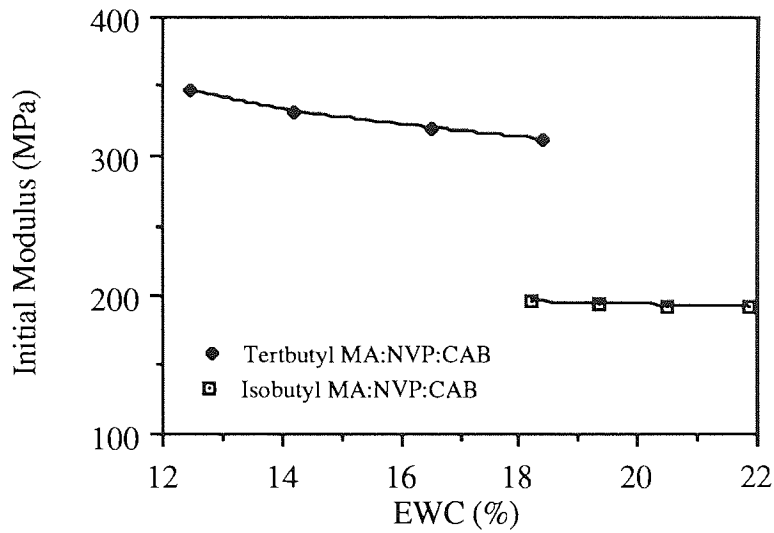


Figure 3.27 Effect of Water Content on the Initial Modulus of 40 : 60
NVP : Iso-butyl MA / Tert-butyl MA with CAB Semi-IPN'S

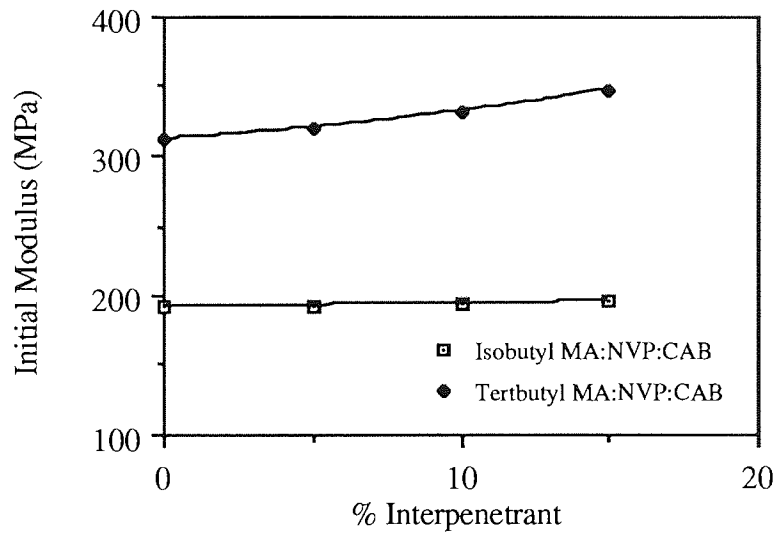


Figure 3.28 Effect of % Interpenetrant on the Initial Modulus of 40 : 60
NVP : Iso-butyl MA / Tert-butyl MA with CAB Semi-IPN'S

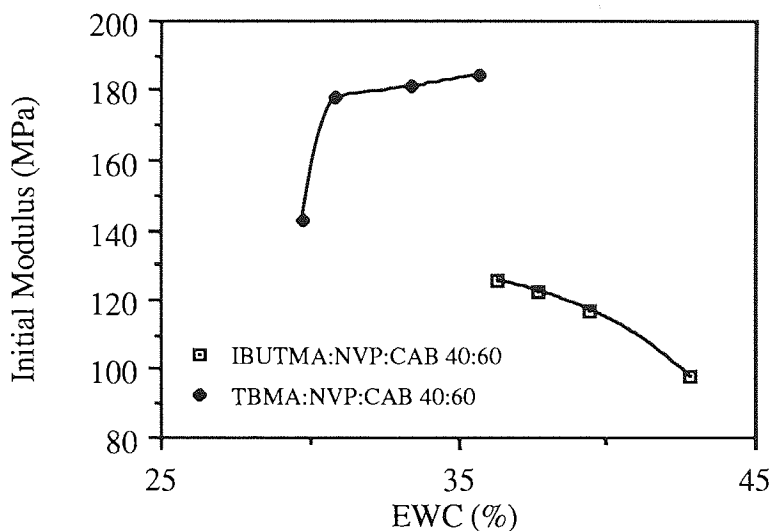


Figure 3.29 Effect of Water Content on the Initial Modulus of 60 : 40
NVP : Iso-butyl MA / Tert-butyl MA with CAB Semi-IPN'S

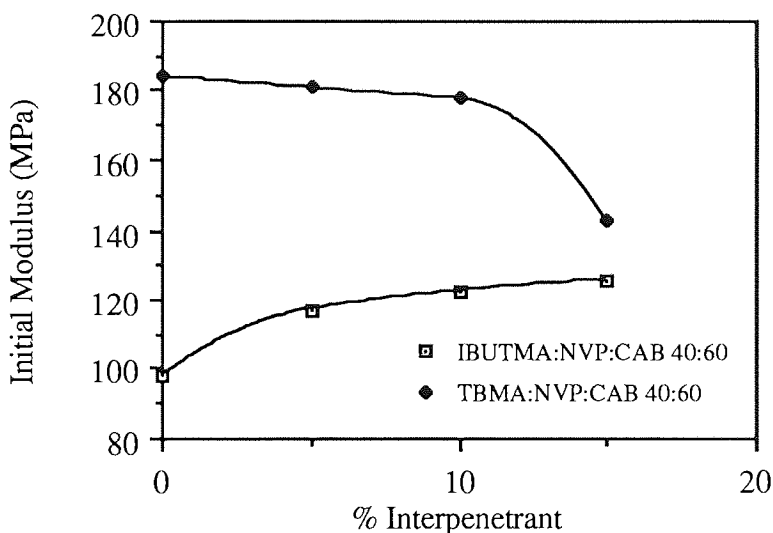


Figure 3.30 Effect of % Interpenetrant on the Initial Modulus of 60 : 40
NVP : Iso-butyl MA / Tert-butyl MA with CAB Semi-IPN'S

Figures 3. 27 - 3.30 compare the initial moduli of samples containing iso-butyl methacrylate and tert-butyl methacrylate. In all cases the tert-butyl methacrylate samples exhibit a greater initial modulus than those containing iso-butyl methacrylate. This is a direct result of the stereochemistry of the molecules. Although both butyl

methacrylates, the tert-butyl methacrylate arrangement produces a considerably stiffer material, resulting in a substantial increase in modulus. The increase in stiffness, observed with the tert-butyl methacrylate, is reflected in the higher glass transition temperature of this material. This is observed in tables 5. 3 and 5. 4, where a higher 'onset' or softening temperature is shown for the TBMA. In addition to the stiffening effect observed with the tert-butyl methacrylate, a lower EWC is also observed than with samples containing iso-butyl methacrylate. Once again this is attributed to the differing arrangements of the methyl groups within the molecules and shows how by careful choice of monomers, a wide range of properties can be achieved.

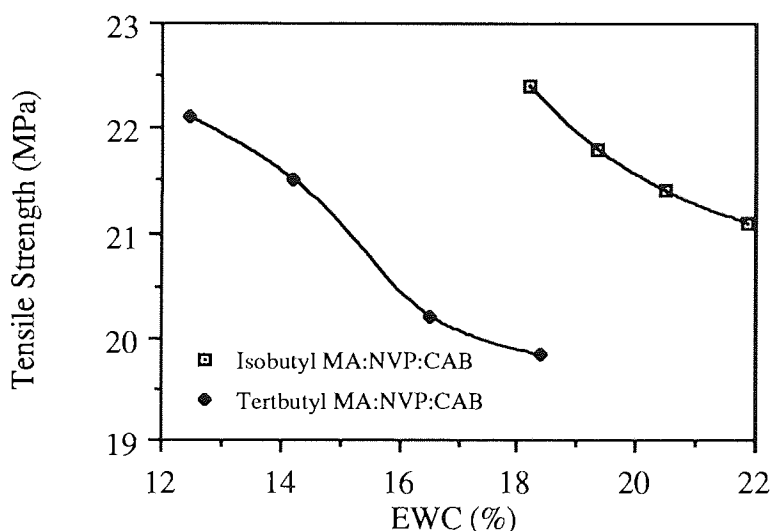


Figure 3. 31 Effect of Water Content on the Tensile Strength of 40 : 60
NVP : Iso-butyl MA / Tert-butyl MA with CAB Semi-IPN'S

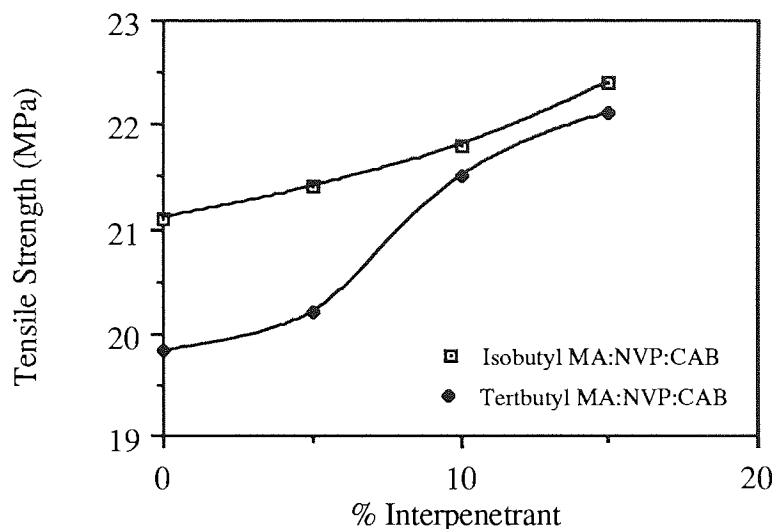


Figure 3.32 Effect of Interpenetrant Concentration on the Tensile Strength of 40 : 60 NVP : Iso-butyl MA / Tert-butyl MA with CAB Semi-IPN'S

Figures 3. 31 - 3.34 compare the relative tensile strengths of samples containing 60% iso-butyl methacrylate or tert-butyl methacrylate. In figures 3. 31 and 3. 32 the tensile strength of the iso-butyl methacrylate containing samples is shown to be greater than those containing tert-butyl methacrylate. This is connected to the relative stiffness of the two families of materials, the tert-butyl methacrylate containing samples that are stiffer and hence, appear to be more brittle yielding in a lower tensile strength. This is also reflected in the lower elongation at break of these samples, seen in figure 3.35.

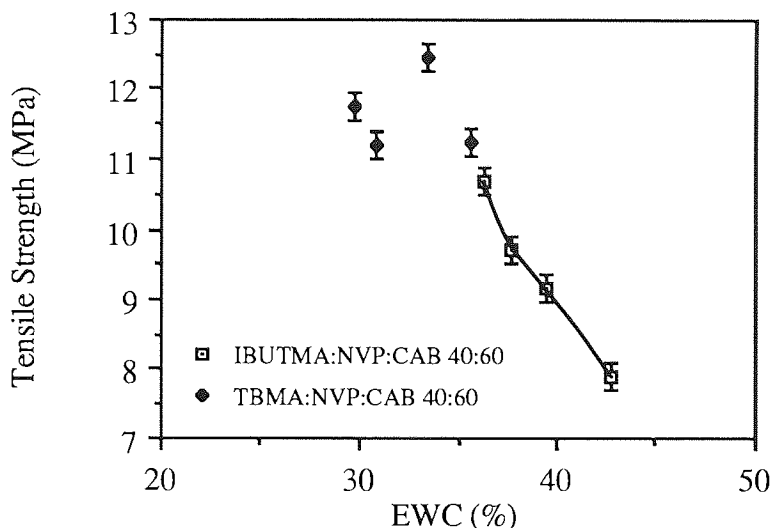


Figure 3.33 Effect of Water Content on the Tensile Strength of 60 : 40 NVP : Iso-butyl MA / Tert-butyl MA with CAB Semi-IPN'S

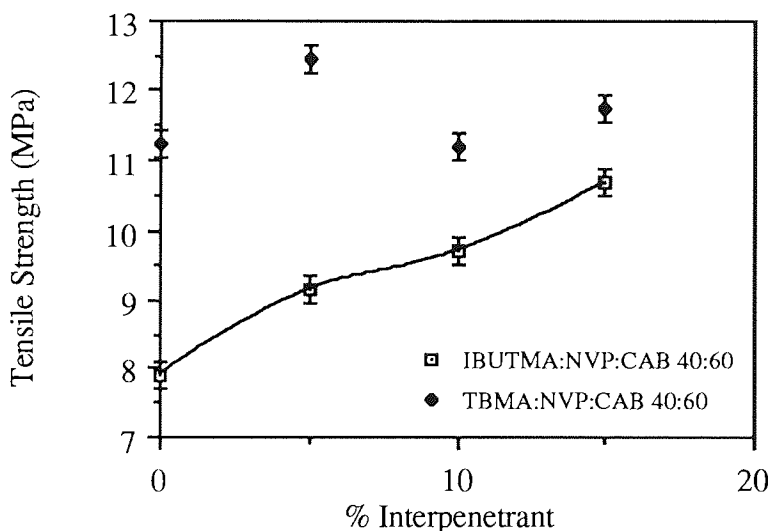


Figure 3.34 Effect of Interpenetrant Concentration on the Tensile Strength of 60 :40 NVP : Iso-butyl MA / Tert-butyl MA with CAB Semi-IPN'S

In figures 3. 33 and 3. 34, which contain less methacrylate, 40 %, and a greater proportion of hydrophilic NVP, the tensile strengths of TBMA containing samples are greater than those containing IBUTMA. This is attributed to the presence of a greater amount of plasticising water which makes the samples more flexible. This is

reflected in figure 3. 36, which shows that TBMA samples having greater values for elongation at break than samples with less water present. The link between tensile strength and elongation at break can be made by looking at figures 3. 33 and 3. 36, where it is seen that the lower the tensile strength the lower the elongation at break.

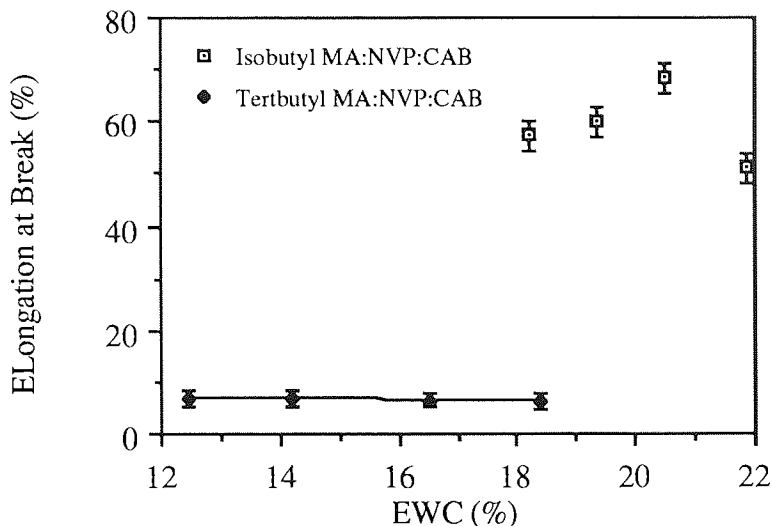


Figure 3.35 Effect of Water Content on the Elongation at Break of 40 : 60
NVP : Iso-butyl MA / Tert-butyl MA with CAB Semi-IPN'S

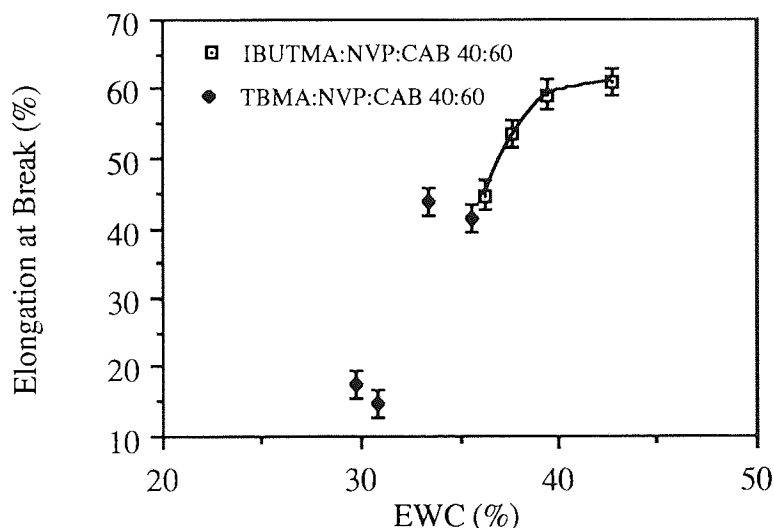


Figure 3.36 Effect of Water Content on the Elongation at Break of 60 : 40
NVP : Iso-butyl MA / Tert-butyl MA with CAB Semi-IPN'S

Figures 3. 35 and 3. 36 show the effect of the equilibrium water content on the elongation at break of samples containing either iso-butyl methacrylate or tert-butyl

methacrylate, in conjunction with N-vinyl pyrrolidone and cellulose acetate butyrate. The elongation is shown to be low in both cases. It is noted that a low EWC is exhibited by the samples. However, if tetrahydrofurfuryl methacrylate samples, seen in figure 3. 20, having similar EWC, are compared to the butyl containing samples, the elongation of these samples is considerably less. This is a direct result of the stiff butyl group being present causing a reduction in the flexibility of these samples.

3. 3 Water Binding Properties of Hydrogels

The equilibrium water content of a hydrogel is its single most important property. However, the various states in which the water may exist in the gel will also influence its properties.

The equilibrium water contents of hydrogel copolymers follow an expected trend. THFFA copolymers have higher EWC's than THFFMA copolymers, due to the hydrophobic nature of the extra methyl group present in THFFMA. Iso-bornyl methacrylate copolymers have the lowest EWC's because these systems have no hydrophilic oxygen atom in the ring, unlike the THFFMA and THFFA. As previously stated in section 3. 2, lower freezing or plasticising water results in a higher initial Young's modulus and reduced elongations, attributed to samples that become so rigid they tend to be brittle.

Water binding studies were carried out using the differential scanning calorimeter, commonly abbreviated to DSC. DSC proves to be a useful technique in providing information on water binding in that small samples are used, the samples are sealed, which minimises the loss of water from within the sample, it is quick and can provide detailed crystallisation and water structuring information, obtained from the melting endotherms. The structure of the water in the polymer is dependent on hydrophilic / hydrophobic interactions in the copolymer system and the water structuring groups present in the monomers. Endotherms often showed more than one peak. Temperature cycling, giving a redistribution of freezing water, often changed these

peaks. The complexity of some of the endotherms that were observed supports the hypothesis that the water in hydrogels exists in a continuum of states, between freezing and non-freezing. Water with a freezing point less than pure water is considered by some workers to be interfacial water, which is not bonded strongly to the hydrophilic groups in the polymer chain but does interact either with the polymer chain or the water strongly bound to the chain. This suggests that not all freezing water is unaffected by the polymeric environment.

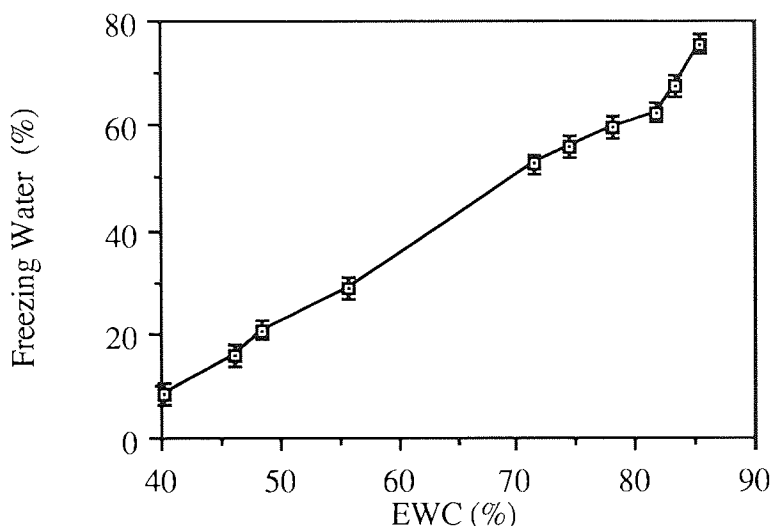


Figure 3.37 Water Binding Properties of NVP : Methacrylate Hydrogel Copolymers

The total amount of water in hydrogels is related to the balance of hydrophilic and hydrophobic components and the steric and polar contributions of backbone substituents³. It appears from looking at figure 3. 37 that in hydrogel copolymers, the freezing water content is dependent upon the equilibrium water content and not necessarily on the chemical structure of the monomers that they contain. Experiments show that it is not only straight forward hydrogel copolymers that observe this principle but the semi-interpenetrating networks made with cellulose acetate butyrate investigated in this work also appear to do so. This phenomenon can be seen in figure 3. 38. However, only samples used in this study were tested so this theory may not be universally true.

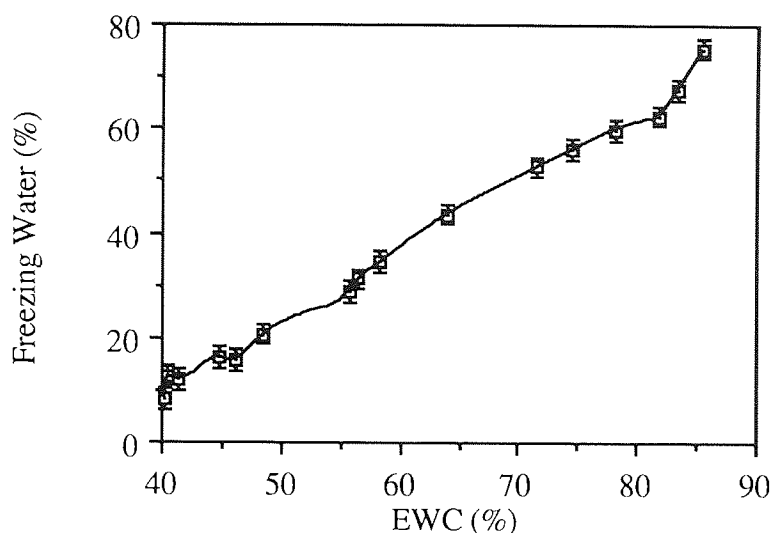


Figure 3. 38 Freezing Water Content for NVP : Methacrylate : CAB Semi-IPN's

The EWC's of methacrylate/acrylate with NVP systems was studied and the order of hydrophilicity of the various methacrylates or acrylate was deduced. THFFA was found to be the most hydrophilic of the materials used throughout this work, followed by THFFMA, iso-bornyl MA, iso-butyl MA and, finally the most hydrophobic material, tert-butyl MA.

3. 4 Surface Properties of Hydrogels

A major use for hydrogel materials is in the biomedical field, where intimate contact with body fluids or tissue occurs. As the surface energy of a polymer is thought to be important in determining its interactions with a biological environment, it is interesting to note the factors which control the surface free energy of these materials.

3.4.1 Dehydrated Surface Properties

Studying the surface properties of hydrogels in the dehydrated state enables the monomer structure to be observed. However, when testing dehydrated materials, especially those which are extremely hydrophilic, hydration rapidly occurs both in air and when water is used as a wetting liquid in the sessile drop technique. This causes

problems in obtaining accurate results, as the readings taken may be results from a partially hydrated sample.

The measured surface energies are a function of both the interactions within the bulk polymer and at the surface. The measured surface free energy is affected by the orientation of the surface groups, which may in turn depend on the polarity of the adjacent phase.

Results are presented in the form of surface free energy versus methacrylate / acrylate or interpenetrant concentration.

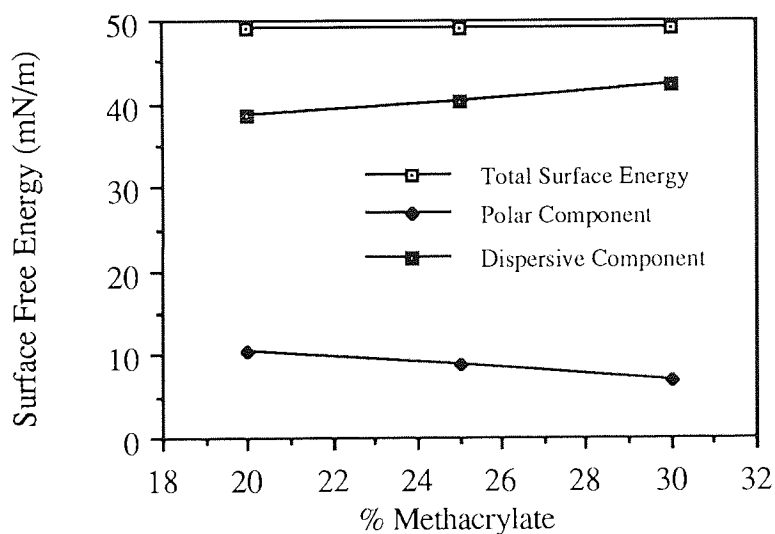


Figure 3.39 Effect of Methacrylate Content on the Surface Free Energy in Dehydrated NVP : Tetrahydrofurfuryl Methacrylate Copolymers

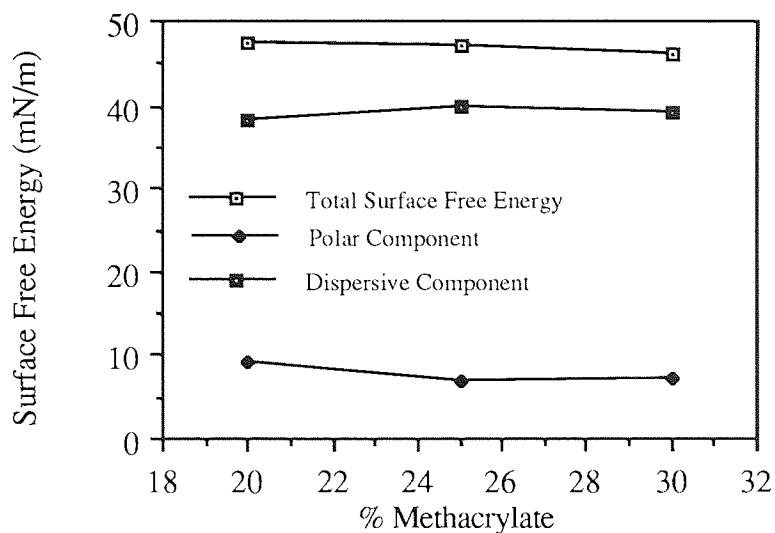


Figure 3.40 Effect of Methacrylate Content on the Surface Free Energy in Dehydrated NVP : Tetrahydrofurfuryl Acrylate Copolymers

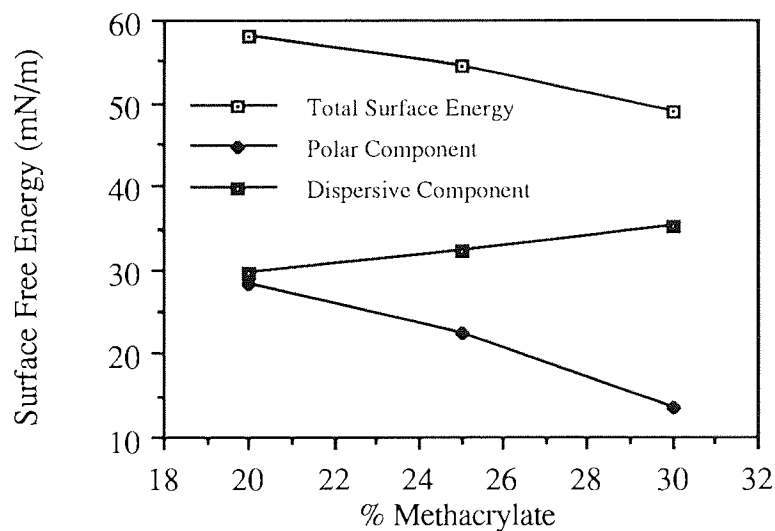


Figure 3.41 Effect of Methacrylate Content on the Surface Free Energy in Dehydrated NVP : Iso-bornyl Methacrylate Copolymers

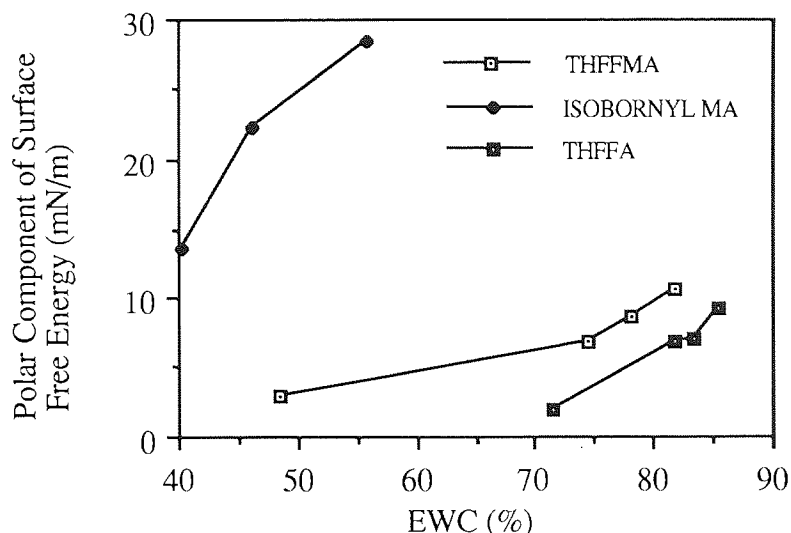


Figure 3.42 Effect of Equilibrium Water Content on the Polar Component of Surface Free Energy for Dehydrated Hydrogel Copolymers

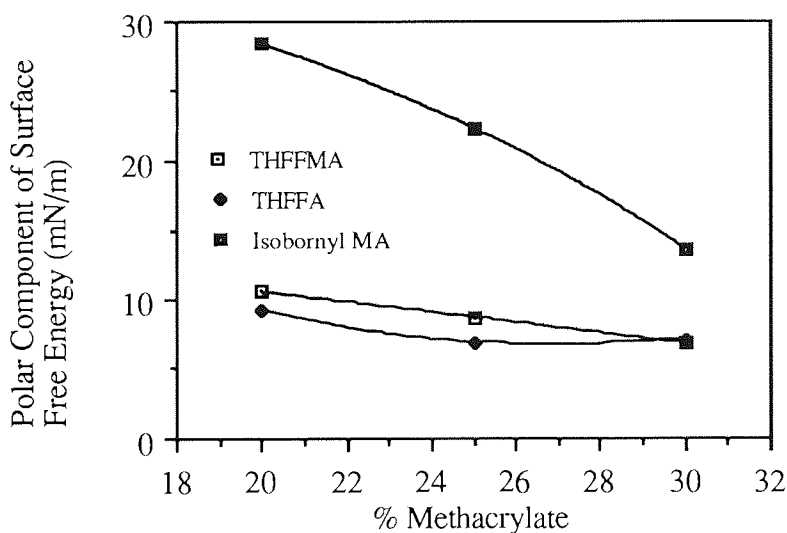


Figure 3.43 Effect of Methacrylate Content on the Polar Component of Surface Free Energy for Dehydrated Hydrogel Copolymers

In hydrogel copolymers the total surface free energy appears to increase with an increase in equilibrium water content, or with increasing amounts of hydrophilic component, NVP. In all samples the dispersive component is the dominating component in the dehydrated system. There is also an increase in the polar component of surface free energy associated the increase in EWC. This is most

pronounced in the iso-bornyl : NVP copolymer samples, as can be seen in figure 3.13. It would also be expected that the THFFA copolymers would have a higher polar component of surface free energy than the THFFMA copolymers, due to the higher equilibrium water content, however this is not the case. THFFA has a low glass transition temperature and hence a low energy to rotation, enabling chains to 'flip' freely. It appears that in this case the polar groups arrange themselves inwardly, giving a low polar component of surface free energy. It has also been shown that surface properties of acrylates are unpredictable. In samples containing THFFMA, chain rotation is restricted, this is due to the sterically hindering α -methyl group on the backbone chain. This reduces the likelihood of chains rearranging themselves, and appears to give a surface which is more random with some polar groups inward and some outward.

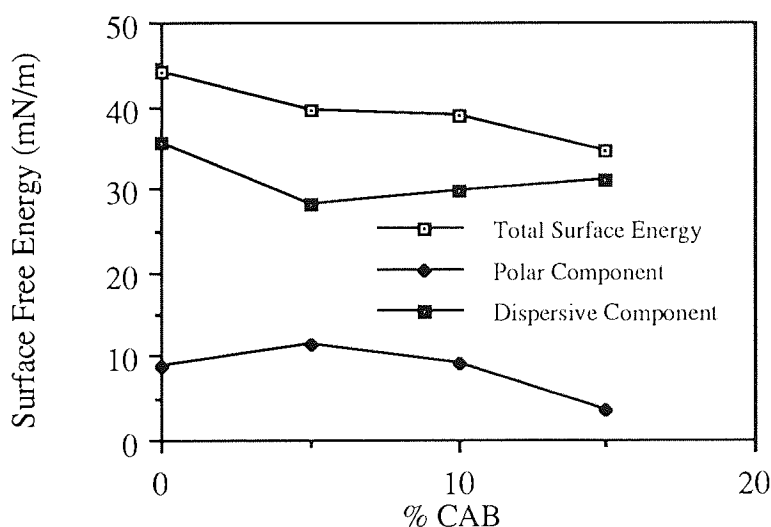


Figure 3.44 Effect of CAB Content on the Surface Free Energy in Dehydrated 40:60 NVP : Tetrahydrofurfuryl Methacrylate with CAB Semi-IPN's

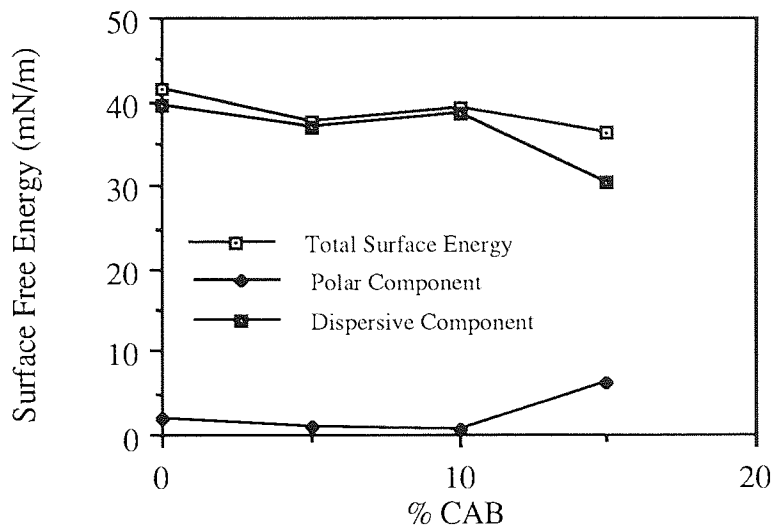


Figure 3.45 Effect of CAB Content on the Surface Free Energy in 40 : 60
Dehydrated NVP : Tetrahydrofurfuryl Acrylate with CAB Semi-IPN's

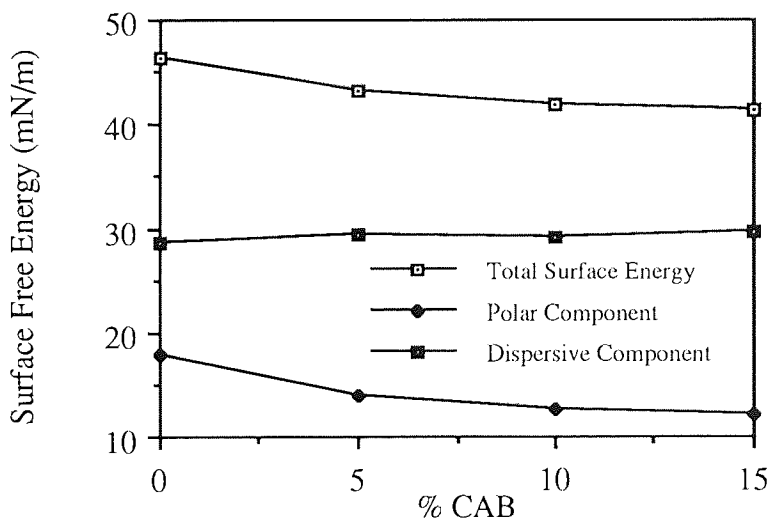


Figure 3.46 Effect of CAB Content on the Surface Free Energy in 40 : 60
Dehydrated NVP : Tert-butyl Methacrylate with CAB Semi-IPN's

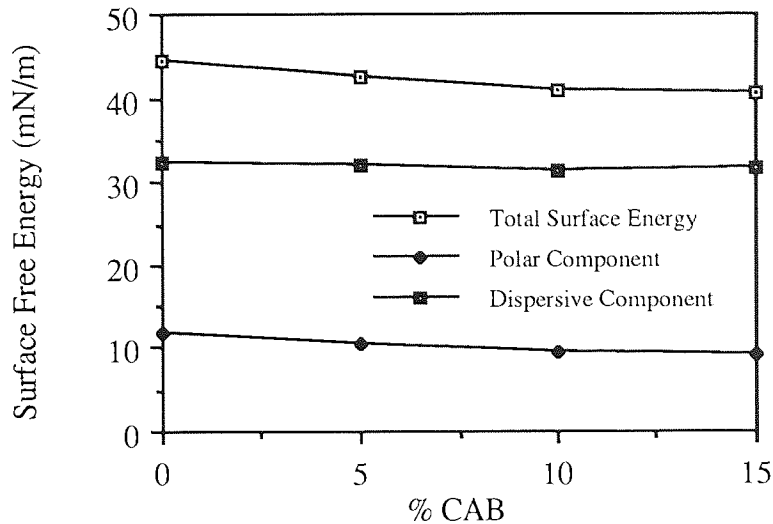


Figure 3.47 Effect of CAB content on the Surface Free Energy in 40 :60
Dehydrated NVP : Iso-butyl Methacrylate with CAB Semi-IPN's

Surface energies of semi-IPN's containing cellulose acetate butyrate are in a similar region to the simple hydrogel copolymers of a similar equilibrium water content, somewhere between 40-50 mN/m. However, in semi-IPN's the filler polymer within the matrix, together with the copolymer in which it is dissolved, will influence the surface properties. A lower equilibrium water content is observed with an increasing amount of cellulose acetate butyrate. This filler polymer has a lower concentration of polar groups which manifests itself as a lower surface free energy when an increasing amount of CAB is incorporated. Once again the total surface energy is dominated by the dispersive component.

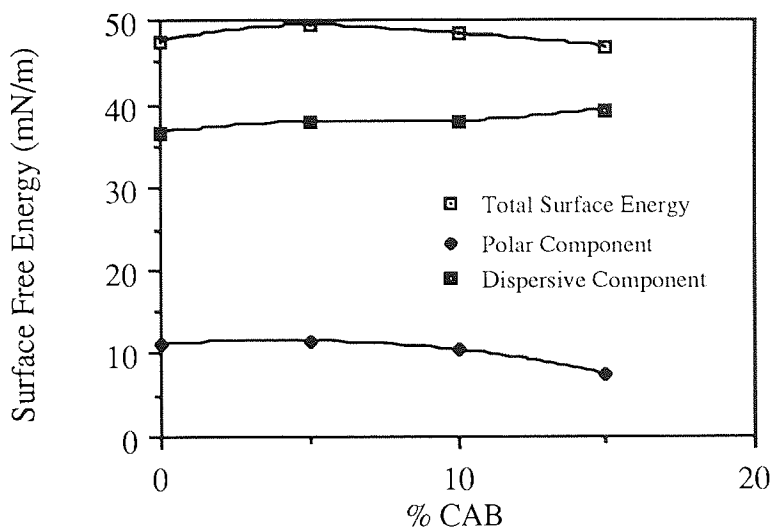


Figure 3.48 Effect of CAB Content on the Surface Free Energy in Dehydrated 60 : 40 NVP : THFFMA with CAB Semi-IPN's

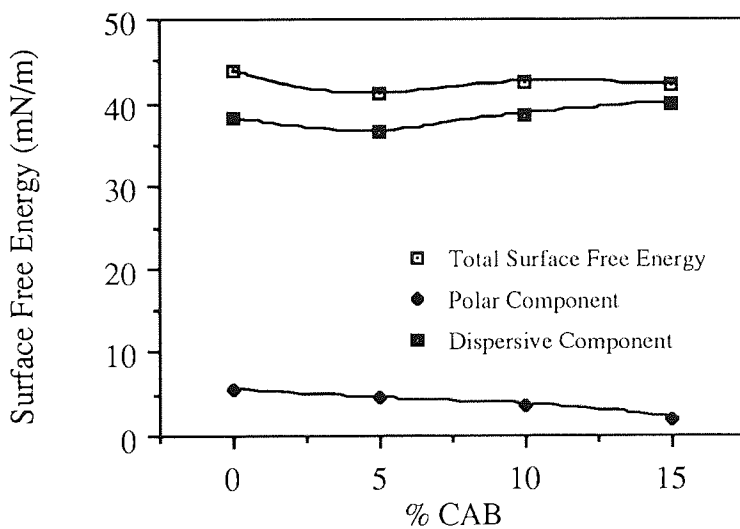


Figure 3.49 Effect of CAB Content on the Surface Free Energy in Dehydrated 60 : 40 NVP : THFFA with CAB Semi-IPN's

Figures 3. 48 and 3. 49 show, as expected, a small increase in the polar component of surface free energy with samples that contain equal percentages of CAB but have an increased amount of NVP. This has the effect of increasing the EWC of the samples and hence the polarity.

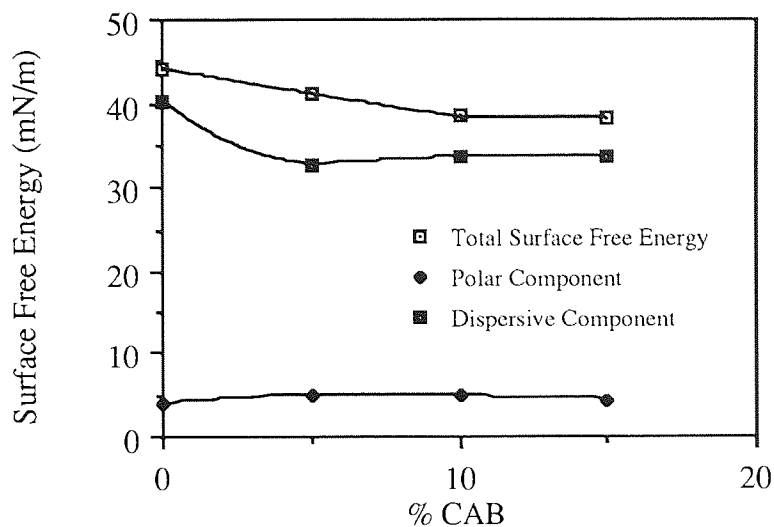


Figure 3.50 Effect of CAB Content on the Surface Free Energy in Dehydrated 60 : 40 NVP : TBMA with CAB Semi-IPN's

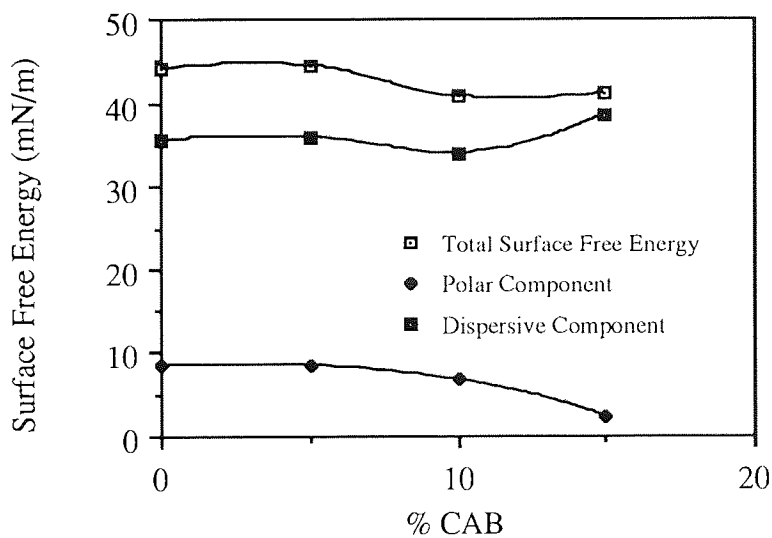


Figure 3.51 Effect of CAB Content on the Surface Free Energy in Dehydrated 60 : 40 NVP : IBUTMA with CAB Semi-IPN's

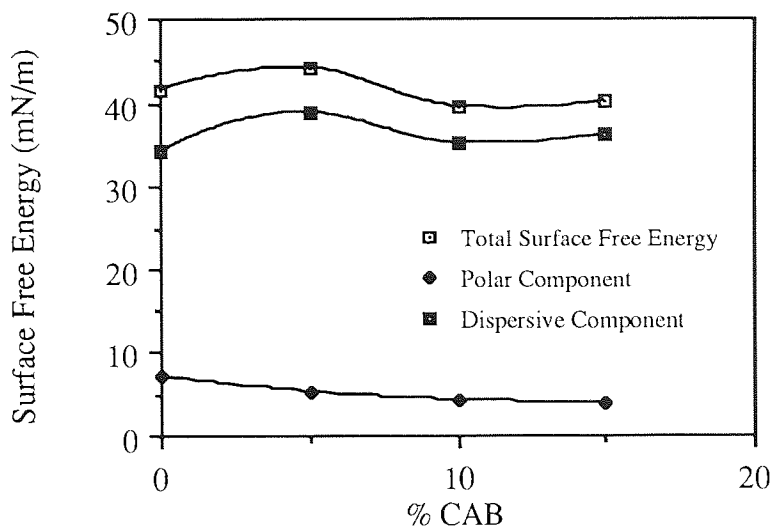


Figure 3.52 Effect of CAB Content on the Surface Free Energy in Dehydrated 60 : 40 NVP : IBMA with CAB Semi-IPN's

Comparing figures 3. 44 and 3. 45 with 3. 48 and 3. 49 respectively, show how changing the ratio of THFFMA / THFFA : NVP affects the surface properties. Increasing the EWC or % NVP in the system again increases the polar component of surface free energy and consequently the total surface free energy. This is not observed in butyl containing samples, in figures 3. 46 and 3. 47, where there is a lower concentration of NVP, 40%, in the samples. Here, the polar component of surface free energy is seen to be slightly lower than those samples containing 60% NVP, figures 3. 50 and 3. 51. However, the difference is very slight and may be due to experimental error.

3.4.2 Hydrated Surfaces Properties

A way of overcoming the problems of hydration which are associated with dehydrated contact angles is to use the polymers in their hydrated state. By using Hamilton's and the captive air bubble technique, an attempt was made to determine the factors involved in the control of surface properties. Although, by using hydrated samples the problems of hydration are overcome, there are problems associated with measurement of angles on hydrated samples. Measurement of contact angles using

an inverted bubble technique is the most difficult type of contact angle to measure correctly since it involves judging where the base of a distorted sphere just impinges on a surface. Furthermore, surfaces of hydrogels may retain a strongly adsorbed water layer at the surface, thereby, dominating the measurements made. Wetting angles of materials with similar water contents may therefore be expected to be similar.

Surface energies of hydrogels in the hydrated state are considerably higher than those in the dehydrated state. This is due to the surface energy of water being higher than those of polymers.

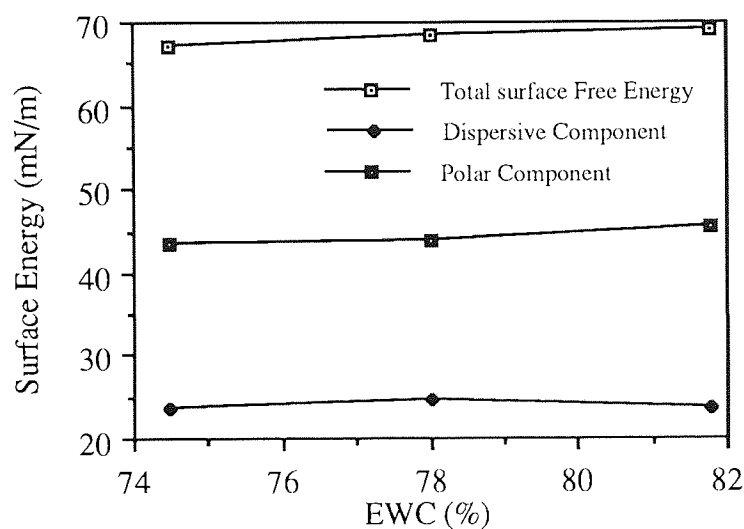


Figure 3.53 Effect of Water Content on the Surface Free Energy in Hydrated NVP: Tetrahydrofurfuryl Methacrylate Copolymers

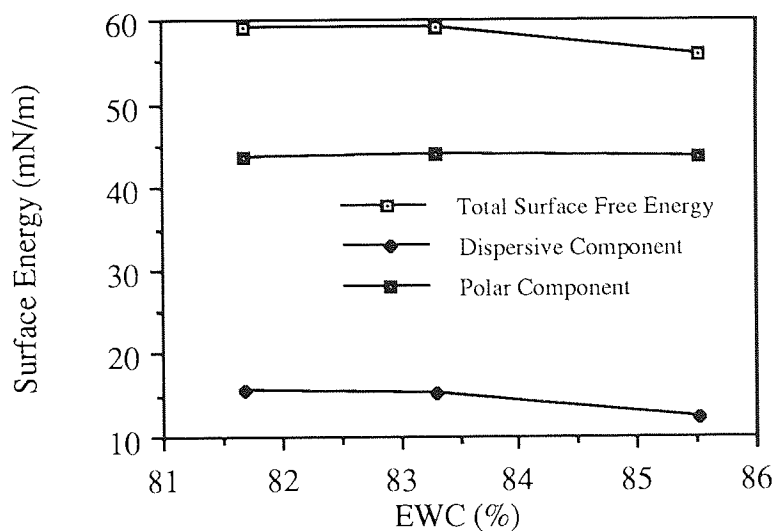


Figure 3.54 Effect of Water Content on the Surface Free Energy in Hydrated NVP : Tetrahydrofurfuryl Acrylate Copolymers

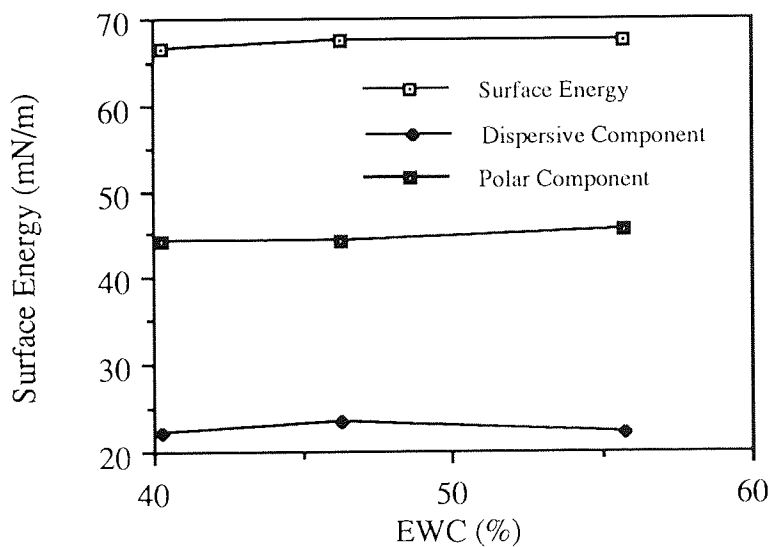


Figure 3.55 Effect of Water Content on the Surface Free Energy in Hydrated NVP : Iso-bornyl Methacrylate Copolymers

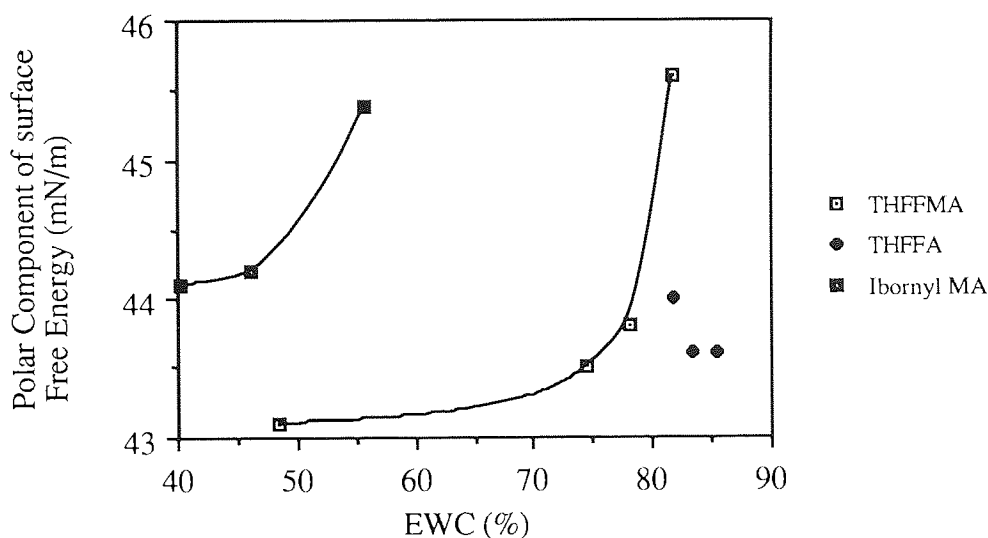


Figure 3.56 Effect of Water Content on the Polar Component of Surface Free Energy in Hydrated NVP : Methacrylate Copolymers

In THFFMA/THFFA:NVP copolymers, the surface energies are in the same region as materials Corkhill synthesised with similar equilibrium water contents³. Equilibrium water content is one of the major controlling factors with surface free energy. In general, systems with an increase in EWC tend to give an increase in surface free energy. However, iso-bornyl methacrylate copolymers, although lower in water content than the THFFMA and THFFA copolymers, have a similar surface free energy. This may be due to the nature of the copolymer structures. Both with and without the presence of water, the IBMA:NVP systems are optically incompatible. This is shown in the white colouring exhibited by the samples when dehydrated and hydrated. However, when hydrated the plasticising water, being the low molecular weight component, detaches itself and migrates to the interface. Hence, a high water content surface results, giving a surface free energy comparable to that of an optically compatible copolymer, such as NVP : THFFMA, which has higher equilibrium water content. The surface free energy of THFFA : NVP copolymers are lower than expected, which is thought to be due to the arrangement of the polymer chains at the surface, polar groups facing inward. However, in all of the samples except NVP : THFFA, as seen in figure 3. 54, typical trends are followed, with increasing amounts of NVP, or EWC, the total surface free energy and polar

component increase, while the dispersive component decreases. In the NVP : THFFA sample the total surface free energy appears to follow the predicted pattern until the point at the highest water content. This is in relation to the large drop in the dispersive component. This may just be an experimental error. As previously mentioned contact angles are hard to measure accurately and as this sample follows all the predicted patterns until this point, it is thought that this is what has occurred in this instance.

Figure 3. 56, shows the effect of equilibrium water content on the polar component of surface free energy, although with NVP : THFFA copolymers, the polar component points are very close. The THFFMA and iso-bornyl methacrylate copolymers show the expected trend, i. e. with increasing equilibrium water content the polar component of surface free energy increases.

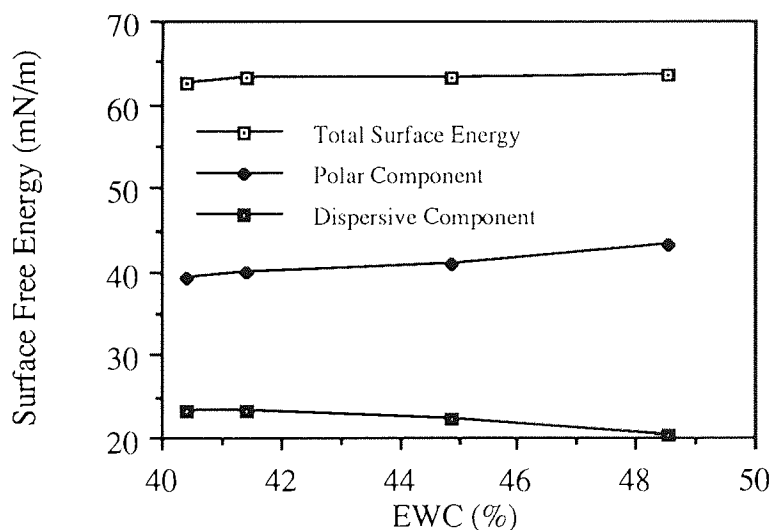


Figure 3.57 Effect of Water Content on the Surface Free Energy in Hydrated 40 : 60 NVP : Tetrahydrofurfuryl Methacrylate with CAB semi-IPN's

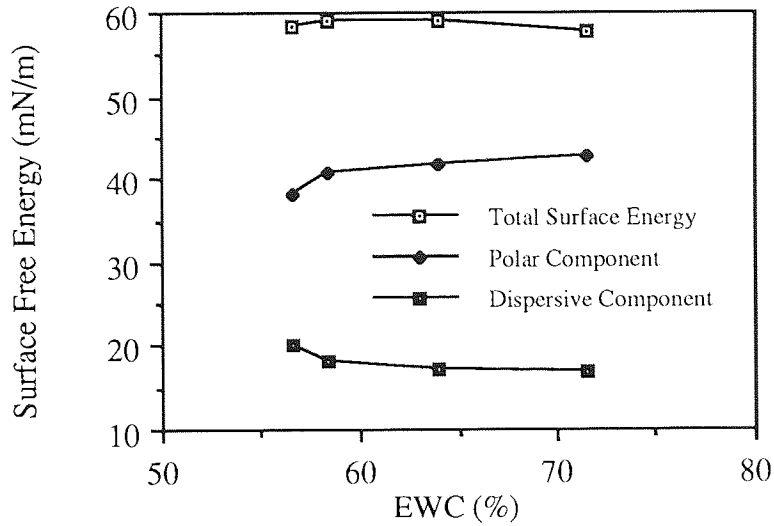


Figure 3.58 Effect of Water Content on the Surface Free Energy in Hydrated 40 : 60 NVP : Tetrahydrofurfuryl Acrylate with CAB semi-IPN's

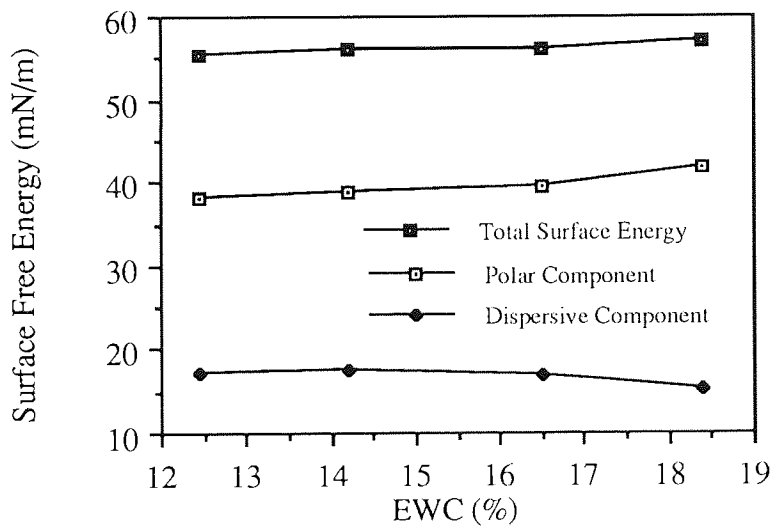


Figure 3.59 Effect of Water Content on the Surface Free Energy in Hydrated 40 : 60 NVP : Tert-butyl Methacrylate with CAB semi-IPN's

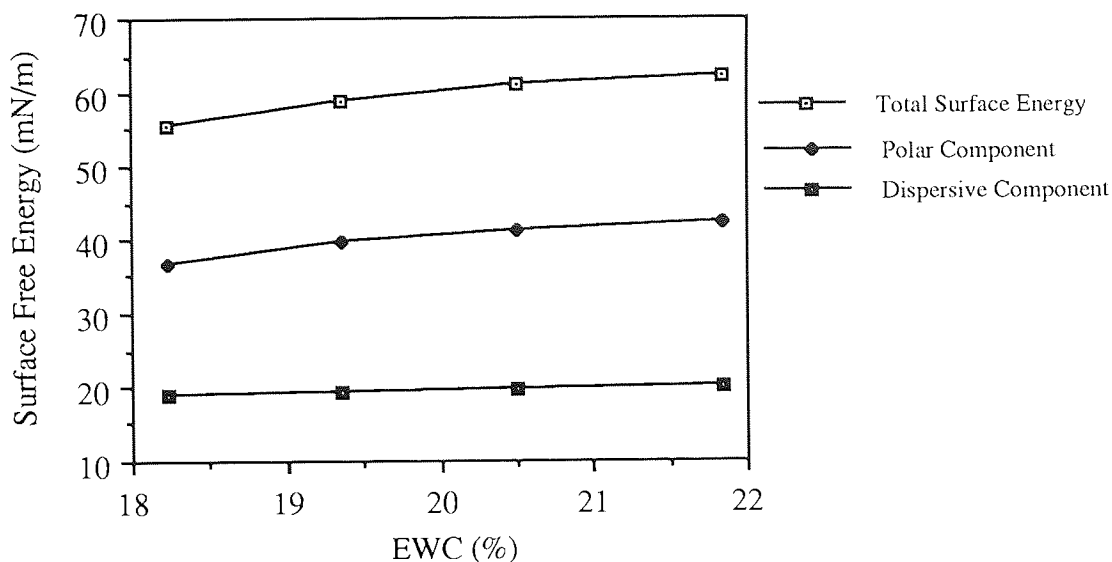


Figure 3.60 Effect of Water Content on the Surface Free Energy in Hydrated 40 : 60 NVP : Iso-butyl Methacrylate with CAB semi-IPN's

Once again the surface energies of the semi-IPN's are in the regions expected if related to their EWC. However, trends follow in a predicted manner, i. e. with an increasing amount of CAB, the total surface free energy decreases, the polar component decreases and the dispersive component increases. Although equilibrium water content is one of the major controlling factors in controlling surface free energy, and appears to be the overriding factor in the examples discussed here, structural changes in the semi-IPN's may also effect the surface energies. In addition the proportion of this energy which is dispersive and the proportion which is polar may also be effected. Although there are difficulties in accurately measuring hydrated contact angles, the technique shows how small surface changes can be detected.

3. 5 Oxygen Permeabilities

The oxygen permeability used in this work is given as Dk , and is calculated from equation 2. 9 given in Chapter 2. The units of Dk are $\times 10^{-11} \text{cc mm}/(\text{cm}^2 \text{ s cm Hg})$.

High oxygen permeabilities have been attributed to bulky side chains, therefore, the effect of the copolymers and semi-IPN's containing cyclic methacrylates was interesting to note.

The oxygen permeabilities of hydrogel materials are harder to determine than very low water content materials because problems are associated with dehydration of the samples. Although the samples are in contact with a potassium chloride saturated lens tissue, a constant stream of gas is passing through. This appears to dehydrate the samples, hence results may be of partly dehydrated samples. If dehydration of the samples occurred results may be lower than expected for samples with high equilibrium water content.

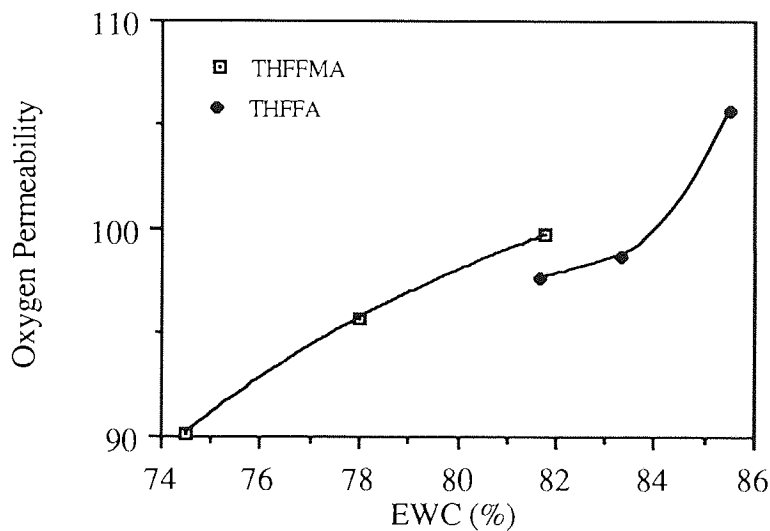


Figure 3.61 Relationship Between Oxygen Permeability and EWC in THFFMA / THFFA : NVP Hydrogels

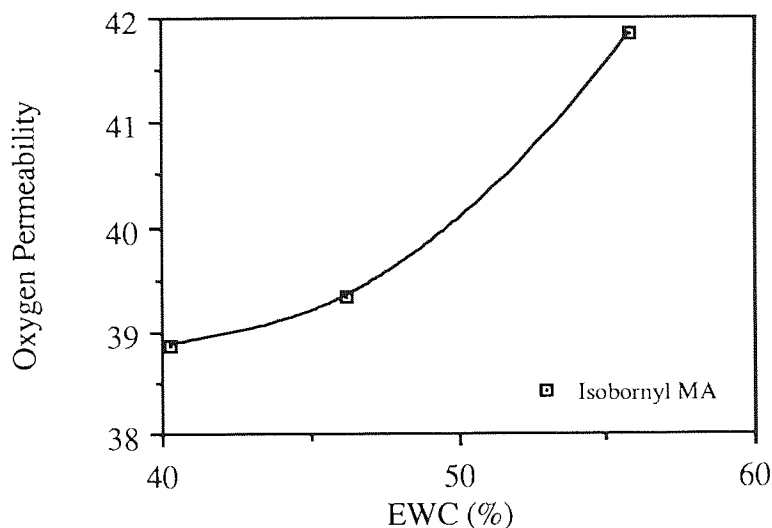


Figure 3.62 Relationship Between Oxygen Permeability and EWC in Iso-bornyl MA : NVP Hydrogels

Hydrogel samples behave in a predicted manner, with an increase in equilibrium water content showing an increase in oxygen permeability. In figure 3. 61, a direct relationship of EWC and oxygen permeability can be seen. At an EWC of approximately 82%, the oxygen permeability in both the THFFMA : NVP and the THFFA : NVP copolymers is in the high nineties. This could be due to the similarities in the THFFMA and the THFFA structures, having only an α -methyl group present in the THFFMA that is not present in the THFFA. The THFFMA containing samples had a slightly higher oxygen permeability at an EWC of 82%, than the THFFA samples. This was again due to the bulkier structure which resulted from the α -methyl group present in the THFFMA samples. It would be interesting to see if other samples with a similar EWC had similar oxygen permeabilities or if structure would effect results.

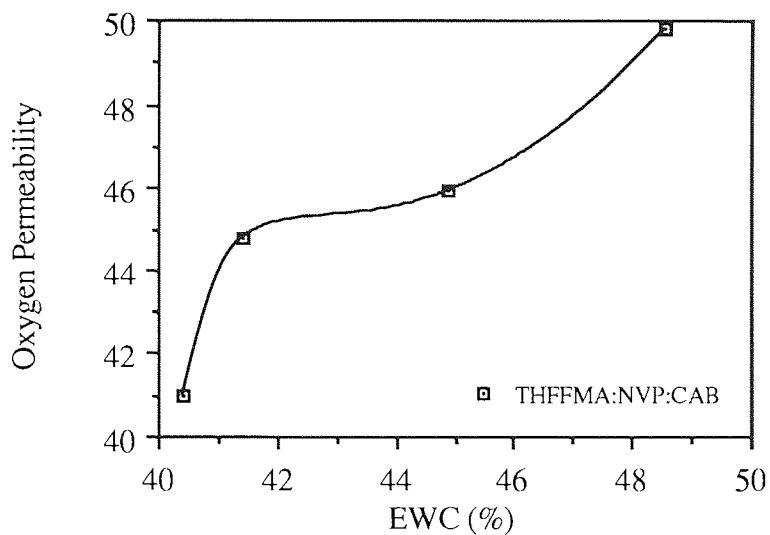


Figure 3.63 Relationship Between Oxygen Permeability and EWC in 60 : 40 THFFMA : NVP with CAB Semi-IPN's

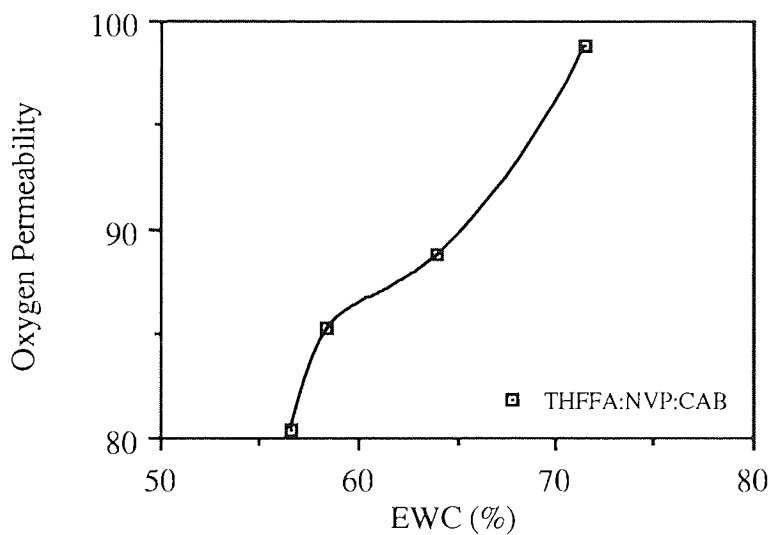


Figure 3.64 Relationship Between Oxygen Permeability and EWC in 60 : 40 THFFA : NVP with CAB Semi-IPN's

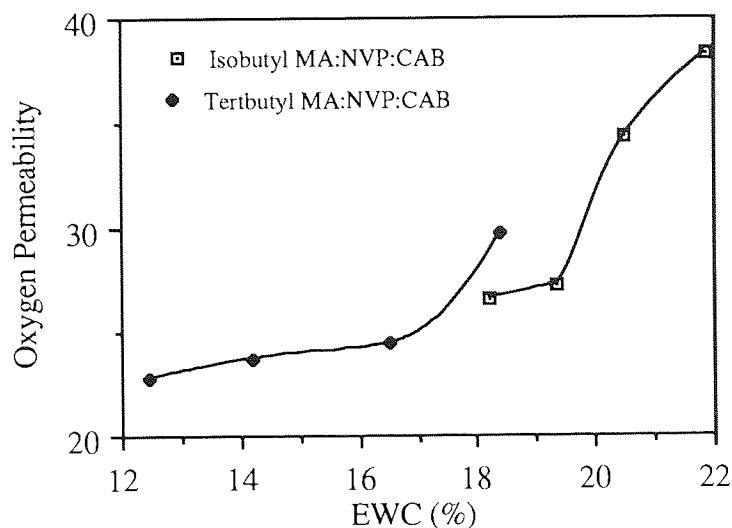


Figure 3.65 Relationship Between Oxygen Permeability and EWC in 60 : 40 Iso-butyl / Tert-butyl MA : NVP with CAB Semi-IPN's

Once again with the semi-IPN samples the oxygen permeability and EWC are related, one increasing with respect to the other. As with simple hydrogel copolymers, semi-IPN's at a given EWC have similar oxygen permeabilities for several systems. This can be seen in figure 3. 65, with tert-butyl methacrylate and iso-butyl methacrylate semi-IPN's. At a water content of 18%, both systems have similar oxygen permeabilities, between 26 and $29 \times 10^{-11} \text{cc mm} / (\text{cm}^2 \text{ s cm Hg})$. TBMA containing samples having a slightly higher oxygen permeability at a similar EWC due to the bulkier side chain. No deduction from these results can be made as to the effect of the structure further than to say that the more water in the system, the higher the oxygen permeability. However, the amount of water in a system can be attributed directly to the structure of the components it contains. It was thought that incorporating CAB into the system, with its bulky nature, may increase the spacing between polymer chains and hence the oxygen permeability. However, this is not the case. As previously mentioned incorporation of this material causes a decrease in EWC, which in turn lowers the oxygen permeability, thus any beneficial effects due to the bulky nature of CAB is offset by this decrease.

3.6 General Conclusions

This Chapter focuses on the development of simple hydrogel copolymers using novel methacrylates and acrylates and semi-IPN's using an established interpenetrant, CAB. Simple systems such as these provide a basis for future work on more complex systems. By noting the strengths and weaknesses of various systems, improvements in specific areas can be made whilst retaining the desirable properties that these materials exhibit.

3.6.1 Effect of Monomer Structure on Properties of NVP Containing Hydrogels

Polymer properties are affected by the structure of the comonomer used with NVP in the production of hydrogels. This is illustrated throughout this chapter. Changes in equilibrium water content, tensile strength, Young's modulus, surface energies and oxygen permeabilities are observed when different comonomers are used.

The EWC of hydrogel systems is dependent on the hydrophilicity / hydrophobicity and the steric and polar contributions of the comonomer. It is no wonder that the most hydrophobic material used was found to be tert-butyl methacrylate, followed by iso-butyl methacrylate, iso-bornyl methacrylate, tetrahydrofurfuryl methacrylate, with the most hydrophilic being tetrahydrofurfuryl acrylate. This was reflected the EWC's the various systems exhibited. In this work the water binding properties were found to be dependent on the EWC rather than polymer structure.

Increasingly hydrophobic, sterically hindered systems produced increasingly stiffer materials. This was reflected in the Young's modulus of the systems. Tensile strength and elongation at break were found to dependent on each other, increasing with respect to each other. The exception is observed with low freezing water content systems. In these materials there is little plasticising water which caused samples to exhibit low elongations. Systems containing more polar components,

such as THFFMA and THFFA, had lower mechanical properties than expected. This was explained by the water in the hydrogel system hydrating these polar materials, in a similar manner to the hydration of pHEMA, resulting in reduction of glass transition temperature, which was reflected in the low Young's modulus.

This study showed that a range of mechanical properties can be achieved at a given EWC by simply changing the structure of the comonomer in the system.

Surface properties of hydrogel copolymers did not differ greatly. A small decrease in the total surface free energy was observed with an increasing amount of methacrylate concentration in the systems.

3.6.2 Effect of CAB as an Interpenetrant on Properties of NVP Methacrylate/Acrylate Copolymer Matrices

In all cases the incorporation of CAB into the NVP:methacrylate/acrylate system, reduced the EWC. Once again the freezing water content appeared to be dependent on the EWC of such systems and not on the chemical composition.

In general incorporation of the interpenetrant CAB into hydrogel matrices produced increases in Young's modulus, tensile strength and elongation at break. At a given EWC a range of mechanical properties were achievable. The greatest percentage increase in mechanical properties was observed with THFFA and THFFMA systems. Simple copolymers of these materials had the lowest mechanical properties of the systems used in this work, hence it is not unexpected that the reinforcing action of the interpenetrant would be the greatest.

The oxygen permeability of both copolymers and semi-IPN's, in this section, is dominated by the EWC and not the chemical composition of the materials.

Simple copolymers were all optically compatible in the dehydrated state. However, when hydrated systems containing iso-bornyl methacrylate became cloudy in appearance. All the other systems remained clear. With the presence of CAB in the system the story is quite different. In all cases the hydrated systems are optically incompatible. In addition dehydrated systems were predominantly incompatible, with only systems containing THFFMA and IBUTMA exhibiting optical clarity in this state. Optical incompatibility is not a concern when considering applications such as synthetic articular cartilage. However, for use in applications such as a synthetic cornea or in the contact lens industry, optical clarity is of the utmost importance. It would, therefore, be desirable to find interpenetrants which would produce optically compatible materials. This idea is followed through in Chapter 4, in the development of semi-IPN's using an ether and an ester polyurethane as the interpenetrant.

CHAPTER 4

Hydrogel Semi-Interpenetrating Polyurethane Polymer Networks

4. 1 Introduction

Chapter 4 continues the work on hydrogel systems similar to those studied in Chapter 3. As previously mentioned in Chapter 3 work on hydrogel systems falls into three distinct sections, there are:

- a Novel methacrylate monomers used in conjunction with NVP
- b Novel methacrylate - NVP copolymers as matrices for an established interpenetrant, CAB
- c Novel methacrylate - NVP copolymers as matrices for novel interpenetrants

Chapter 3 was concerned with sections a and b, Chapter 4 concentrates on section c. As polyurethane interpenetrants appear to give a range of desirable properties, ether polyurethanes, (PU1), as previously used by Corkhill, and new ester polyurethanes, (PU2), were incorporated into the range of methacrylate monomers used throughout this work using the general technique described in section 2.2.1. A series of polyesters was examined and Goodridge code 5706P was chosen as the most soluble, (PU2).

Comparisons were made between the resulting polymers to see the effect, if any, of changing the interpenetrating species.

The term compatibility may be used in different ways. True compatibility of polymers involves complete intermixing of polymer chains with no segregation and a single glass transition temperature consequent of molecular homogeneity. Additionally it is possible for materials to be compatible at this molecular level but to show degrees of phase separation or molecular aggregation at different levels. Compatibility within the discussion of experimental results in this thesis refers to optical compatibility. That is any molecular segregation produces regions of association smaller than the wavelength of light and / or of similar refractive index.

Table 4. 1 shows the compatibility of semi-IPN's in their dehydrated and hydrated states. Mechanical and surface properties together with comment on the clarity of dehydrated and hydrated semi-IPN's are presented in subsequent sections and appendix 1. Tables 4. 2-4. 6 show the polymers that were synthesised in this section together with their equilibrium water contents, (EWC).

Some preliminary observations on the effect of the compatibility of both matrix monomers and IPN polymers are apparent. It is clear that there is no universal order of compatibility. For THFFMA the compatibility with polymers follows the series PU2>PU1>CAB; for THFFA PU2~PU1>CAB; For IBUTMA PU2~PU1~CAB; for TBMA PU2~PU1>CAB and for IBMA PU2~PU1>CAB. When the compatibility data for dehydrated (D) and hydrated (H) system is considered for each IPN the information maybe summarised as follows:

<u>Interpenetrant</u>	<u>Compatible (D)</u>	<u>Compatible (H)</u>	<u>Incompatible (D/H)</u>
CAB		THFFMA/IBUTMA	THFFA/TBMA/ IBMA
PU1	THFFA	THFFMA/IBUTMA	TBMA/IBMA
PU2	THFFA/THFFMA	IBUTMA	TBMA/IBMA

Table 4. 1 Compatibility of Interpenetrants with Methacrylate/Acrylate : NVP copolymers

The greatest degree of compatibility with the methacrylate monomers used here is found with the ester containing polyurethane, PU2. The ether containing polyurethane shows slightly lower compatibility and CAB the least. The methacrylate monomers become more hydrophobic along the series THFFA>THFFMA>IBUTMA>TBMA>IBMA and this seems to be a reflected in the order of compatibility. At the outset of this work the polar tetrahydrofurfuryl based monomers were chosen as a primary means of enhancing semi-IPN compatibility and the ester containing polyurethane, (PU2), was selected as an added means of enhancing this effect. The data presented here shows that a measure of success has been achieved.

One important general effect of the compatibility data revealed here is its consequence for elongation at break results. When an SIPN shows incompatibility in the dehydrated state, its consequent phase separation will, predictably, result in poor and erratic elongation. Incompatibility, (opalescence), that is only produced when the SIPN is hydrated will not affect the integrity and continuity of the polymer matrix to the same extent. The compatibility data would predict that all TBMA and IBMA systems would have low elongations, (relative to the THFFMA based system), as a result of their incompatibility. The results seen in figures 4.5, 4.13 and 4.23, showing the THFFMA, IBMA and TBMA systems respectively, bear this theory out.

<u>Composition</u>	<u>EWC (%)</u>
NVP : THFFMA 60 : 40	64
NVP: THFFMA: PU 1 60: 40:5	59
NVP: THFFMA:PU 1 60:40:10	57
NVP: THFFMA:PU 1 60:40:15	54
NVP: THFFMA: PU 2 60:40:5	56
NVP: THFFMA:PU 2 60:40:10	54
NVP: THFFMA:PU 2 60:40:15	52

Table 4. 2 NVP : Tetrahydrofurfuryl Methacrylate : Polyurethane Semi-IPN's

<u>Composition</u>	<u>EWC (%)</u>
NVP : THFFA 60 : 40	81
NVP: THFFA: PU 1 60: 40: 5	74
NVP: THFFA: PU 1 60: 40: 10	73
NVP: THFFA: PU 1 60: 40: 15	70
NVP: THFFA: PU 2 60: 40: 5	77
NVP: THFFA: PU 2 60: 40: 10	74
NVP: THFFA: PU 2 60: 40: 15	71

Table 4. 3 NVP : Tetrahydrofurfuryl Acrylate : Polyurethane Semi-IPN's

<u>Composition</u>	<u>EWC (%)</u>
NVP : ISOBORNYL MA 60:40	31
NVP: IBMA:PU 1 60:40:5	27
NVP: IBMA:PU 1 60:40: 10	29
NVP: IBMA: PU 1 60:40:15	28
NVP: IBMA:PU 2 60:40:5	27
NVP: IBMA: PU 2 60:40: 10	23
NVP: IBMA: PU 2 60:40:15	26

Table 4. 4 NVP : Iso-bornyl MA : Polyurethane Semi-IPN's

<u>Composition</u>	<u>EWC (%)</u>
NVP : ISOBUTYL MA 60 : 40	43
NVP: IBUTMA: PU 1 60: 40: 5	39
NVP: IBUTMA: PU 1 60:40:10	40
NVP: IBUTMA: PU 1 60:40:15	39
NVP: IBUTMA: PU2 60: 40: 5	38
NVP: IBUTMA: PU 2 60:40:10	35
NVP: IBUTMA: PU 2 60:40:15	33

Table 4. 5 NVP : Iso-butyl MA : Polyurethane Semi-IPN's

Composition	EWC (%)
NVP : TERTBUTYL MA 60:40	39
NVP: TBMA: PU 1 60: 40: 5	38
NVP: TBMA: PU 1 60:40: 10	39
NVP: TBMA: PU 1 60:40: 15	38
NVP: TBMA: PU 2 60: 40: 5	38
NVP: TBMA: PU 2 60:40: 10	30
NVP: TBMA PU 2 60:40: 15	32

Table 4. 6 NVP : Tert-butyl MA : Polyurethane Semi-IPN's

For each monomer combination the EWC's were not dependent on the particular polyurethane.

4. 2 A Comparison of the Mechanical Properties of Ester (PU2) and Ether (PU1) Polyurethanes

Semi-IPN's were made with two series of comparable compositions of N-vinyl pyrrolidone: methacrylate monomer and a polyurethane interpenetrant, where the interpenetrant was either an ether or an ester polyurethane. Equilibrium water contents with compositions of the semi-IPN's were measured and are presented in tables 4.2 - 4.6. The effect of the ether polyurethane, PU1, and ester polyurethane, PU2, on mechanical properties are presented in figures 4.1 - 4.23, in relation to the percentage of interpenetrant incorporated and the equilibrium water content. The data are presented in the same order as contained in tables 4.1 - 4.5. Thus figures 4.1-4.5 present mechanical property data for THFFMA : NVP 40 : 60 together with a percentage of polyurethane. In each case both Young's modulus and tensile strength are presented as a function of both EWC and % interpenetrant, whereas elongation at break which is experimentally less precise and more subject to error, is presented simply as a function of EWC. The raw data is presented in appendix 1. An exception to this method of presentation is found with samples containing THFFA,

here the parallel between EWC and % interpenetrant is so close that the data are simply presented as a function of EWC.

Throughout this section the symbol ■ on the graphs represents the NVP with methacrylate or acrylate copolymer with no interpenetrant present.

4. 2. 1 Mechanical Properties of Semi-IPN's Prepared with Tetrahydrofurfuryl Methacrylate

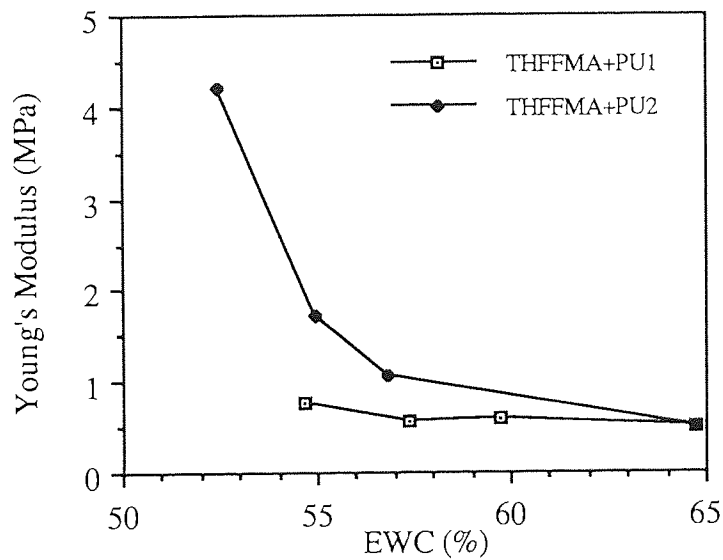


Figure 4. 1 A Comparison of Initial Young's Modulus with EWC in 60 : 40 NVP : THFFMA SIPN's Prepared with PU1 and PU2

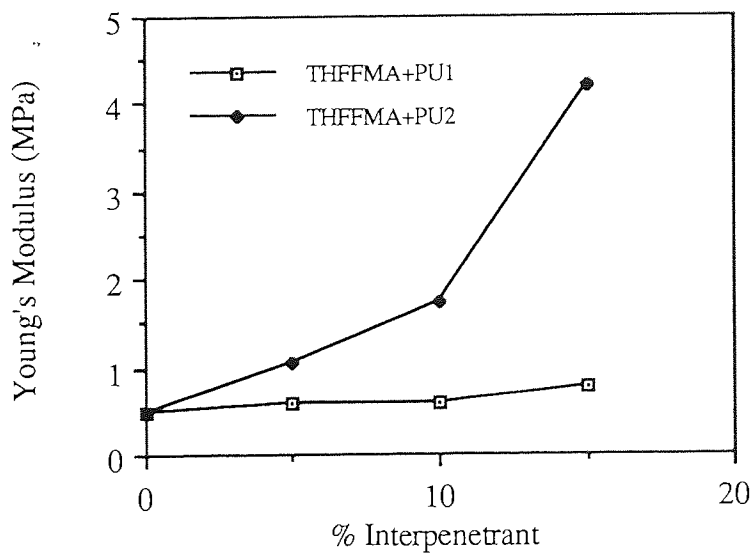


Figure 4. 2 A Comparison of Young's Modulus with Interpenetrant Concentration in 60 : 40 NVP : THFFMA SIPN's Prepared with PU1 and PU2

Figures 4. 1 and 4. 2 show essentially the same thing, that the incorporation of PU2 increases the initial Young's modulus significantly more than PU1 and that it does so at any given EWC.

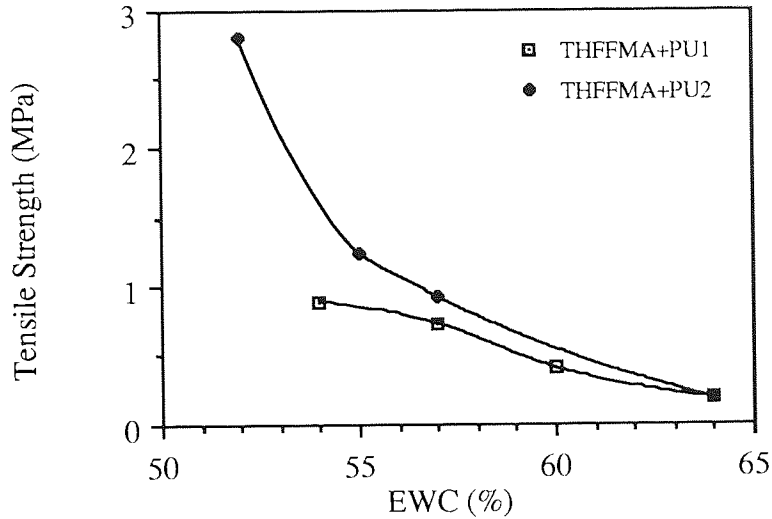


Figure 4. 3 A Comparison of Tensile Strength with EWC in 60 : 40 NVP : THFFMA SIPN's Prepared with PU1 and PU2

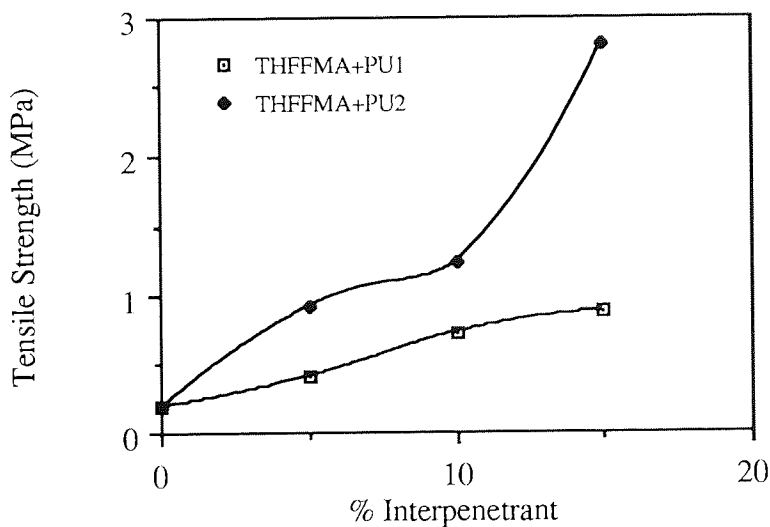


Figure 4. 4 A Comparison of Tensile Strength with Interpenetrant Concentration in 60 : 40 NVP : THFFMA SIPN's Prepared with PU1 and PU2

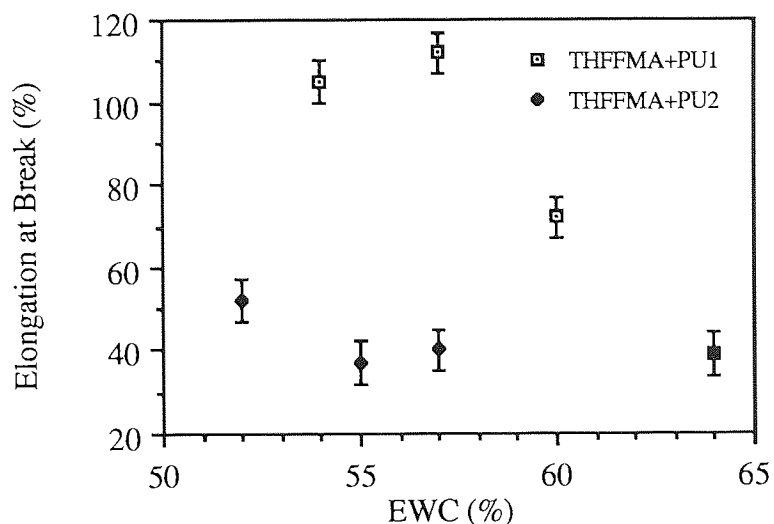


Figure 4. 5 A Comparison of Elongation at Break with EWC in 60 : 40
NVP : THFFMA SIPN's Prepared with PU1 and PU2

Figures 4. 1-4. 5 show how the incorporation of an ester polyurethane, (PU2), into 60 : 40 NVP : THFFMA semi-IPN's improves the mechanical properties relative to the case when an ether polyurethane, (PU1), is used. Previously Corkhill¹ used ether polyurethanes to strengthen hydrogel systems. This work shows that considerable improvements can be made by changing the structure of the interpenetrating species, without deleterious effects on other physical properties of the gels. Figure 4. 5, showing the elongation at break with EWC, illustrates that PU1 containing samples give higher elongation at break for a given EWC. In presenting the results obtained with the acrylate, because of the close parallel between % interpenetrant and EWC, the data is simply related to EWC, (figures 4. 6 - 4. 8).

4. 2. 2 Mechanical Properties of Semi-IPN's Prepared with Tetrahydrofurfuryl Acrylate

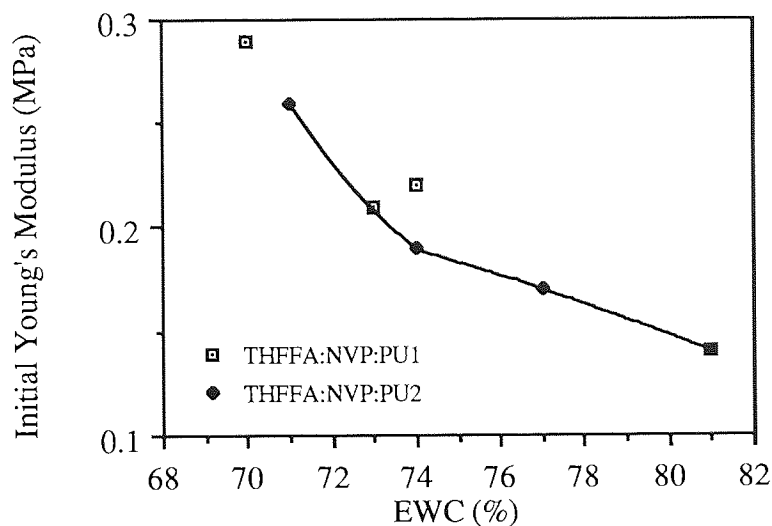


Figure 4. 6 A Comparison of Young's Modulus with EWC in 60 : 40 NVP : THFFA SIPN's Prepared with PU1 and PU2

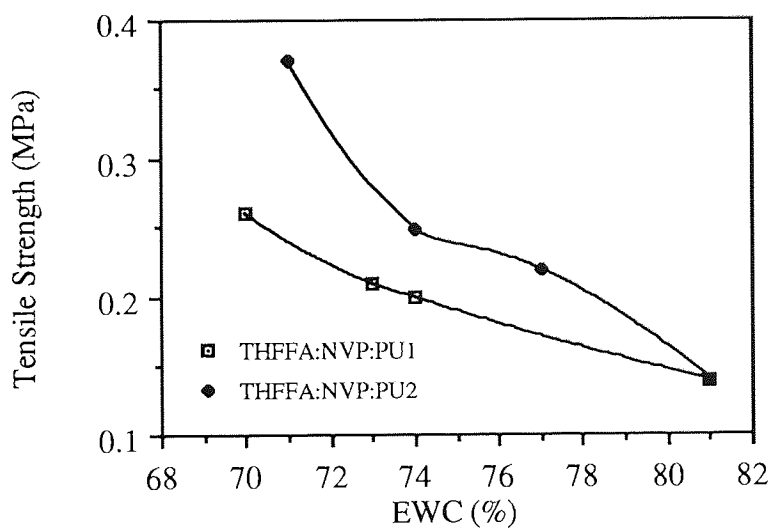


Figure 4. 7 A Comparison of Tensile Strength with EWC in 60 : 40 NVP : THFFA SIPN's Prepared with PU1 and PU2

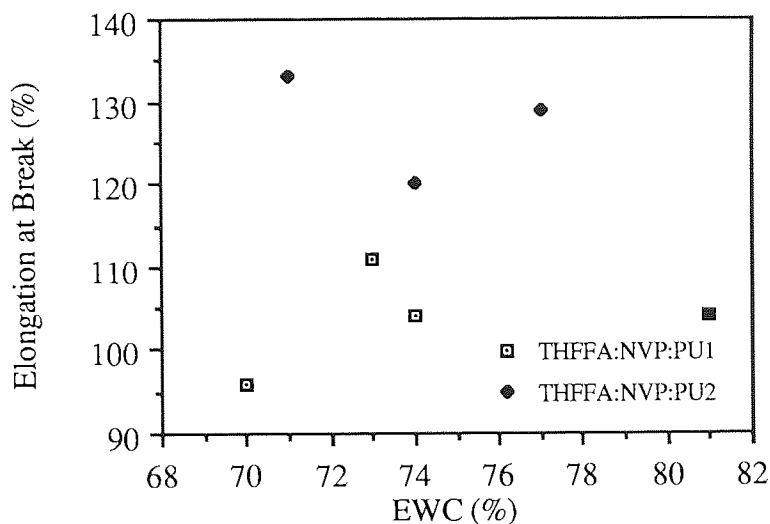


Figure 4. 8 A Comparison of Elongation at Break with EWC in 60 : 40
NVP : THFFA SIPN's Prepared with PU1 and PU2

In the cases of the tensile strength and Young's modulus both polyurethanes have an advantageous effect, both increasing with increasing percentages of either polyurethane. This is accompanied by a decrease in EWC which makes it extremely difficult to attribute the effect directly to the polyurethane. The fact that the results are non-identical however (see figures 4.7 and 4.8) shows that there is some specificity associated with the polyurethane interpenetrant and that the ester polyurethane has some advantage over the ether polyurethane. Figure 4. 8 shows the elongation at break of THFFA : PU samples and indicates that samples containing PU2 have a higher elongation at break than samples of a similar EWC containing PU1. Given the high standard deviations associated with elongation at break it is not wise to read a great deal into the results.

4. 2. 3 Mechanical Properties of Semi-IPN's Prepared with Iso-bornyl Methacrylate

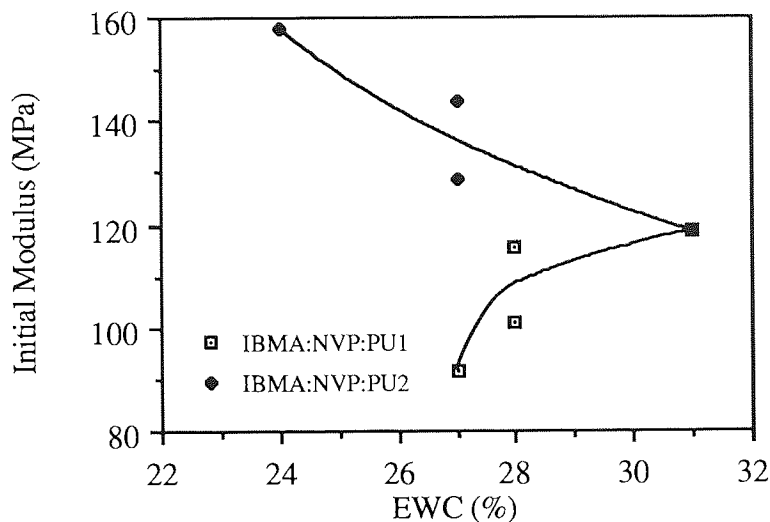


Figure 4. 9 A Comparison of Initial Modulus with EWC in 60 : 40 NVP : Iso-bornyl MA SIPN's Prepared with PU1 and PU2

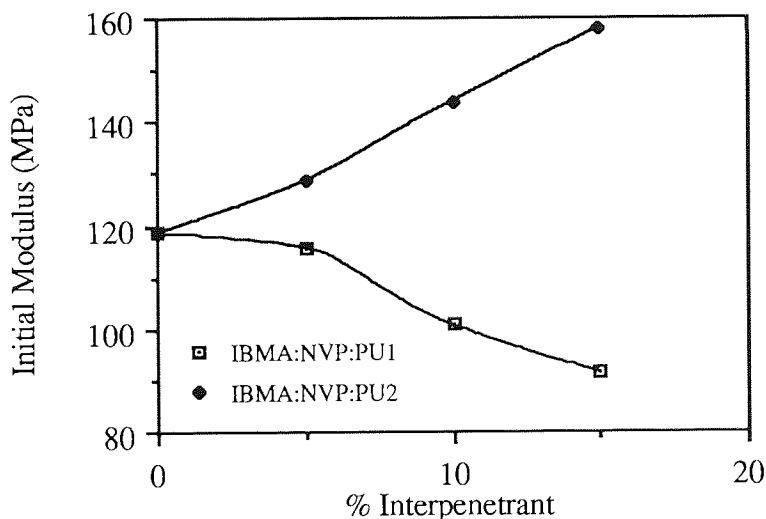


Figure 4.10 A Comparison of Initial Modulus with % PU in 60 : 40 NVP : Iso-bornyl MA SIPN's Prepared with PU1 and PU2

Figures 4. 9 and 4. 10 show the change in the initial Young's modulus with EWC and percentage interpenetrant respectively. This shows that opposite patterns emerge when increasing amounts of either ester or ether polyurethane are incorporated into the hydrogel system. If the percentage of polyether urethane in the system is

increased there is a fall in the initial modulus but the reverse is observed when the polyester urethane is incorporated. One conclusion for this is that the NVP : IBMA backbone is less stiff than the ester polyurethane. Although the ester polyurethane in its condensed undiluted form is stiffer, this does not necessarily predict the relative stiffness of the two chains when they are dispersed in an aqueous medium. This is because the polyurethane - polyurethane interchain forces, e. g. dipole - dipole, will have virtually disappeared in the dispersed system. When they are dispersed the polyurethane stiffness will be much more dependent on the inherent energy barrier to rotation of the backbone.

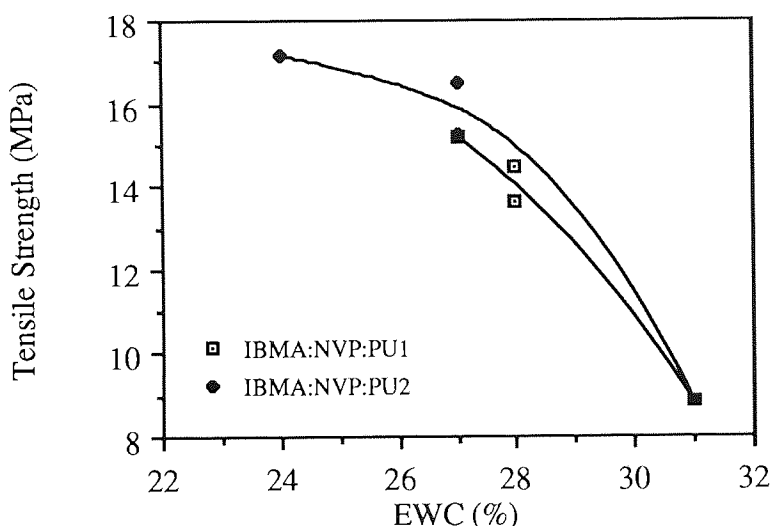


Figure 4.11 A Comparison of Tensile Strength with EWC in 60 : 40
NVP : Iso-bornyl MA SIPN's Prepared with PU1 and PU2

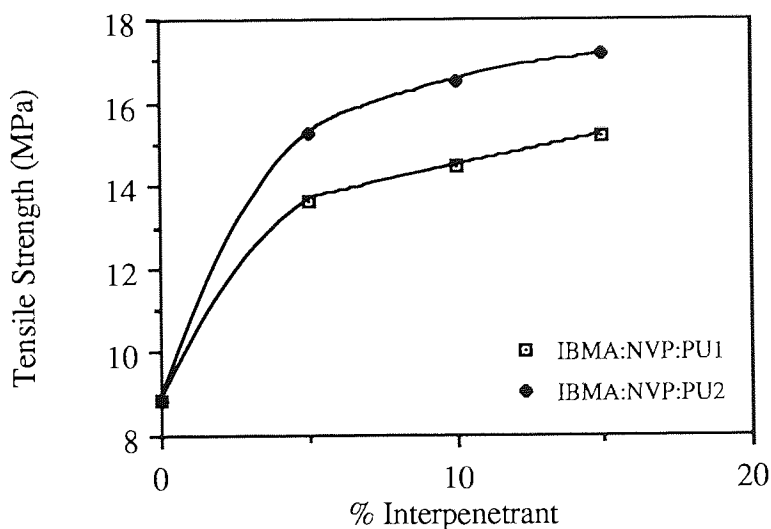


Figure 4.12 A Comparison of Tensile Strength with % PU in 60 : 40
NVP : Iso-bornyl MA SIPN's Prepared with PU1 and PU2

Turning to tensile strength, figures 4. 11 and 4. 12 show that a drop in tensile strength is observed with an increase in EWC or a decrease in percentage interpenetrant. Patterns for both the polyurethanes used are similar, however, the polyester urethane gave slightly higher tensile strengths.

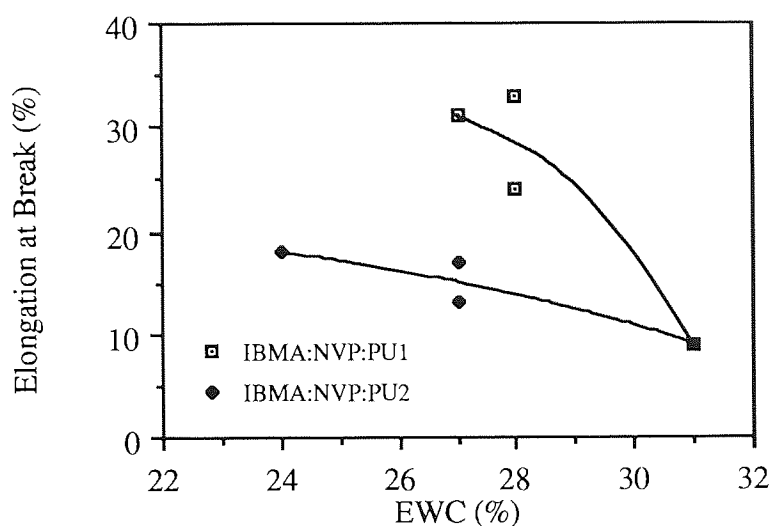


Figure 4.13 A Comparison of Elongation at Break with EWC in 60 : 40
NVP : Iso-bornyl MA SIPN's Prepared with PU1 and PU2

The clear difference between the behaviour of the IBMA and THFFMA systems is that the former have a much lower elongation at break. This is in part but not wholly related to EWC and we can see that in both cases, comparing figures 4. 5 and 4. 13 that increasing the percentage interpenetrant increases elongation at break. It is the elongation at break, at a given modulus that controls the tensile strength, since this is simply the force / unit area required to rupture the polymer.

A reversal of the roles of the ether and ester are seen when comparing the initial modulus and elongation at break (figures 4. 9 and 4. 13). This underlines an aspect of behaviour referred to earlier in comparing the two polyurethanes. The ether polyurethane is a less stiff, more extensible polymer and the ester polyurethane a more stiff, somewhat less extensible polymer. This suggests that in the dispersed state, the polymers are retaining the relative characteristics which they show in the

condensed state. This difference between the polyurethanes is complimented by differences in the inherent mechanical properties of the hydrogel matrices into which they are incorporated. This point is illustrated by the huge differences in modulus of the THFFMA systems, figure 4. 2, and the IBMA system, figure 4. 10, and emphasised here in the behaviour of elongation at break, figures 4. 5 versus 4. 13. In broad terms, the more hydrophobic, sterically hindered IBMA produces systems that are inherently stiffer because of the interdependent effects of steric hindrance of the matrix polymer (i. e. iso-bornyl groups versus tetrahydrofurfuryl groups) and the EWC that they produce. Although the elongations and moduli of the IBMA and THFFMA systems are different the positive effect of introduction of the interpenetrant is to increase tensile strength. In the case of the THFFMA systems (figure 4. 4) this is a much more dramatic effect in proportional terms than is the case with the inherently stiffer and stronger IBMA system (figure 4.12). It can be seen in figure 4.12 that both the ester and ether containing polyurethanes produce an increase in the tensile strength. In the case of the ether polyurethane (PU1) this is done by advantageously increasing the elongation at break (figure 4. 13) whereas in the case of the ester polyurethane, (PU2), the increase results from an increase in initial modulus. This family of results nicely illustrates how the initial modulus, tensile strength and elongation at break compliment each other.

4. 2. 4 Mechanical Properties of Semi-IPN's Prepared with Iso-butyl Methacrylate

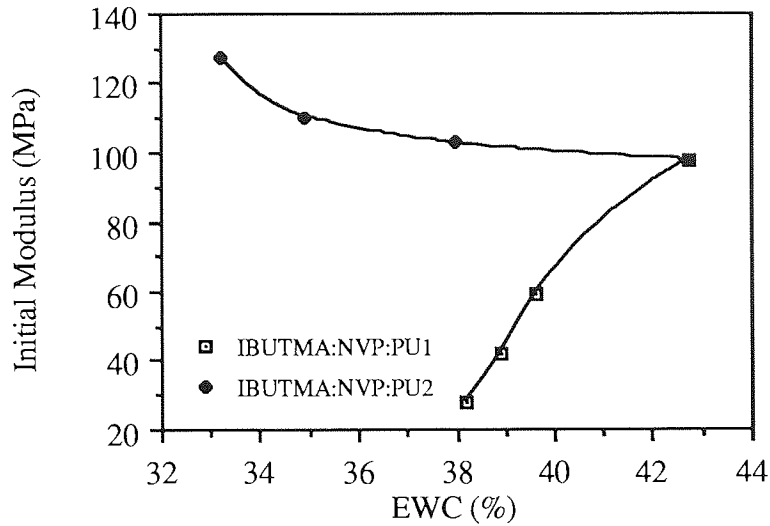


Figure 4.14 A Comparison of Initial Modulus with EWC in 60 : 40 NVP : Iso-butyl MA SIPN's Prepared with PU1 and PU2

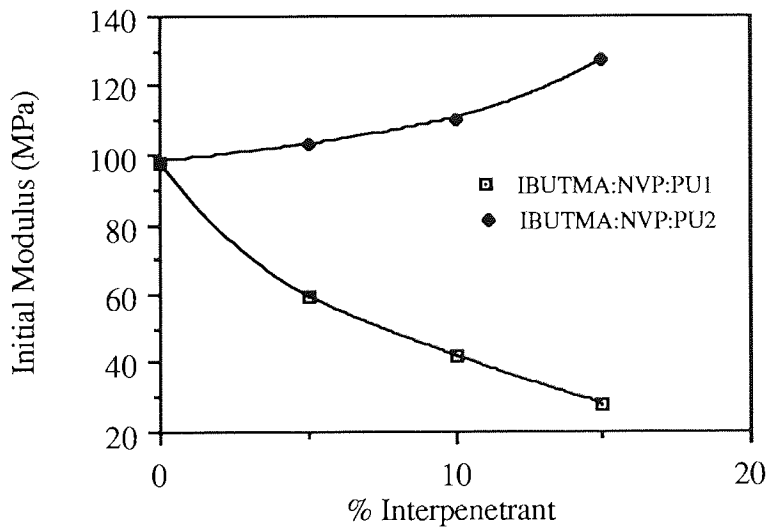


Figure 4.15 A Comparison of Initial Modulus with % PU in 60 : 40 NVP : Iso-butyl MA SIPN's Prepared with PU1 and PU2

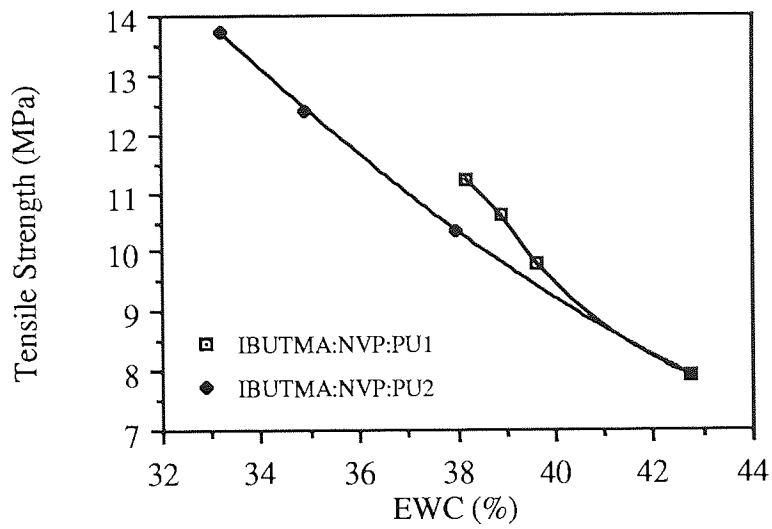


Figure 4.16 A Comparison of Tensile Strength with EWC in 60 : 40
NVP : Iso-butyl MA SIPN's Prepared with PU1 and PU2

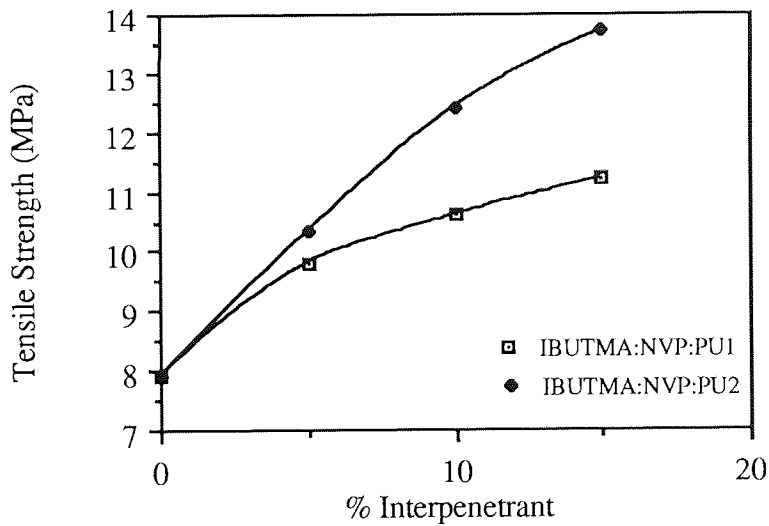


Figure 4.17 A Comparison of Tensile Strength with % PU in 60 : 40
NVP : Iso-butyl MA SIPN's Prepared with PU1 and PU2

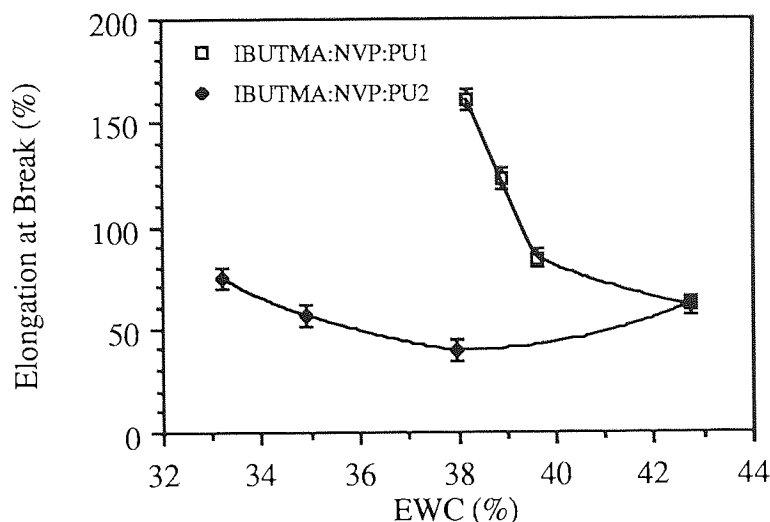


Figure 4.18 A Comparison of Elongation at Break with EWC in 60 : 40
NVP : Iso-butyl MA SIPN's Prepared with PU1 and PU2

The IBUTMA system appears to be more similar to the hydrophobic IBMA system than the hydrophilic THFFMA system. Results which emerge are of intermediate values with similar patterns to the IBMA system. However, owing to the EWC being more extended, patterns can be more clearly observed reinforcing the differences in the ether and ester polyurethanes.

Inspection of figure 4. 18 confirms that the pattern of behaviour, with respect to elongation at break for IBMA : NVP matrices, reflects that previously seen and commented on with IBMA. The pattern of behaviour which is distinct for the ether and ester polyurethanes (PU1 and PU2), is exactly parallel in the IBMA and IBUTMA systems. The magnitude of the elongations at break is however quite different. In comparing figures 4. 13 and 4. 18, which show elongation at break behaviour for the IBMA and IBUTMA systems respectively, a further interesting point emerges. Although EWC is an important factor in determining mechanical properties, the nature of the polymer matrix has the dominant influence,. This is brought home by comparing the elongation at break at 33% water in iso-butyl based systems (figure 4. 18) with the simple iso-bornyl copolymer at 31% (no interpenetrant) shown in figure 4. 13. The elongation at break in the former case is

around 71% where in the latter case it is hardly 10%. Both copolymers are clear in the dehydrated state. Although the similarity of behaviour of the IBMA and IBUTMA systems has been commented on, semi-IPN's based on the latter are broadly compatible in the dehydrated state, where those based on the former are incompatible, as reflected in optical clarity. This undoubtedly contributes to the very large magnitude of difference in elongation at break between the two systems.

4. 2. 5 Mechanical Properties of Semi-IPN's Prepared with Tert-butyl Methacrylate

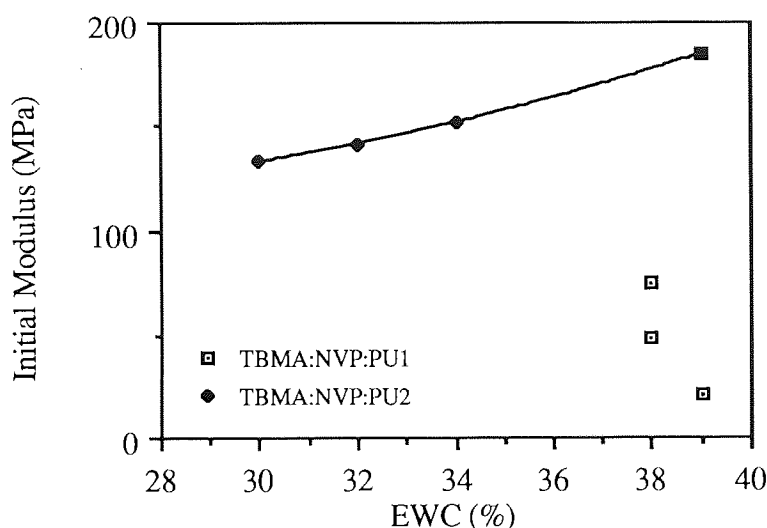


Figure 4.19 A Comparison of Initial Modulus with EWC in 60 : 40
NVP : Tert-butyl MA SIPN's Prepared with PU1 and PU2

In samples containing tert-butyl methacrylate results show that as the percentage of polyurethane changes, there is little effect on the EWC and no specific pattern emerges.

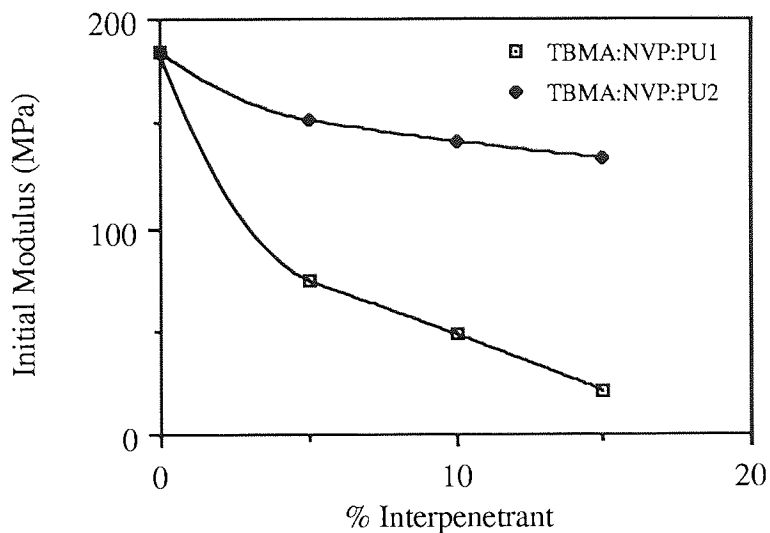


Figure 4.20 A Comparison of Initial Modulus with % PU in 60 : 40
NVP : Tert-butyl MA SIPN's Prepared with PU1 and PU2

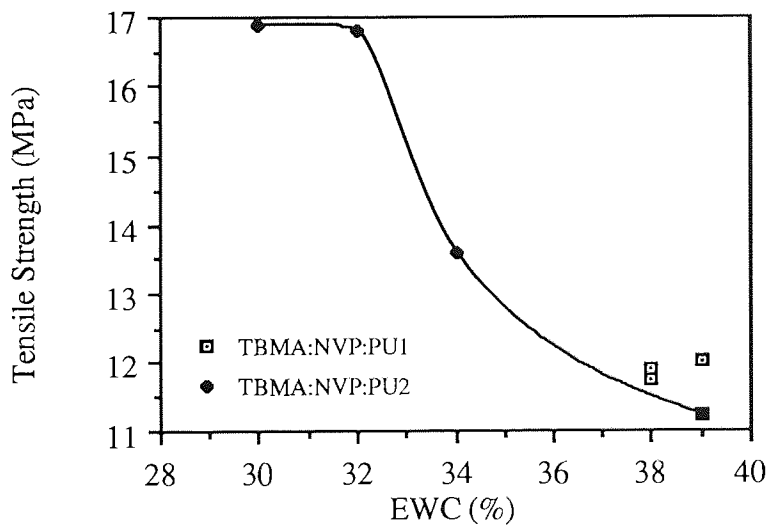


Figure 4.21 A Comparison of Tensile Strength with EWC in 60 : 40
NVP : Tert-butyl MA SIPN's Prepared with PU1 and PU2

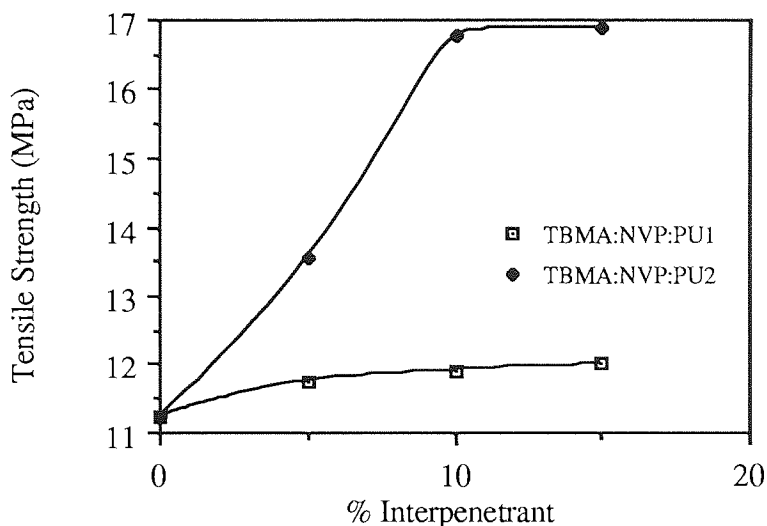


Figure 4.22 A Comparison of Tensile Strength with % PU in 60 : 40
NVP : Tert-butyl MA SIPN's Prepared with PU1 and PU2

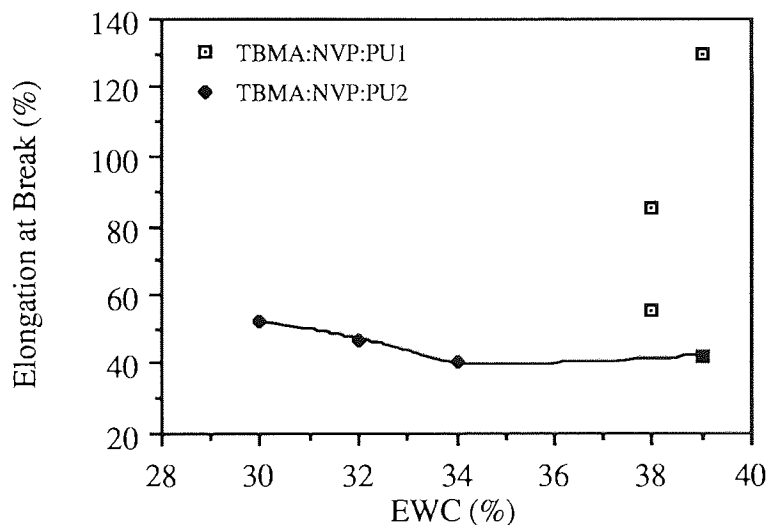


Figure 4.23 A Comparison of Elongation at Break with EWC in 60 : 40
NVP : Tert-butyl MA SIPN's Prepared with PU1 and PU2

The selection of tert-butyl methacrylate as a monomer to continue the sequence of monomers showing different degrees of steric hindrance and hydrophobicity, presents the expectation of increased hydrophobicity with respect to the isomeric isobutyl methacrylate. The decrease in EWC of the NVP : MA 60 : 40 copolymer from

43% for IBUTMA to 39% for TBMA is consistent with this change. The SIPN's produced are in general less compatible than those found with the IBUTMA copolymers and those two factors taken together (i. e. increasing hydrophobicity and decreasing compatibility) provide a basis for understanding the properties of the resultant semi-IPN's, which are similar in general form to those found with IBUTMA but show some significant differences in detail. The initial moduli of the 60 : 40 NVP : TBMA / PU1 and PU2 semi-IPN's are shown in figures 4. 19 and 4.20. Although the general form of these two figures reflects those shown for the comparable IBUTMA systems figures 4. 14 and 4. 15 the initial modulus of the TBMA 60 : 40 matrix copolymer is approximately twice that of the IBUTMA system. As a result incorporation of both the ether and ester polyurethanes (PU1 and PU2) produces a decrease in the initial modulus with the effect being very much greater for the ether polyurethanes (PU1). The comparable IBUTMA systems showed a decrease with the ether polyurethane but an increase with the ester polyurethane. When taken together with the results for the IBMA system, figure 4. 10, which is a moderate intermediate between that of IBUTMA and TBMA, it appears that incorporation of the ester polyurethanes as interpenetrants will decrease the initial modulus of matrices based on copolymers which themselves have an initial modulus greater than 150 MPa, but increasing the initial moduli of matrices whose initial moduli are in the region of 120 MPa or less.

The ether polyurethane almost invariably plasticises the system and decreases the initial modulus. The only case in which an increase in the initial modulus was observed with the ether polyurethane interpenetrant, was that of the THFFA : NVP system , figure 4. 6. The effect with the THFFMA is neutral, figure 4. 2. The initial modulus of the THFFA and THFFMA copolymer matrices are 0. 2 and 0. 5 MPa respectively, lower than the three hydrophobic methacrylates studied. It is clear that the work carried out here with ester polyurethane produces dramatically different results from those obtained with ether polyurethane to the extent that these two systems can be regarded as quite distinct polymers, as regards SIPN technology.

On the basis of these observations the initial moduli of the TBMA : NVP : PU systems can now be seen to fall into a predictable pattern in relation to which the only somewhat unusual feature is the great similarity in EWC of the initial matrix copolymer and the SIPN's produced with 5, 10, and 15% interpenetrant. The fact that all these systems (including the unmodified matrix copolymer) are incompatible in the dehydrated and hydrated state produce a degree of unpredictability in EWC's which do not represent a balance of hydrophobic and hydrophilic components in the system. Despite the fact that the EWC's are the same, incorporation of ether polyurethane produces a massive plasticisation of NVP etc. matrix, figure 4. 23. This increase in flexibility and decrease in the initial modulus have a mutually balancing effect which means, unusually, that the tensile strength of the systems remain substantially constant, figure 4. 21. It is important to note, however, that the near identical tensile strengths correspond to quite different stress strain curves, see figures 4. 21 and 4. 22. The behaviour of the ester polyurethane differs interestingly from that of the ether polyurethane. The ester polyurethane : TBMA systems show a slight progressive decrease in initial modulus with an increase in interpenetrant concentration (figure 4. 20) which is coupled with an increase in elongation at break (figure 4.23).

4. 3 Surface Properties

It is always important in multicomponent systems of the sort examined here to measure surface properties. There are many advantages in the measurements in the dehydrated state since such measurements indicate any tendency for the interpenetrant to be positively absorbed at the surface. A higher concentration of interpenetrant at the surface would influence surface behaviour in a non predictable manner. Surface properties of polyurethane semi-IPN's described earlier in this chapter were carried out in the dehydrated state and the results are presented in the same sequence as has been previously used for mechanical properties. These results are shown in figures 4. 24- 4. 33. Samples gave results of total surface free energy in the same region as the CAB SIPN's, the dispersive component once again the dominating component in the dehydrated system. Results obtained were similar for both ether and ester polyurethane containing samples, slight differences were observed but were felt to be within experimental error and therefore insignificant.

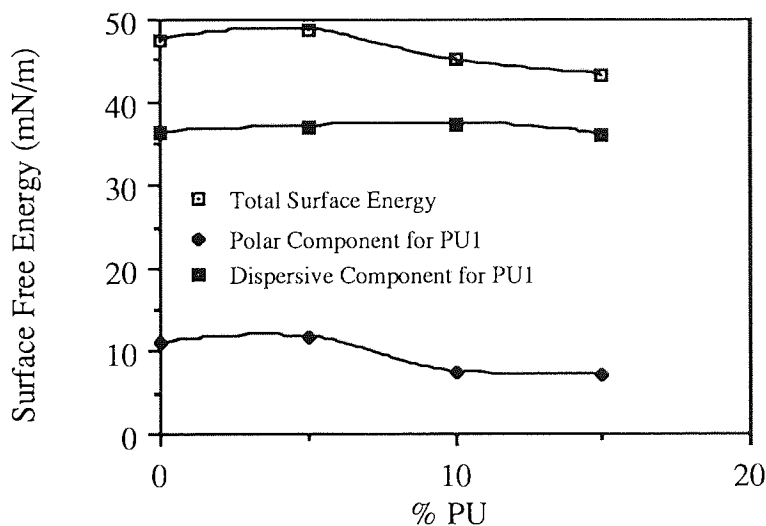


Figure 4.24 Effect of PU1 Content on the Surface Free Energy in Dehydrated NVP 60 : THFFMA 40 : PU Semi-IPN's

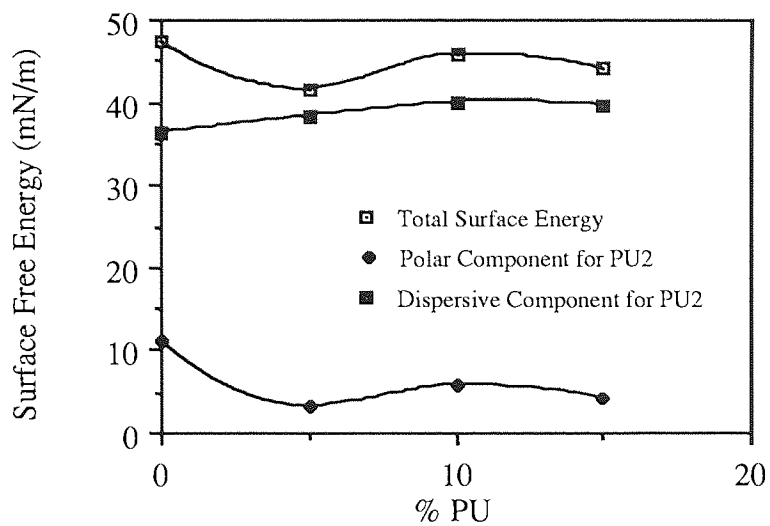


Figure 4.25 Effect of PU2 Content on the Surface Free Energy in Dehydrated NVP 60 : THFFMA 40 : PU Semi-IPN's

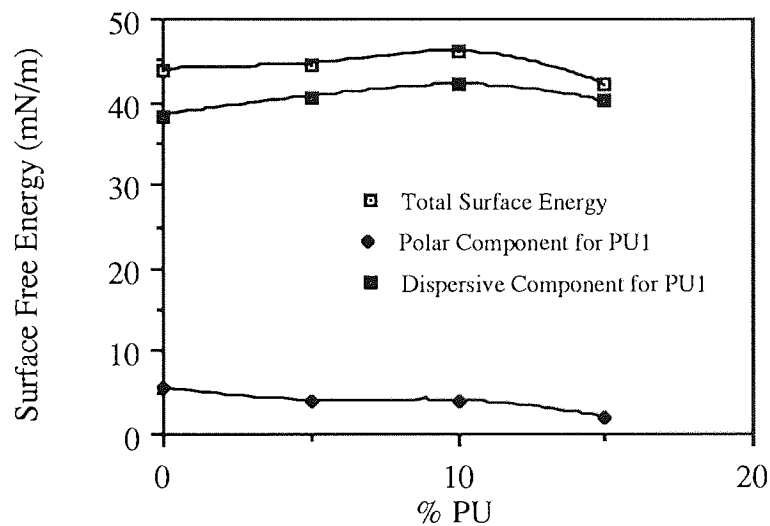


Figure 4.26 Effect of PU1 Content on the Surface Free Energy in Dehydrated NVP 60 : THFFMA 40 : PU Semi-IPN's

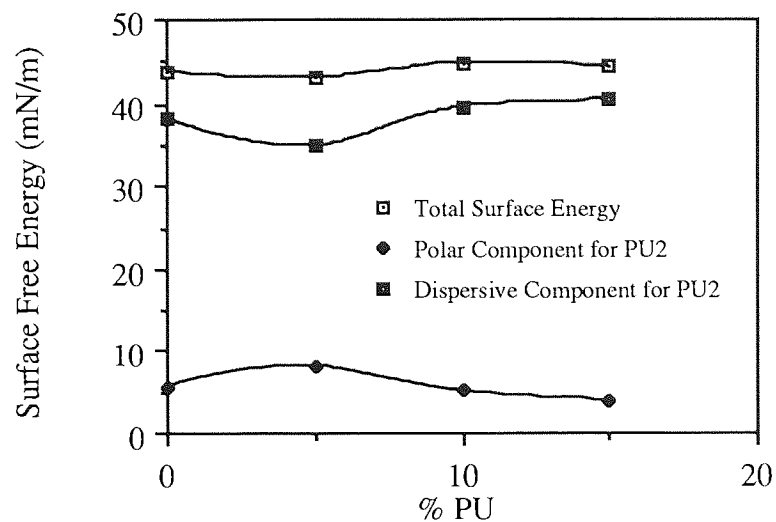


Figure 4.27 Effect of PU2 Content on the Surface Free Energy in Dehydrated NVP 60 : THFFA 40 : PU Semi-IPN's

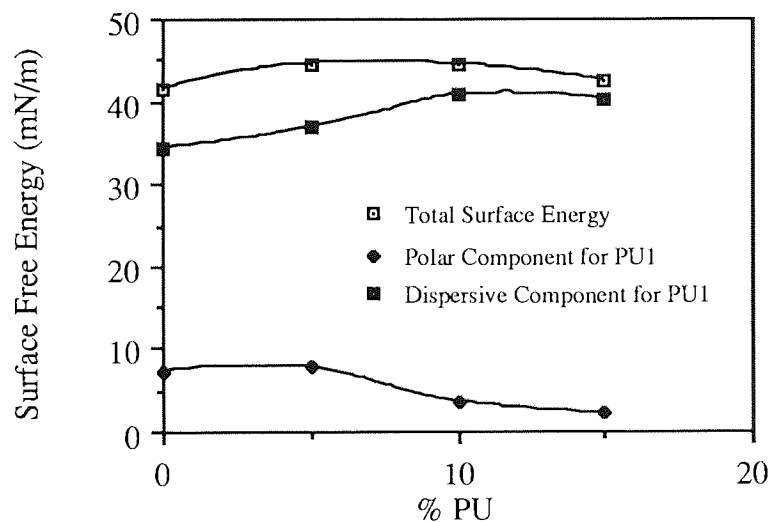


Figure 4.28 Effect of PU1 Content on the Surface Free Energy in Dehydrated NVP 60 : IBMA 40 : PU Semi-IPN's

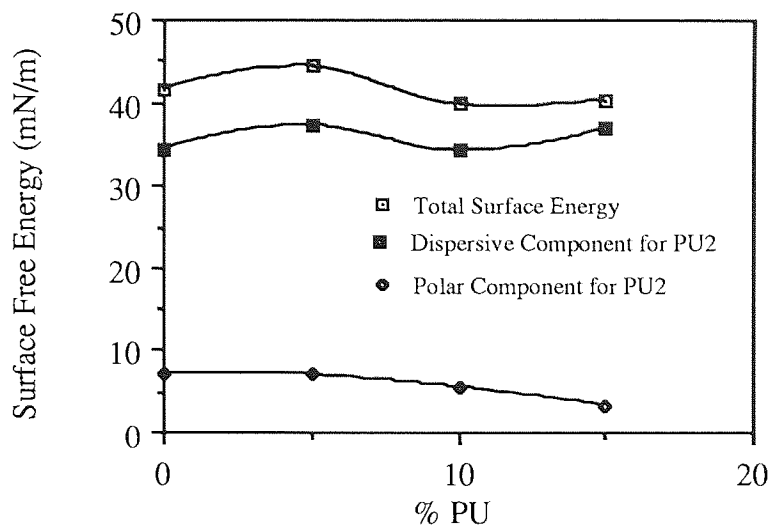


Figure 4.29 Effect of PU2 Content on the Surface Free Energy in Dehydrated NVP 60 : IBMA 40 : PU Semi-IPN's

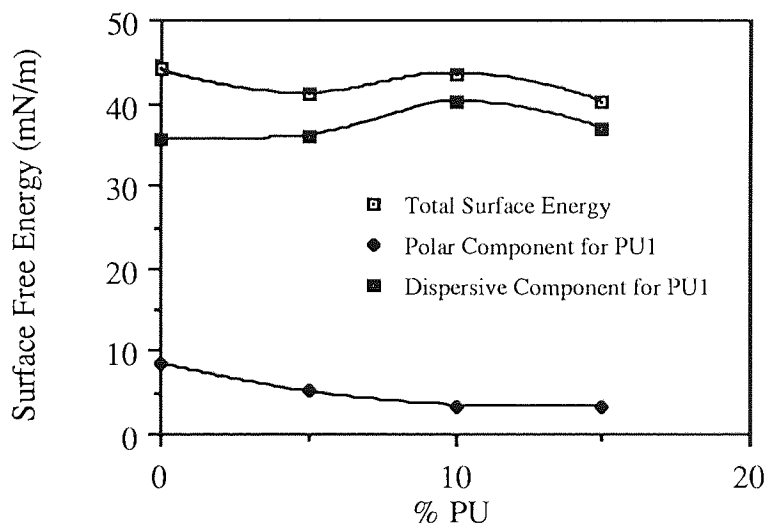


Figure 4.30 Effect of PU1 Content on the Surface Free Energy in Dehydrated NVP 60 : IBUTMA 40 : PU Semi-IPN's

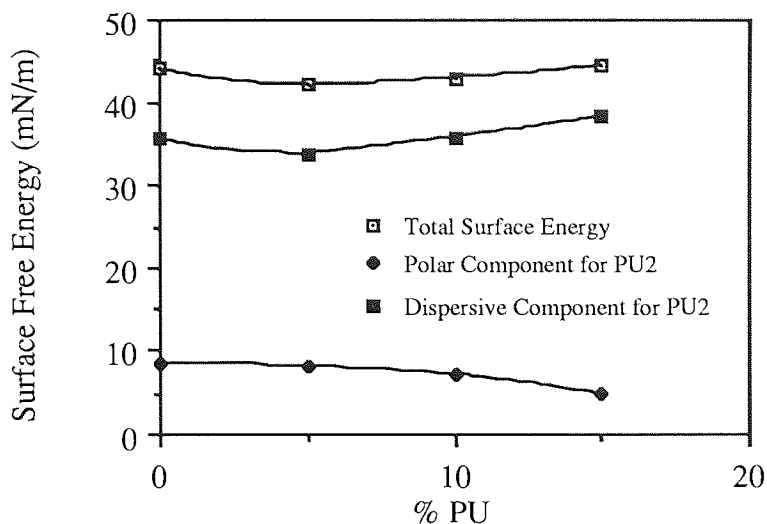


Figure 4.31 Effect of PU2 Content on the Surface Free Energy in Dehydrated NVP 60 : IBUTMA 40 : PU Semi-IPN's

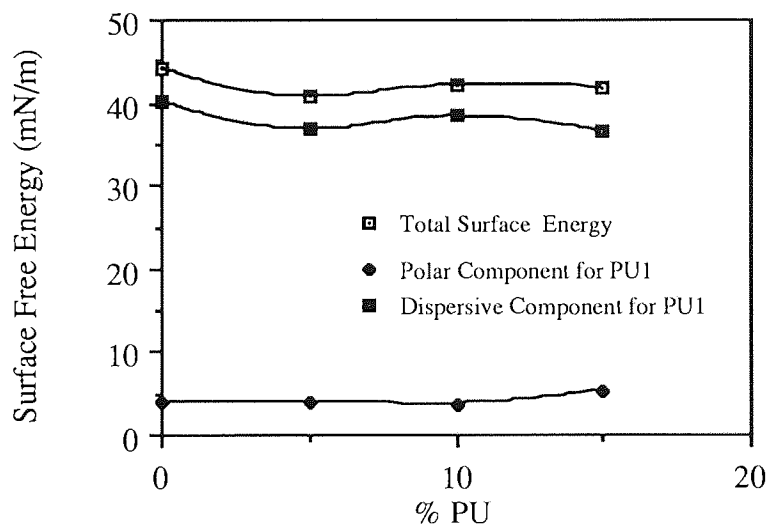


Figure 4.32 Effect of PU1 Content on the Surface Free Energy in Dehydrated NVP 60 : TBMA 40 : PU Semi-IPN's

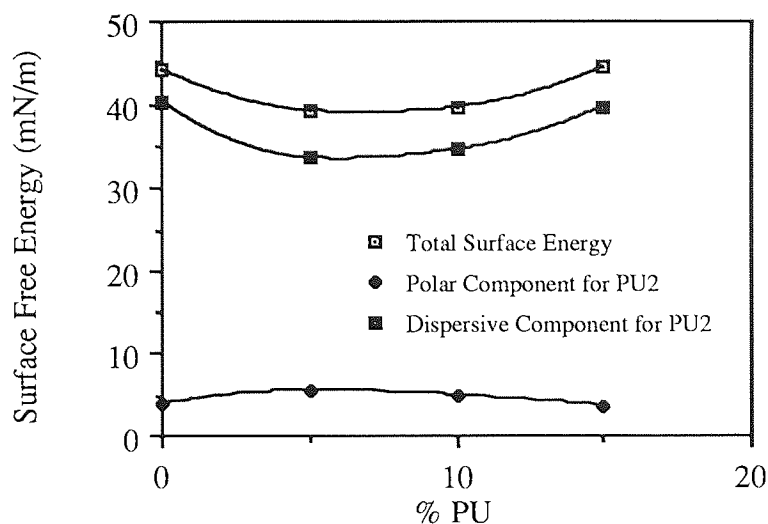


Figure 4.33 Effect of PU2 Content on the Surface Free Energy in Dehydrated NVP 60 : TBMA 40 : PU Semi-IPN's

The forgoing information on the effects using polyurethane as an interpenetrant on the surface energies of dehydrated materials tells a fairly familiar story. There is a general trend for polyurethane incorporation to produce, on average, a very slight decrease in the polar component, accompanying a slight increase in dispersive component. The total surface free energy of the system remains practically unchanged. One of the previously noted effects of some polyurethane interpenetrants was a slight enhancement of the cell adhesion properties of the semi-IPN's compared to the unmodified hydrogel with no accompanying modification of surface energy¹. This aspect of behaviour has not yet been studied for these polymers and it may be that the same type of behaviour may be encountered with these materials studied here. The results presented here can conveniently be summarised as indicating that neither ether or ester polyurethane incorporation has any marked advantages or disadvantages to the surface free energy of the dehydrated materials. The results are consistent with a reasonable compatibility of the monomer / polyurethane combinations examined here. There is no evidence of abnormally high concentration or clustering of polyurethane at the semi-IPN surface.

4. 4 General Conclusions

This chapter concentrates on the development of semi-IPN's using novel polyurethanes as interpenetrants within novel methacrylate : NVP matrices. Several important points have emerged highlighting the differences between ether and ester polyurethanes and the differing contributions of hydrophilic and steric hindrance contributions made in matrix polymers.

In general the at a given percentage of either polyurethane the equilibrium water content was approximately the same. Water binding studies have not been carried out on this range of materials, however it would be very interesting to note if the water structuring is unaffected, as is the EWC, by changing the nature of the polyurethane

Although it is clear that no universal order of compatibility exists, different materials prefer different interpenetrants. It is fair to say that out of the interpenetrants used that the ester polyurethane, PU2, shows the greatest compatibility with the monomer matrices used in this study. The ether containing polyurethane shows slightly lower compatibility and CAB the least.

In comparing the effect of changing the interpenetrating species on the mechanical properties, the ester containing polyurethane increased the Young's modulus, tensile strength and the elongation at break considerably more than the ether polyurethane. The mechanical properties increase or decrease depending on the matrices which the polyurethane is incorporated. In general the incorporation of the ester polyurethane will decrease the initial modulus of matrices based on copolymers which themselves have an initial moduli greater than 150M Pa, but will increase the initial moduli of matrices whose initial moduli are in the region of 120 MPa. The ether polyurethane reduces the Young's modulus of most of the polymer matrices used in this section. It does however increase the initial modulus in THFFA containing matrices, and has little effect on the modulus of THFFMA containing samples. This would suggest

that the glass transition temperature of the ether polyurethane is in a similar region to the NVP:THFFMA matrix.

Surface properties of semi-IPN's do not appear to significantly change when the interpenetrating species is changed. Results show total surface free energies in a similar region to semi-IPN's made with CAB.

CHAPTER 5

Low Water Content Semi-Interpenetrating Polymer Networks

5.1 Introduction

Given the interesting results obtained with medium/high equilibrium water content semi-IPN's it was desirable to extend this technology to very low equilibrium water content materials (<5%). The resulting semi-interpenetrating polymer networks would hopefully have high wettability and oxygen permeability, a consequence of using the novel methacrylates shown in figures 2. 6-2. 13, but with a considerable increase in toughness. Materials with such a combination of properties would be desirable in a range of applications, these include bone and teeth replacements, rigid gas permeable contact lenses and / or augmentation.

As with the high EWC semi-IPN hydrogels, where all the preliminary work was done with CAB which formed a sound basis for extension into other interpenetrant materials, CAB was once again used in the preliminary investigations of low EWC materials. It is anticipated that CAB will give indications of types of behavioural differences, oxygen permeability etc., and that this range of behaviour will ultimately be extendible when a wider range of interpenetrants is successfully explored. Given the extensive range of linear polymers either commercially available or synthesisable it is an extremely time consuming process to carry out an extensive investigation. Future success on extending semi-IPN technology depends upon successful exploration of a wider range of interpenetrant polymers than those investigated here. Whilst it is true to say a wide range of polymer classes available have been initially investigated as interpenetrants, a far wider range of less readily available potential materials could be used to extend this work. Solubility parameters provide a useful indication of potential interpenetrant / monomer solubility but give no more than a general guide to behaviour.

Monomers	% CAB	% CAB	% CAB	% CAB
THFFMA	0	5	10	15
THFFA	0	5	10	15
TBMA	0	5	10	15
IBUTMA	0	5	10	15

Table 5.1 Rigid Semi-IPN Compositions

Solubility of the interpenetrant polymer in the methacrylate monomer, in the absence of NVP, was found to be the main restricting feature in the development of this range of materials. NVP was found to be a better solvent for polyurethanes than the methacrylates and the acrylate used in this work. Its better solvating capabilities are attributed to it having fewer bulky side groups than the other methacrylates and the acrylate which cause steric hindrance, and its greater polarity. THFFMA was found to have the greatest capacity, out of the range of methacrylates, for dissolving polymers. This, however, only dissolved up to 5% of ester polyurethane, PU2, and polycarbonate, PC. No amount of ether polyurethane, PU1, would dissolve in this sample and both of these systems were incompatible, see table 5. 2. This was expressed in the lack of opacity which the samples showed. Other monomers were found not to dissolve any significant amount of any of the interpenetrants other than cellulose acetate butyrate.

Monomer	Interpenetrant	Compatibility
THFFMA	CAB	Incompatible
THFFMA	PU2	Incompatible
THFFMA	PC	Incompatible
THFFA	CAB	Incompatible
TBMA	CAB	Incompatible
IBUTMA	CAB	Incompatible

Table 5.2 Compatibility of Semi-IPN Systems

Mechanical properties via tensiometry proved to be a problem when dealing with low water content materials. Unless the samples were extremely tough, they tended to break when attempting to cut them from the membrane sheet. Efforts were made to make a dumbbell shaped sample directly, however owing to the differences in polymerisation shrinkage, samples were not always the same size. The samples that resulted also had edges that were less than smooth and this would cause higher stress concentration to occur in these 'crack' tips. Hence results obtained could be lower than true values. Placing sheets of sample in hot water and attempting to cut when the samples were still warm, and therefore more pliable, was attempted. This, although the most successful technique, also had limitations as the samples rapidly cooled down and once again became brittle, which resulted in cracking upon cutting frequently occurring. Due to these problems extensive tensometry was not carried out on these materials. It was hoped that using polyurethane as an interpenetrant would produce a less brittle polymer than using cellulose acetate butyrate, however, on first inspection this does not appear to be the case.

5. 2 Effect of Interpenetrant Concentration on Surface Free Energy

Samples were tested in their dehydrated state, as described in section 2. 6 and all samples had an equilibrium water content less than 5%. Samples containing THFFA were below their glass transition at room temperature, and as a consequence showed inconsistent results.

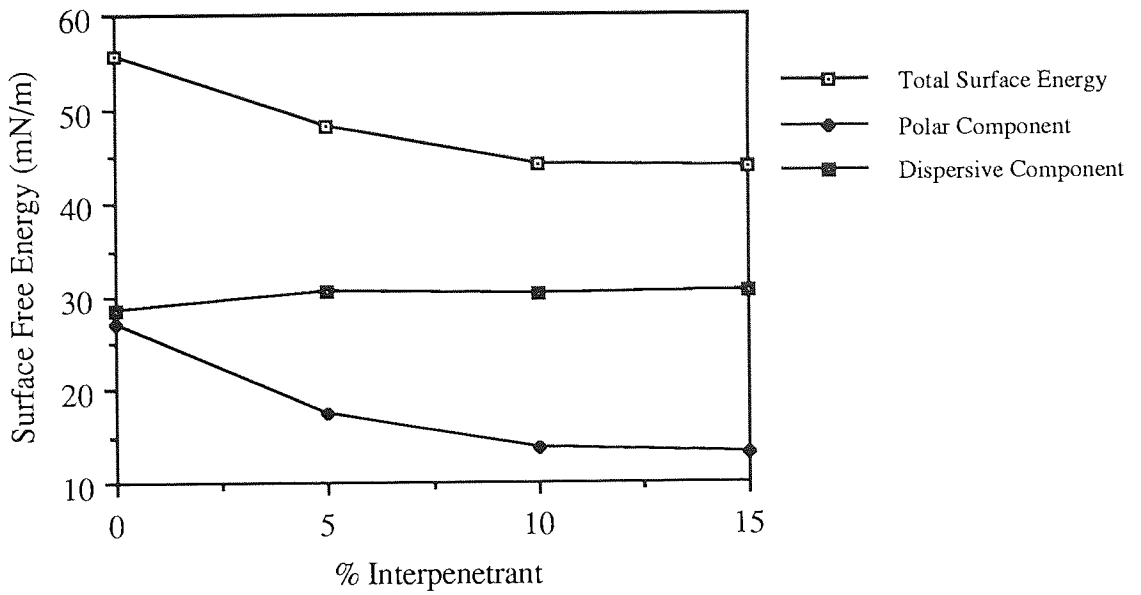


Figure 5. 1 Effect of CAB Concentration on Surface Free Energy in THFFMA Samples

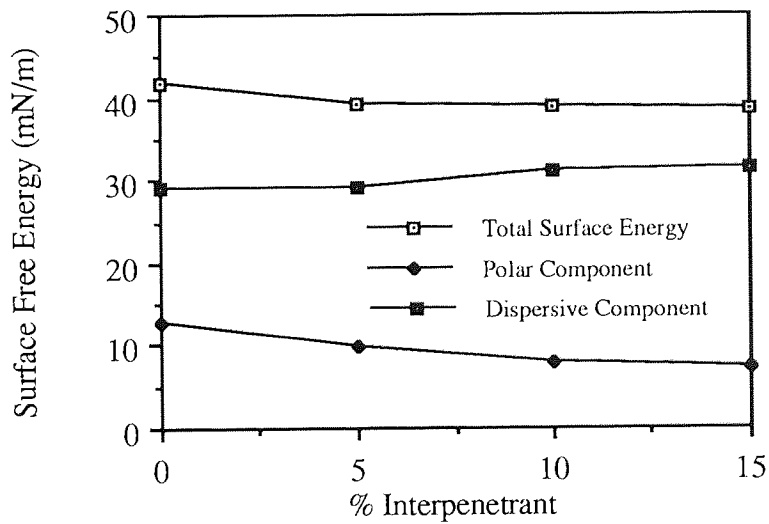


Figure 5. 2 Effect of CAB Concentration on Surface Free Energy in Tert-butyl Methacrylate Samples

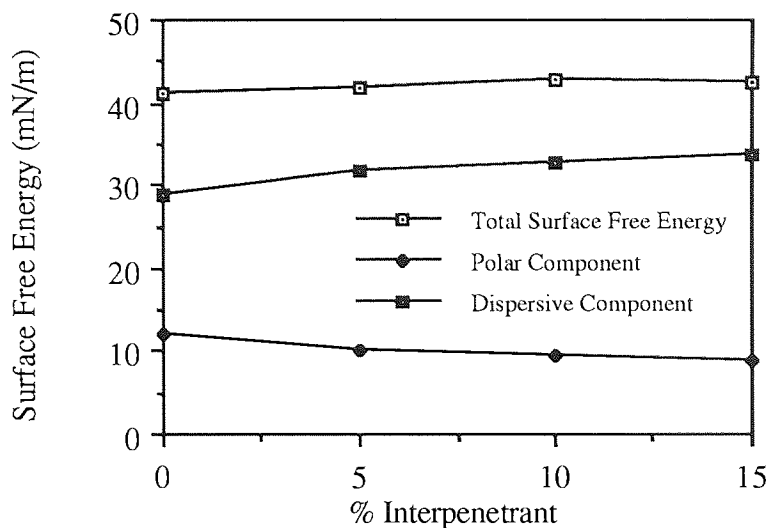


Figure 5. 3 Effect of CAB Concentration on Surface Free Energy in Iso-butyl Methacrylate Samples

All the samples show surface free energies in a similar region to the dehydrated hydrogel CAB semi-IPN samples. The dispersive component once again dominates the surface free energy of the system.

5.2.1 Effect of Interpenetrant on Polar Component of Surface Free Energy

Surface properties, in particular the polar component of surface free energy, were investigated in relation to the percentage of cellulose acetate butyrate incorporated into several methacrylates.

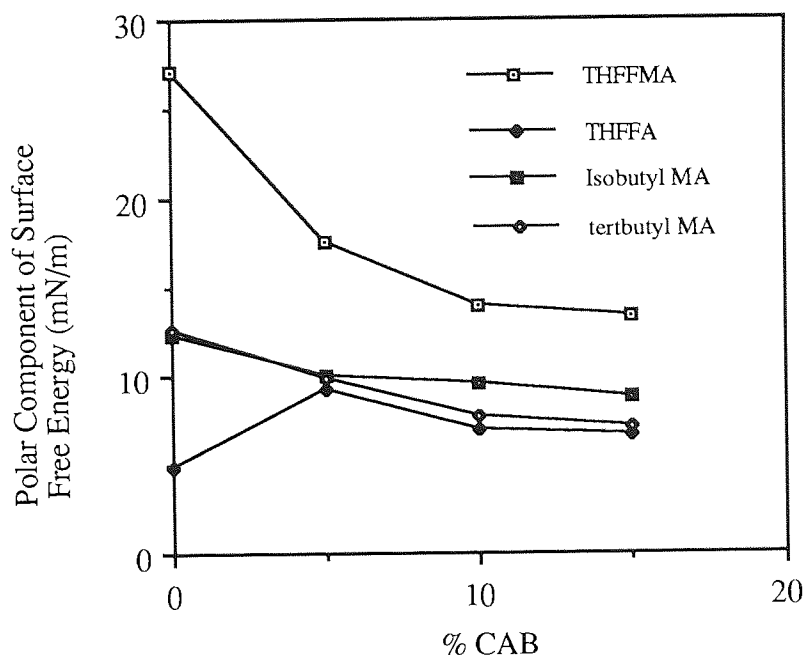


Figure 5. 4 Effect of CAB Content on the Polar Component of Surface Free Energy

In all cases with increasing percentages of the CAB, the polar component of surface free energy is reduced. This effect has previously been observed in hydrogel samples, where incorporating CAB leads to ester groups expressing themselves at the surface and hence a reduction in polar component of surface free energy is observed. All of the systems shown in figure 5. 4 are incompatible which may lead to a higher concentration of CAB in the systems being expressed at the surface, causing the polar component of surface free energy to fall as increasingly large amounts of CAB are incorporated. This effect is most pronounced in samples containing THFFMA, which is the most polar in the range of methacrylates used in this work. Other samples are of lower polarity, more similar to that of CAB, and hence additions of CAB have a lesser effect.

The THFFA homopolymer at room temperature is below its glass transition temperature and has a rubbery texture with a low wettability. With the addition of CAB, the glass transition increases significantly and forms a material with significantly better wettability. However, as with the other samples with increasing

amounts of CAB, the wettability once again is reduced. It may be thought that the THFFA, being a more polar material, would have a higher polar component of surface free energy than the THFFMA but this however, is not the case. This is explained by the fact that in the THFFMA, the α -methyl group having a high energy to rotation, produces a surface which is more random than the THFFA's surface, which tends to express the polar groups inwardly, resulting in a low polar surface.

5. 3 Relationship between Interpenetrant Concentration and Oxygen Permeability

Figures 5. 5 and 5. 6 illustrate the effect of cellulose acetate butyrate on the oxygen permeability of a range of methacrylates.

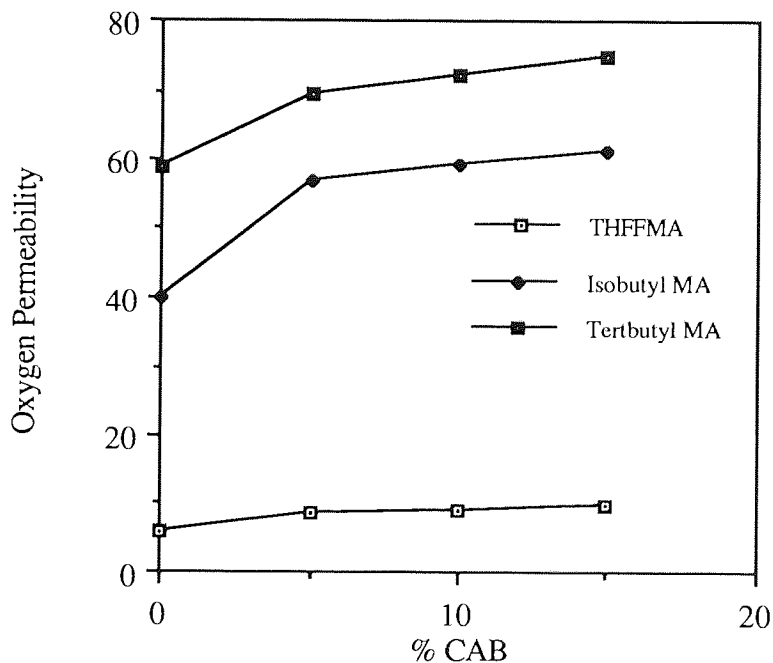


Figure 5. 5 Effect of the CAB Content on the Oxygen Permeability of Methacrylate Semi-INP's

Units of oxygen permeability, Dk , are 10^{-11} cc mm/(cm² s cm Hg).

As seen in figure 5. 5, when an increasing amount of cellulose acetate butyrate is incorporated into the chosen methacrylates the oxygen permeability also increases.

This is due to the bulky nature of the CAB structure which causes a less efficient packing arrangement of polymer chains to occur. This allows for larger 'gaps' to be present in the structure, resulting in an increasing in oxygen mobility within the structure. In addition this graph shows how the bulkier structure of the tert-butyl methacrylate results in a higher oxygen permeability than the iso-butyl methacrylate and the even less bulky THFFMA. If tables 5. 3 - 5. 5 are studied, it appears to follow that for higher 'onset' temperatures, and hence the higher glass transition temperatures, an increase in oxygen permeability results. It is noted that the packing arrangement of polymer chains is related to both the glass transition temperature and the oxygen permeability.

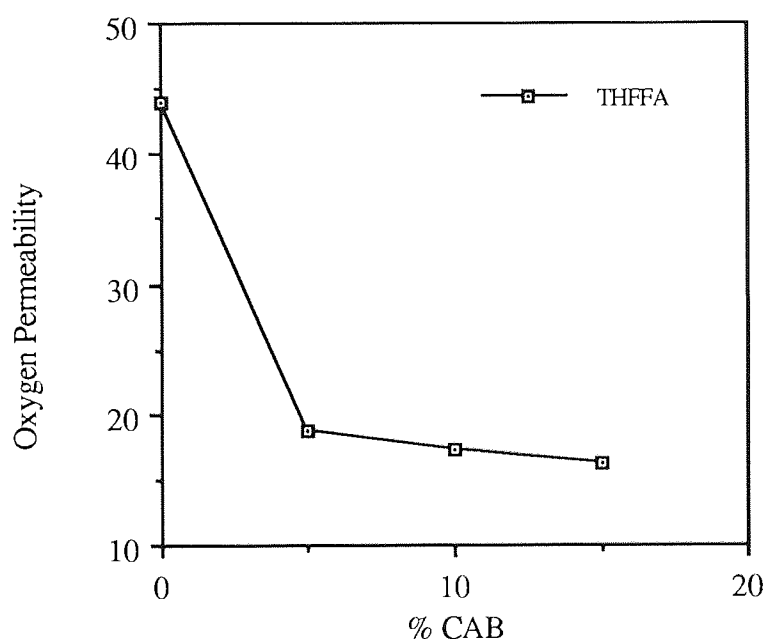


Figure 5.6 Effect of the CAB Content on the Oxygen Permeability of Tetrahydrofurfuryl Acrylate

The oxygen permeability of the THFFA : CAB samples show that the inclusion of CAB causes the oxygen permeability to fall, figure 5. 6. This differs from the results obtained for the other samples shown in figure 5. 5 and is explained by the THFFA homopolymer being below its glass transition temperature at room temperature. However, when combined with CAB the Tg is raised to above room temperature and this gives the molecules within the matrix significantly less mobility in the semi-IPN

than in the homopolymer. Backbone rotation is reduced which reduces the movement of oxygen molecules. However, with increasing amounts of CAB, creating a more porous structure, it would be expected that the oxygen permeability would rise. This is not the case but no significant loss in oxygen permeability is observed either.

5. 4 Relationship Between Oxygen Permeability and Polar Component of Surface Free Energy

As both the polar component of surface free energy and the oxygen permeability of a material need to be within a certain range for the material to be suitable in contact lens applications, it is desirable to investigate how these two properties relate, and if indeed they do relate to each other. Figure 5. 7 illustrates the polar component of surface free energy and the oxygen permeability of methacrylate : CAB semi-interpenetrating polymer networks. It is noted that the polar component of surface free energy for CAB is approximately 6.4 mN/m.

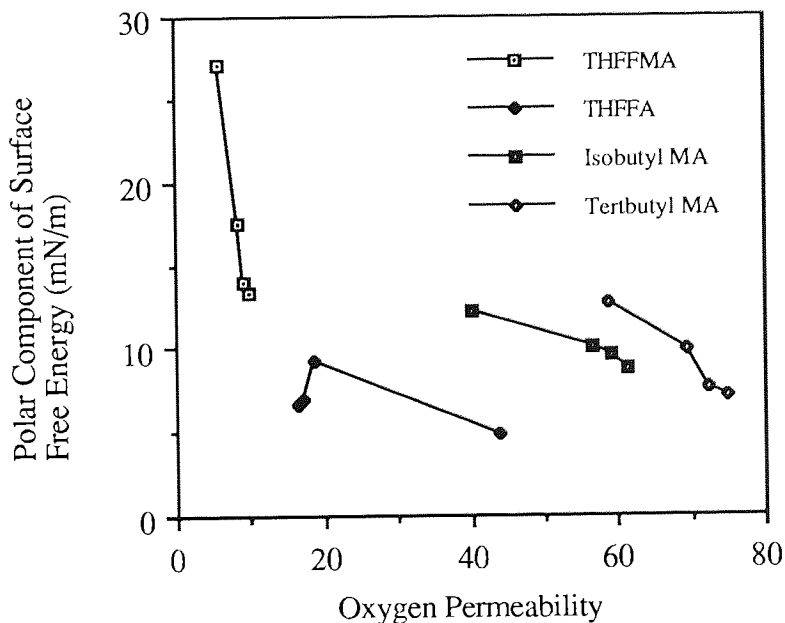


Figure 5. 7 Relationship of Polar Component of Surface Free Energy and Oxygen Permeability in Methacrylate / Acrylate : CAB Semi-IPN's

As can be seen in figure 5. 7 the general trend, for any family of materials tested here, is that when the oxygen permeability increases, the polar component of surface free energy decreases. It appears that the butyl groups in the CAB tend to pack in the surface of the polymer which results in a fall in the polar component of surface free energy, when increasing amounts are incorporated into the samples. The drop in oxygen permeability is less pronounced in the tetrahydrofurfuryl methacrylate samples. In addition the polar component of surface free energy is the highest in the families of materials used in this study. This makes it a good material to base further experimental compositions upon in order to develop materials suitable for contact lens applications.

5. 5 Thermal Mechanical Analysis

Although previously mentioned, the mechanical properties of low water content materials are difficult to measure in the traditional way, using tensiometry. However, using thermal mechanical analysis can give an idea as to how incorporating increasing amounts of interpenetrants into homopolymers can effect the temperature of 'onset' or the temperature at which the materials begin to soften. In addition this technique gives us information about the practical aspects of this project, using an interpenetrant as a reinforcing agent, especially in these non-hydrogel systems. However, an indication of the reinforcing action of interpenetrants in dehydrated hydrogels can also be obtained.

<u>Composition</u>	<u>Onset Temperature °C</u>
THFFMA	51.64
THFFMA:CAB 95:5	51.93
THFFMA:CAB 90:10	54.25
THFFMA:CAB 85:15	56.08

Table 5. 3 'Onset' Temperature of THFFMA : CAB Semi-IPN's

<u>Composition</u>	<u>Onset Temperature °C</u>
IBUTMA	55.71
IBUTMA:CAB 95:5	63.65
IBUTMA:CAB 90:10	66.32
IBUTMA:CAB 85:15	69.42

Table 5. 4 'Onset' Temperature of Iso-butyl MA: CAB Semi-IPN's

<u>Composition</u>	<u>Onset Temperature °C</u>
TBMA	74.25
TBMA:CAB 95:5	84.25
TBMA:CAB 90:10	91.97
TBMA:CAB 85:15	98.05

Table 5. 5 'Onset' Temperature of Tert-butyl MA: CAB Semi-IPN's

Tables 5. 3-5. 5, especially tables 5. 4 and 5. 5, show that the softening temperature is considerably lower than the glass transition temperatures expected for the homopolymers of these methacrylates⁴⁰. Reported values of T_g for the methacrylate homopolymers used in this work are as follows; THFFMA 47°C⁴⁷, TBMA 115°C, IBUTMA 60°C and IBMA 114°C⁴⁰. It is, however important to note that the onset temperature is the point at which deformation begins, the glass transition temperature is a characteristically the mid point of a transition which may span 30°C or more. It is therefore no wonder that results are so much lower than other published glass transition temperatures quoted for the methacrylates used in this work. Although this is not a precise method of determining glass transition temperatures, it is a reproducible technique giving results within 2°C of each other. The patterns that emerge from these results are somewhat predictable, tert-butyl MA generally having the highest onset followed by iso-bornyl MA and THFFMA having the lowest

values. In all cases the onset temperature increases with increasing amounts of CAB, which is an indication that the interpenetrant is acting to stiffen the matrix.

5. 6 General Conclusions

Chapter 5, although highlighting the difficulties involved in producing semi-IPN's in the absence of NVP, shows some of the advantageous effects that can be achieved by forming materials of this type. Considerable increases in toughness are achieved, this is reflected in the increase in onset temperature, in otherwise brittle materials. In addition another useful effect is the increase in oxygen permeability obtained with the incorporation of the bulky CAB into the system. Surface properties in these systems show similar patterns to those obtained with dehydrated materials, as seen in previous chapters. Once again THFFMA containing materials exhibiting the highest polar component of surface free energy. In relating the oxygen permeability to the polar component of surface free energy, a loss of oxygen permeability is associated with an increase in polar component. This is a familiar story, control of this effect would be advantageous.

CHAPTER 6

Oxygen Permeable Materials

6.1 Introduction

Oxygen permeability is a characteristic specific to a particular material. It is dependent on temperature, pressure, thickness and the equilibrium water content in hydrogel materials. Oxygen transport through contact lenses is of great importance for the proper functioning of the cornea. Placing a contact lens in the eye alters the oxygen flux causing normal corneal metabolism to be no longer maintained⁷². Swelling of the cornea occurs when the oxygen tension on the precorneal tear film is below approximately 70-90 mm Hg, and when oxygen flux into the corneal epithelium decreases below the value of $5.5 \times 10^{-6} \text{ cm}^3 \text{ of O}_2 / \text{cm}^2 \text{ s}$. Therefore, it is desirable to know the materials most suitable for use in the design of contact lenses. Materials having high oxygen permeability have often been shown to have a low polar component of surface free energy, and hence low wettability. As wettability is a major factor when considering the fabrication of contact lenses, it is desirable to design a material which has both high oxygen permeability and high wettability.

Silicon-containing polymers with high oxygen permeabilities have been extensively investigated for medical purposes^{70,71}. Silicone rubber, itself, was one of the materials first suggested for use as a contact lens. However, it is difficult to harness this material into a clinically acceptable contact lens due to its hydrophobic nature and the difficulty in generating a hydrophilic surface on the material with any degree of permanence. A range of tris-(trimethylsiloxy)- γ -methacryloxypropyl silane or 'TRIS' containing polymers were synthesised, TRIS's structure is shown in figure 6. 1. This material has been shown to enhance oxygen permeability⁷¹, however, it has a glass transition temperature below room temperature. This is a disadvantage when a lathe cutting technique, the most widely used processing method for non-hydrogel lenses, is employed in the processing of lens materials. Materials with a yield temperature greater than 50°C would be useful to enable lenses free of distortion to be produced. Also, as with silicone rubber based lenses, it has a very low polar component of surface free energy making it necessary to enhance

Samples were all tested at standard room temperature and pressure; it is well documented that these parameters have significant effects on oxygen permeability⁷⁶. Errors may occur due to 'pin holes' being present in the sample which are unobserved by the eye. In addition edge and boundary effects can occur, particularly in rigid gas permeable contact lenses, having a set shape that may not be pliable enough at the edges, leaving small gaps where the lens meets the column which gas passes through. Taking a range of readings over a range of sample thicknesses and taking an average reading could alleviate this problem, provided a calibration had been carried out on a suitable range of samples of known permeability, such as PMMA, at various thicknesses. However, this is not always practical in that it is a very timely procedure and a range of thicknesses of lenses may not be readily available.

6. 2 Effect of 'TRIS' on Methacrylate Copolymers and Terpolymers

Copolymers of 'TRIS' :MA were synthesised and the effect this had on the oxygen permeability, surface properties and glass transition temperatures of the materials was investigated.

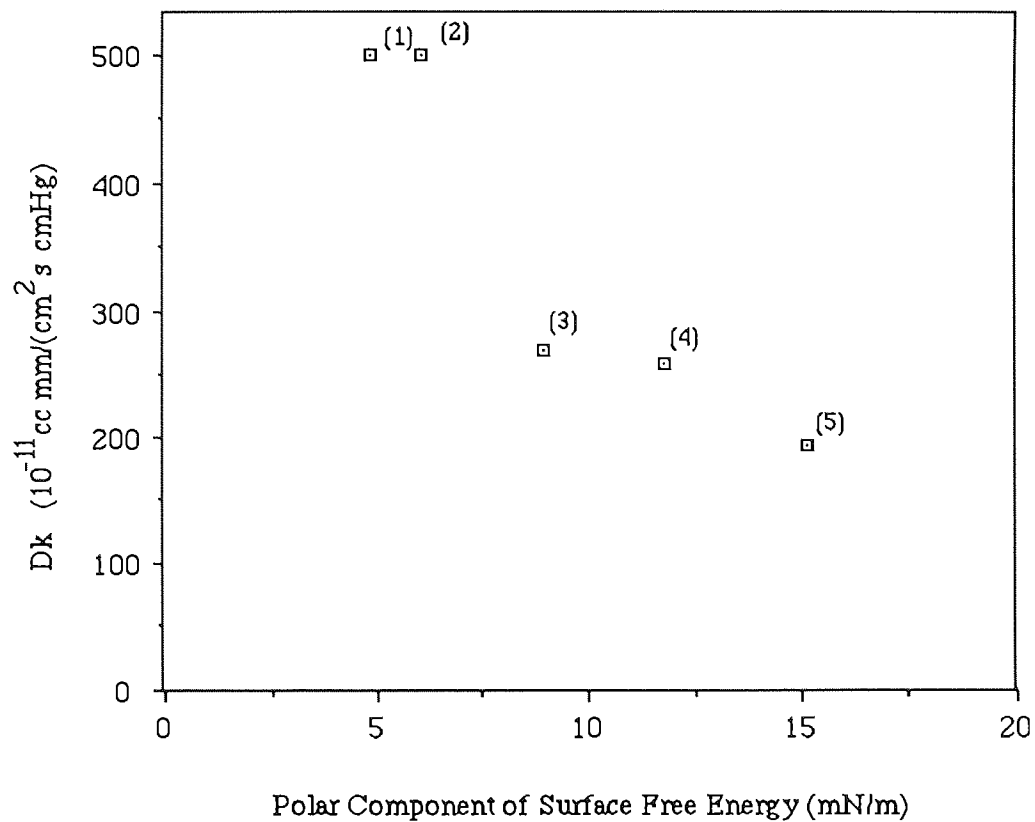


Figure 6.2 Effect of Polar component of Surface Free Energy on Oxygen Permeability for a range of TRIS : Methacrylate Copolymers

Key

- (1) TRIS
- (2) TRIS:Hexafluoro-iso-propyl MA 50:50
- (3) TRIS:Tertiary butyl MA 50:50
- (4) TRIS:Iso-bornyl MA 50:50
- (5) TRIS:Tetrahydrofurfuryl MA 50:50

6.2.1 Relationship between Surface Polarity and Oxygen Permeability

Figure 6. 2 shows the oxygen permeability of methacrylate : TRIS copolymers as a function of their polar component of surface free energy. From this graph while it is apparent the oxygen permeability of TRIS homopolymer is excellent, its polar component of surface free energy is the lowest of this range of polymers. The oxygen permeability, as predicted, increases considerably with the inclusion of TRIS into any of the chosen range of methacrylates, which in turn enhances the polarity of the TRIS. The addition of hexafluoro-iso-propyl methacrylate gives rise to a small increment in the polar component of surface energy and hence its wettability, but has little adverse effect on the oxygen permeability. The fluoro-carbon bonds allow more oxygen to pass through than hydro-carbons and although this network is glassy and immobile, it is not as tightly packed and oxygen molecules can move more readily through the material. In addition the glass transition temperature of this combination is higher than the TRIS homopolymer, instantly making it a more desirable material. Unfortunately the increase in polarity is only small, therefore a balance of desirable properties had to be found. It was noted that THFFMA gave the greatest enhancement of surface properties in TRIS copolymers. Therefore, on the basis of these results, a range of terpolymers containing differing amounts of TRIS, hexafluoro-iso-propyl methacrylate and THFFMA were made. The effect the different compositions have on oxygen permeability with respect to the polar component of surface free energy can be seen in figure 6.3.

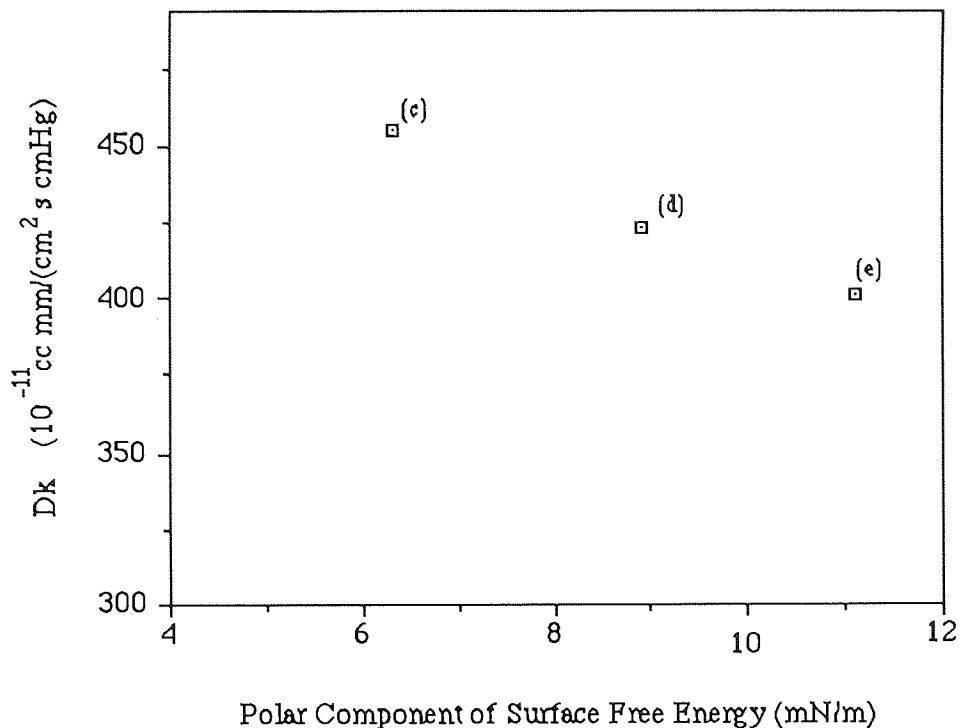


Figure 6. 3 Polymers Increasing the Polar Component of Surface Free Energy whilst retaining a High Oxygen Permeability

Key

- (a) TRIS
- (b) TRIS:Hexafluoro-iso-Propyl MA 50:50
- (c) TRIS:Hexafluoro-iso-Propyl MA:THFFMA 47.5:47.5:5
- (d) TRIS:Hexafluoro-iso-Propyl MA :THFFMA 45:45:10
- (e) TRIS:Hexafluoro-iso-Propyl MA :THFFMA 42.5:42.5:15

Figure 6. 3 shows that significant increases in surface polarity can be achieved by the addition of small percentages of tetrahydrofurfuryl methacrylate and this is achieved without substantial reductions in oxygen permeability.

6. 3 Effect of 4-META on the Surface Properties and the Oxygen Permeability of Methacrylate Copolymers

All the samples synthesised in this section have been made with TRIS : MA 50 : 50, with small additions of 4-META, seen in figure 6. 4. 4-META is added in increasing proportions following the method outlined in Chapter 2. The 4-META is dissolved using tetrahydrofuran as a solvent prior to adding the other components in the system. In small amounts the effect of using solvents in systems such as these has been reported to have no significant effect⁷⁷. The effect of 4-META on the polar component of surface free energy in relation to the oxygen permeability was studied.

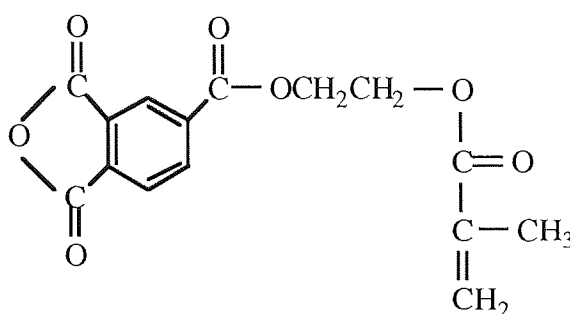


Figure 6. 4 4-Methacryloxyethyl Trimellitate

The units of oxygen permeability, D_k , used through out this work are $\times 10^{-11}$ cc mm / (cm² s cm Hg).

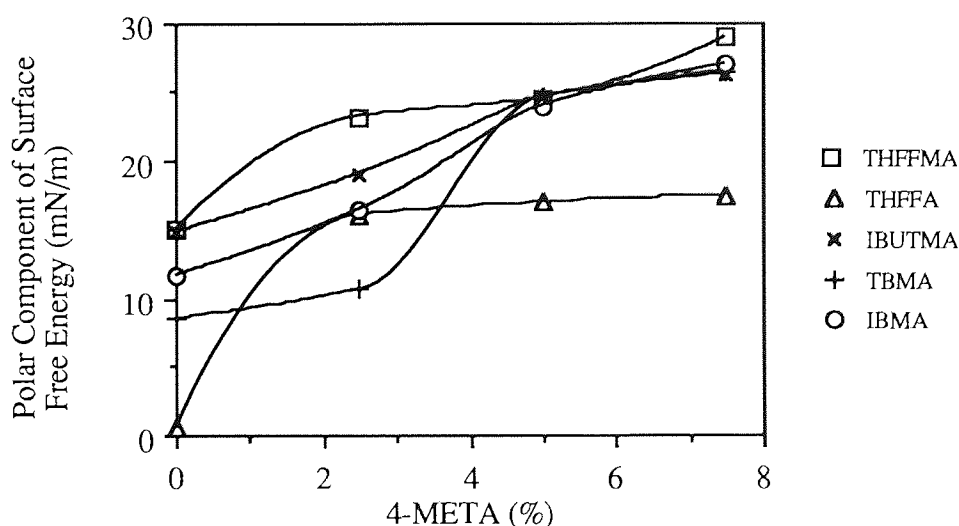


Figure 6. 5 Effect of 4-META on the Polar Component of Surface Free Energy in TRIS : MA 50:50 copolymers

As can be seen from figure 6. 5 with small incremental increases in 4-META, in all samples, quite substantial increases in the polar component of surface free energy occurs. If particular samples are studied more closely in relation to the oxygen permeability, in figures 6. 6-6. 10, patterns begin to emerge.

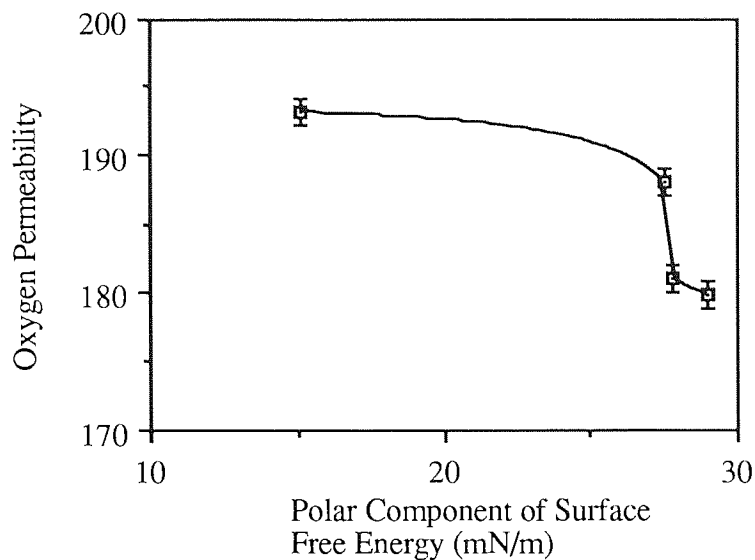


Figure 6. 6 Relationship between the Polar Component of Surface Free Energy and Oxygen Permeability with increasing amounts of 4-META in TRIS 50 : THFFMA 50 : copolymers

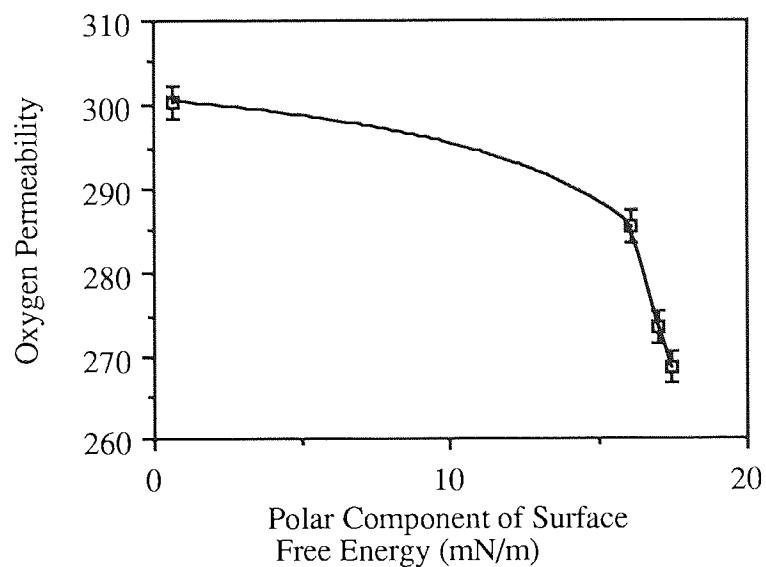


Figure 6.7 Relationship between the Polar Component of Surface Free Energy and Oxygen Permeability with increasing amounts of 4-META in TRIS 50 : THFFA 50 : copolymers

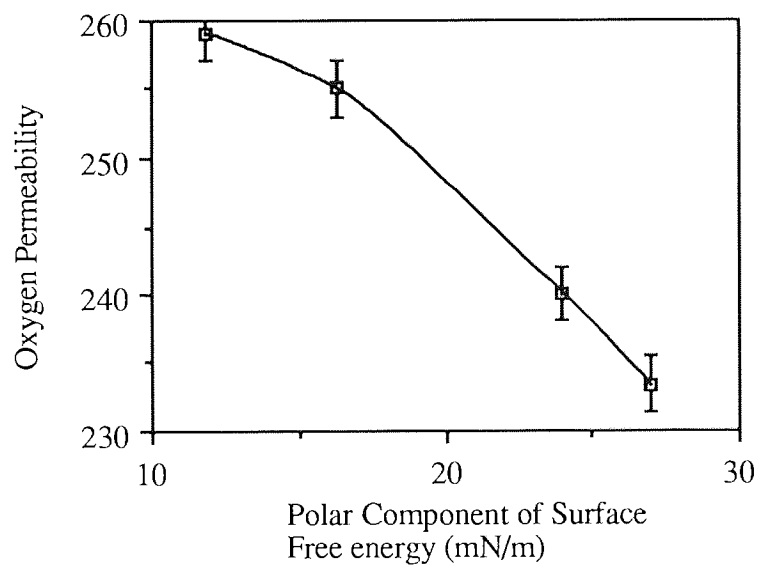


Figure 6.8 Relationship between the Polar Component of Surface Free Energy and Oxygen Permeability with increasing amounts of 4-META in TRIS 50 : Iso-bornyl MA 50 : copolymers

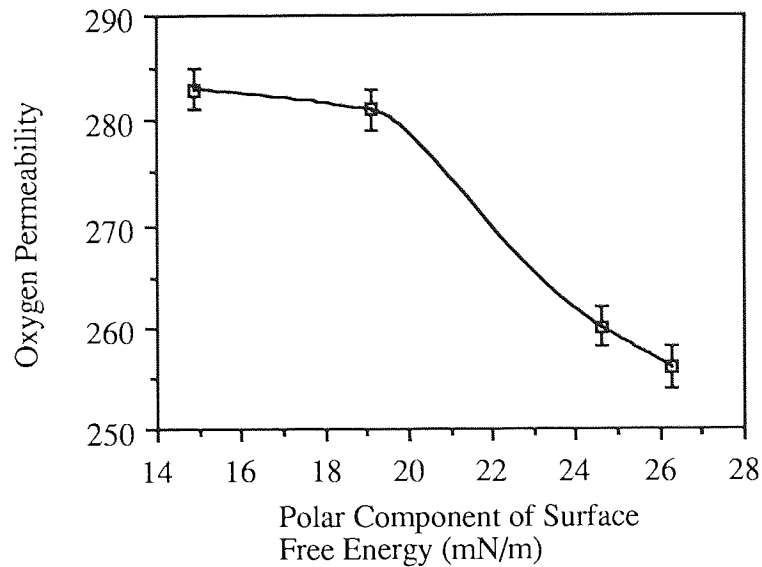


Figure 6. 9 Relationship between the Polar Component of Surface Free Energy and Oxygen Permeability with increasing amounts of 4-META in TRIS 50 : Iso-butyl MA 50 : copolymers

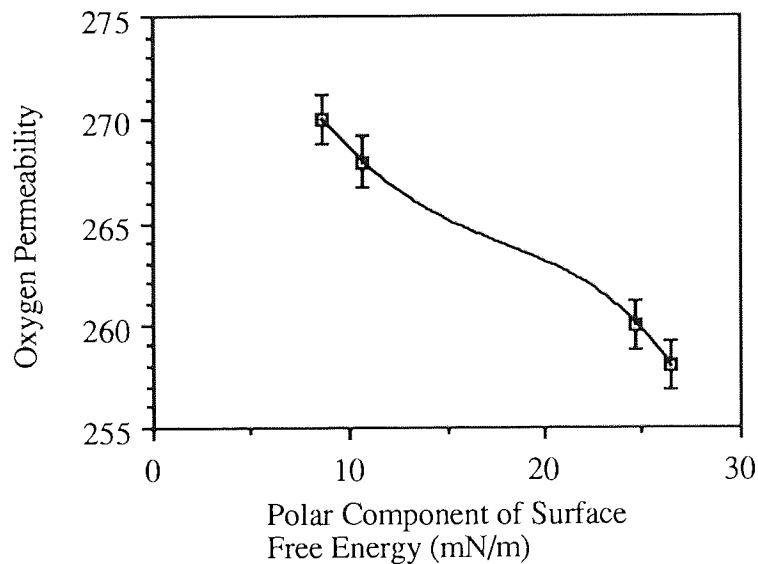


Figure 6. 10 Relationship between the Polar Component of Surface Free Energy and Oxygen Permeability with increasing amounts of 4-META in TRIS 50 : Tert-butyl MA 50 : copolymers

Figures 6. 5 - 6. 10 illustrate the effect of adding 4-META into methacrylate copolymers. With an increase in the 4-META concentration there is an increase in the polar component of surface free energy. However, there will be a limit to the

achievable polar component, as with an increasing amount of 4-META there will come a point when mutual hydrogen bonding will occur, lessening the effect of the anhydride groups at the surface. This effect should be less marked than COOH-COOH bonding in methacrylic acid, which has been used previously in materials as a wetting agent. This is due to the 'long leash' between bond and polar group, allowing the polar group to be freer to concentrate at the surface. It was hoped, and was demonstrated, that small concentrations would have disproportionately high effects. As the concentration increased, the materials behaved more like a conventional polar monomer, inter-chain bonding reducing chain mobility and thus permeability. The greatest percentage gain in polarity, with the least derogatory effect in the oxygen permeability, tends to be with 2.5% of 4-META. Figures 6.6-6.10 show that a good gain in polarity can be achieved with a modest fall in permeability. However, with figures 6.6 and 6.7, samples made with THFFMA and THFFA, with an increasing amount of 4-META there is a diminishing return effect. Hence, it is deduced that the principle works, that the more polar groups present, the more they bond with each other, thus setting up an immobile layer which lowers oxygen permeability. However, when at a low concentration, the polar groups want to 'get-out' of the bulk material and flee to the surface. It is thought that samples containing THFFMA and THFFA show a greater loss in oxygen permeability due to their structure being less bulky than the IBMA, IBUTMA and TBMA, hence making the polar coupling more noticeable in these samples.

6. 4 Thermal Mechanical Analysis

As previously seen in chapter 5, thermal mechanical analysis can be a useful technique in determining the 'onset' or softening temperatures of rigid materials giving an indication of the stiffness, or mechanical properties of those materials. In this chapter, when considering rigid gas permeable contact lens applications, the 'onset' temperature would give an indication of the ability of the material to undergo processing techniques without deforming. Compositions exhibit yield temperatures, or softening temperatures, which may be several degrees lower than T_g. Yield

temperatures above 50°C have been reported to be preferable to cope with local heat generated in lathe cutting and polishing. Table 6. 1 shows the softening temperatures for copolymers of TRIS : MA 50 : 50.

<u>Composition</u>	<u>Onset Temperature °C</u>
TRIS : THFFMA	35
TRIS : Iso-butyl MA	43
TRIS : HFIPMA	50
TRIS : TBMA	69
TRIS : Iso-bornyl MA	74

Table 6. 1 Thermal Mechanical Analysis Data for TRIS : MA Copolymers

As expected when copolymerising with TRIS, which has a glass transition temperature lower than room temperature, onset temperatures are lower than those obtained with the homopolymers of these materials. Copolymerisation with TRIS, although lowering onset temperatures in all cases, is not necessarily a straight forward relationship. Components that have different reactivity ratios give differences in packing leading to different resistances to deformation. In addition, results obtained for the softening of several of these materials cover a wide range of temperatures. This may be due to residual monomer being present, which may in addition lower the onset temperature, and the conversion being incomplete allowing plasticisation to occur.

Although results are clear, reproducible and give information about conversion, these results more importantly give information, together with surface and oxygen permeability data, about the choice of materials for multicomponent systems. Table 6. 2 shows the three component system of TRIS : HFIPMA : THFFMA, which was shown to have a good combination of surface and oxygen permeability properties.

<u>Composition</u>	<u>Onset Temperature °C</u>
TRIS : HFIPMA 50 : 50	50
TRIS : HFIPMA : THFFMA 47.5:47.5:5	69
TRIS : HFIPMA : THFFMA 45:45:10	56
TRIS : HFIPMA : THFFMA 42.5:42.5:15	51

Table 6. 2 Thermal Mechanical Analysis Data for TRIS : HFIPMA : THFFMA Terpolymers

If to samples of TRIS : HFIPMA, additions of THFFMA are added, it would be expected that as the softening temperature of this material is similar to the copolymer of TRIS : HFIPMA, the onset temperature would be similar. However, this table is a prime example of the effect of different packing affecting the resistance to deformation, which causes the onset temperature to significantly rise with the inclusion of THFFMA into the system.

Table 6. 3 gives some examples of multicomponent systems which have been composed from data shown earlier in this chapter.

<u>Composition</u>	<u>Onset Temperature °C</u>
TRIS:HFIPMA:THFFMA 47:5:47.5:5	69
MAA:TRIS:IBUTMA 10:10:80	83
4-META:TRIS:THFFMA:TBMA 5:20:15:60	73

Table 6. 3 Multicomponent Systems with High Onset Temperatures

This table shows that although it is difficult to deduce how materials will act looking purely on a molecular basis, instinctive choices of monomer can produce systems with suitable properties which are required for contact lens processing techniques.

6.5 General Conclusions

Since for contact lens applications a degree of surface polarity is important. Methacrylic acid has often been used as a wetting agent due to its polarity. An attempt was made to replace methacrylic acid, which although polar adversely affects oxygen permeability. This is because methacrylic acid has very little bulk and strong polar attraction. In addition to modifying surface properties it produces a high degree of interchain attraction and consequently dramatically reduces oxygen permeability. The use of methacrylates with bulky side groups but with polar components were investigated as possible replacements. Firstly THFFMA was used in conjunction with TRIS and HFIPMA. THFFMA has a polar oxygen atom in the ring structure, this enhances polarity and again reduced oxygen permeability, see figure 6.3, but with a less dramatic effect than that associated with methacrylic acid. An equally polar molecule 4-META was also investigated. Incorporation of this molecule was found to produce an optimum balance of properties at low concentrations, see figures 6.5-6.10. The net effect was to identify a combination of TRIS based polymers that produced attractive balance of mechanical, surface and transport properties than is possessed by currently available commercial materials.

Although a final 'ideal' contact lens composition has not been identified, this chapter has illustrated the wide range of properties that can be achieved by carefully combining materials which possess one or more of the desirable properties required for a contact lens.

CHAPTER 7

Conclusions and Suggestions for Further Work

7.1 Conclusions

This study set out to determine and control the factors involved in polymer behaviour. By careful choice of monomers and interpenetrants, a range of properties such as mechanical, oxygen permeability, surface and equilibrium water content, were achievable.

Initial work involved the production of simple hydrogel copolymers. N-vinyl pyrrolidone was chosen as the hydrophilic component in the systems because it is widely used for producing high equilibrium water content materials. Bulky methacrylates with hydrophilic groups were chosen as comonomers. One of the limiting factors with hydrogel polymers are their poor mechanical properties. It was thought, and shown, that bulky methacrylates with high glass transition temperatures would improve the mechanical properties of these systems at a given equilibrium water content significantly more than linear methacrylates. In addition methacrylates of this type have a lower density than linear materials which would hopefully have an advantageous effect on the oxygen permeability of such systems. This effect was not displayed in hydrogel systems, where adding methacrylate to the system reduced the EWC, which in turn reduced the oxygen permeability, but was displayed in the low equilibrium water content materials. The bulkiest methacrylate in the study, tert-butyl methacrylate, showed the highest oxygen permeability followed by iso-butyl methacrylate and tetrahydrofurfuryl methacrylate. Methacrylates with hydrophilic groups were chosen in an attempt to produce a wettable surface, a desirable property if considering contact lenses as a potential use. Tetrahydrofurfuryl methacrylate was found to be the most promising comonomer studied giving the best balance of desirable properties when considering biomaterial production.

Studies showed that monomer structure was one of the major controlling factors of polymer properties, however it was not the overriding factor. In general simple copolymers behaved in a manner which first inspection of monomer structure predicted. Improvements in mechanical properties occurred with incorporation of

high glass transition temperature components and a reduction of EWC, with increasing percentages of methacrylate in the system, however, this is not always the case. In samples containing THFFMA and NVP, it was thought that the tensile strength and initial Young's modulus would be considerably higher than those observed. This may be explained by the fact that the THFFMA homopolymer does not reach an equilibrium water content after 33 months⁴³, which may cause the glass transition temperature of fully hydrated THFFMA to be considerably lower than that of the dehydrated sample. Therefore, a Tg of approximately 47°C which is reported for dehydrated THFFMA may be several degrees higher than the actual value if this material were in a copolymer with NVP and could be isolated between the hydrophilic component and then hydrated. This would cause the energy to rotation to drop, and hence, stiffness or Young's modulus would be lower than expected by looking only at the properties the material would be expected to exhibit in the dehydrated state. This illustrates that although many polymer properties can be predicted there will always be exceptions to the general rules.

Formation of semi-interpenetrating polymer networks present exciting potential in the production of polymers with novel properties. Firstly semi-IPN's were used to improve the poor mechanical properties that high water content hydrogels exhibit. This was highly successful and at a given water content materials could be made with significantly improved mechanical properties. However, this was not the only use semi-IPN's presented. By the incorporation of a large bulky material, such as CAB, improvements in oxygen permeability were observed. Surface properties were in a similar region to hydrogel copolymers of similar EWC in this study, however, this will not be the case with all semi-IPN systems, surface energies of semi-IPN's would be hard to predict with experimental work being the only real way of finding out what is occurring at the polymer surface. Unlike simple hydrogel systems it is hard to predict at first inspection the properties of systems like this will act. Compatibility of systems is reflected in the clarity of materials in the dehydrated and hydrated states, incompatibility in the dehydrated state shows phase separation and predictably resulted in poor and erratic elongation. Incompatibility, (opalescence),

that is only produced when the SIPN is hydrated did not affect the integrity and continuity of the polymer matrix to the same extent. Work on semi-IPN's was split into several sections, novel methacrylate - NVP copolymers as matrices for an established interpenetrant, CAB; novel methacrylate - NVP copolymers as matrices for novel interpenetrants; non-hydrogel methacrylate - CAB systems.

Simple semi-IPN hydrogel systems, especially compatible systems, show great potential for biomedical applications. Systems using CAB as an interpenetrant have already been studied for such applications as articular cartilage², with the use novel methacrylates in conjunction with CAB a wider range of controllable properties have been established. This information can be used as a data base when developing more complex systems. Polyurethanes have been used for many years now in medical applications with varying degrees of success, using ether and ester polyurethanes as interpenetrants highlighted the range of polymer properties than are achievable. By looking at the compatibility of the two materials in each systems, differences in mechanical behaviour could be explained. Ether polyurethanes have been previously used as interpenetrants with a degree of success. The ester polyurethanes appear, from this preliminary work, to be a better system. Ester polyurethanes are more compatible with the monomers used in this study and gave greater improvements in mechanical properties. These type of systems holds great interest for future work in mimicking biological materials such as an artificial articular cartilage and an artificial cornea.

In non-hydrogel semi-IPN systems the major problem was finding interpenetrants which would dissolve in the range of novel methacrylate monomers used throughout this work in the absence of NVP. Predissolving interpenetrants before the addition of monomer allowed for a range of methacrylate:CAB systems to be developed. Limited success was achieved with the use of other interpenetrants, THFFMA was found to be the best solvent for the ester polyurethane and polycarbonate, however, 5% was the maximum amount of either of these polymers which could be incorporated. Methacrylate : CAB semi-IPN's were considerably tougher than

methacrylate homopolymers. Although mechanical properties of these systems were found to be difficult to test using tensiometry, increases in the softening temperature, an indication of glass transition temperature and hence stiffness, with increasing amounts of CAB, were shown by the use of thermal mechanical analysis. In addition to improvement of mechanical properties oxygen permeability was enhanced with increasing amounts of CAB.

As oxygen permeability is a major controlling factor involved in the suitability of a material in the production of contact lenses, it was desirable to integrate the knowledge gained from systems containing novel methacrylates into systems containing a highly oxygen permeable component. Tris-(trimethylsiloxy)- γ -methacryloxypropyl silane, TRIS, has been shown to significantly enhance oxygen permeability, however, TRIS has other properties which make it a less than ideal contact lens material. The least desirable property TRIS exhibits is a low polar component of surface free energy. This would prevent tears forming a stable film over a contact lens. Secondly TRIS has a glass transition temperature less than room temperature. Lathe cutting and polishing techniques generate local heat, so to produce lenses free of distortion by this technique a glass transition temperature greater than 50°C is desirable. By simple copolymerisation with the range of methacrylates used throughout this work, glass transition temperatures were raised enough to make lathe cutting as a processing technique a viable option. In addition, and more importantly, the polar component of surface free energy was significantly enhanced, THFFMA gave the greatest improvement. Fluorinated polymers have also shown high oxygen permeabilities, hexafluoro-iso-propyl methacrylate was added as a third component in TRIS:THFFMA systems. Although this material has a slightly lower oxygen permeability than TRIS its polar component of surface free energy was higher. The terpolymers which resulted showed significantly increased polar component of surface free energy without substantial reductions in oxygen permeability. Combining materials in this way demonstrates how desirable properties from a selection of materials can be harnessed to produce one product with a balance of properties. Another way of further enhancing surface wettability was to

incorporate 4-methacryloxyethyl trimellitate into TRIS:methacrylate copolymers. This material was found to enhance the polar component of surface free energy at small concentrations with little effect on oxygen permeability. The greatest percentage gain in polarity, with the least detrimental effect in the oxygen permeability, was with the addition of 2.5% of 4-META.

Although a final 'ideal' contact lens composition has not been identified a wide range of properties that can be achieved by carefully combining materials which possess one or more of the desirable properties required for a contact lens. In addition to the contact lens industry, the polymers developed in this work may have other uses in the biomedical field where their unique properties may be utilised and developed.

7.2 Suggestions for Further Work

In suggesting future work on hydrogel systems, changing the hydrophilic component in the system may increase the compatibility of systems which are presently incompatible. Although NVP is commonly used for producing higher water content hydrogels it tends to form blocky polymers. It was suggested that NVP be replaced with acryloylmorpholine which may give a better sequence distribution, leading to more compatible systems, particularly with iso-bornyl methacrylate which are cloudy. These systems may be clear if polymer chains were 'broken' into shorter chains. Short chain poly(ethylene glycols), PEG's, have been used to enhance surface properties and using PEG's as interpenetrants or ethylene glycol as a comonomer may produce materials with unique surface properties.

Enhancement of mechanical properties may be achieved by replacing THFFMA with tetrahydropyranyl methacrylate or tetrahydropyran-2-yl methacrylate in hydrogel systems without a deleterious effect to the surface properties. Although these materials have no flexibilising HO-CH₂, they do have high glass transition temperatures and are hydrophilic.

Further enhancement of the polar component of surface free energy in systems containing 4-META may occur if this material were ring opened, with little effect on the oxygen permeable of these systems.

Cell adhesion and spoliation studies would be an indication of clinical performance, therefore it would be desirable to carry out such studies on the families of materials developed throughout this work.

References

- 1 Corkhill, P. H. , Novel Hydrogel Polymers, PhD Thesis,
Aston University, March 1988
- 2 Corkhill, P. H. , Trevett, A. S. and Tighe, B. J. , The potential
of hydrogels as synthetic articular cartilage, UK Conference 'New engineering
concepts and alternative materials for prosthesis', Leeds 1990, reprint in Proc.
Inst. Mech. Engrs. , 1990, 147-155, Vol. 204
- 3 Bray, J. C. and Merrell, E. W. , Poly(vinyl)alcohol) hydrogels for
synthetic articular cartilage, Journal of Biomedical Materials Research, 1973,
Vol. 7, 431-443
- 4 Shahgaldi, B. Amis, A. Wheatley, F. , McDowell, J. and Bentley, G. ,
Repair of cartilage lesions using biological implants, The Journal of Bone
and Joint Surgery, 1991, Vol. 73-B, No. 1
- 5 Hogan, M. J. and Alvarado, J. A. , Weddell, eds, histology of the
Human eye, An Atlas and Text Book, Chapter 3, The Cornea, Published by
Saunders, 1971
- 6 Wichterle, O. and Lim, D. , hydrophilic gels for biological use, Nature,
1960, 185, 117-118
- 7 Yasuda, H. , Olf, H. G. , Christ, B. , Lamaze, C. E. and Peterlin, A. ,
Movement of water in homogeneous water swollen polymers, Water
structure at the water-polymer interface, Ed. Jellinek, H. H. G. , Plenum,
N.Y. , 39-55
- 8 Nelson, R. A. , the determination of moisture in cellulosic materials using
differential scanning calorimetry, Journal of Applied Polymer Science, 1977,
Vol. 21, 645-654
- 9 Hiltner, J. , Cassidy, J. J. and Baer, E. , Mechanical properties of
biological polymers, Journal of Materials Science, Vol. 15, 1985, 455-482
- 10 Murakami, T. , The lubrication in natural synovial joints and prostheses,
JSME International Journal, 1990, Series III., Vol. 33, No. 1, 465-474

- 11 Noguchi, T. , Yamamuro, T. , Oka, M. , Kumar, P. , Kotoura, Y. , Hyon, S. and Ikada, Y., Poly(vinyl alcohol) hydrogel as a artificial articular cartilage: Evaluation of biocompatibility, *Journal of applied Biomaterials*, 1991, Vol. 2, 101-107
- 12 Roorda, W.E., Bodde, H.E., de Boer, A.G. and Junginger, H., Synthetic hydrogels as drug delivery systems, *Pharm. Weekl. (Sci)*, 1986, Vol. 8, 165-189
- 13 Pedley, D. G. , Skelly, P. J. and Tighe, B. J. , Hydrogels in biomedical applications, *British Polymer Journal*, 1980, Vol 12, 99-110
- 14 Park, G. B. , Burn wound coverings - A review, *Biomat. Med. Dev. Art. Org. ,* 1978, Vol. 6, No. 1, 29-37
- 15 Ng, C. O. and Tighe, B. J. , Polymers in contact lens applications VI. The 'dissolved' oxygen permeability of hydrogels and the design of materials for the use in continuous-wear contact lenses, *The British Polymer Journal*, Dec. 1976, 118-123
- 16 Trevett, A. S. , The mechanical properties of hydrogel polymers, PhD Thesis, Aston University, October 1991
- 17 Sperling, L. H. , *Interpenetrating Polymers Networks and Related Materials*, Published by Plenum Press, 1981
- 18 Platzer, N. *Multicomponent polymer systems*, *Applied polymer science*, 2nd ed. , 1985, Chapter 10, 219-237
- 19 Yoe, J. , Sperling, L. and Thomas, D. , Poly(n-butyl acrylate) / polystyrene interpenetrating polymer networks and related materials. II. Aspects of molecular mixing via modulus - temperature studies, *Polymer Engineering and Science*, 1981, Vol. 21, No. 11, 696-701
- 20 Hourston, D. and McCluskey, J. , Semi- and fully interpenetrating polymer networks based on polyurethane-polyacrylate systems. VIII. The influence of the degree of crosslinking of the second formed network on the morphology and properties of polyurethane-polymethylacrylate interpenetrating polymer networks, *Journal of Applied Polymer Science*, 1986, Vol. 31, 645-655

- 21 Frisch, K. C. ,Klempner, D. and Xiao, H. X. Recent studies on interpenetrating polymer networks, *Polymer Engineering and Science*, 1985, vol 25, no. 12, 758-764
- 22 Falcetta, J. J. , Frienos, G. D. and Niu, G. , (to Bausch and Lomb inc.), Solid article formed from a polymer network with simultaneous interpenetration, *Fr. Demande* 2,365,606, 1978
- 23 Dror, M. , Elsabee, M. Z. and Berry, G. C. Interpenetrating polymer networks for biomedical applications, *Biomat. , Med. Dev. , Art. Org. ,* 1979, Vol. 7, No. 1, 31-39
- 24 Mueller, K. F. and Heiber, S. J. , Gradient-IPN-nodified hydrogel beads: Their synthesis by diffusion -polycondensation and function as drug delivery agents, *Journal of Applied Polymer Science* 1982, Vol. 27, 4043-4064
- 25 Bae, Y. B. , Okano , T. , Ebert, C. , Heiber, S. , Dave, S. and Kim, S. W., Heterogeneous interpenetrating polymer networks for drug delivery, *Journal of Controlled Release*, 1991, Vol 16, 189-196
- 26 Nair, P. D. , Mohanty, M. , Rathinam, M. , Jayabalan, V. , N. ,Studies on the effect of degree of hydrophilicity on tissue response of polyurethane IPN's, *Biomaterials*, 1992, Vol. 13, No. 8, 537-542
poly(urethane) interpenetrating polymer networks,
- 27 Desai, N. and Hubbell, J. Surface physical interpenetrating networks of poly(ethylene terephthalate) and poly(ethylene oxide with biomedical applications, *Macromolecules*, 1992, 25, 226-232
- 28 Caravia, L. , Dowson, D. , Fisher, J. , Corkhill, P. H. and Tighe, B. J. , A comparison of friction in hydrogel and polyurethane materials for cushion-form joints, *Journal of Materials Science : Materials in Medicine*, 1993, Vol. 4, 515-520
- 29 Dror, M. , Elsabee, M. and Berry, G. , Gradient interpenetrating polymer networks. I. poly(ether urethane) and polyacrylamide IPN, *Journal of Applied Polymer Science*, 1981, Vol. 26, 1741-1757

- 30 Chatterji, P. and Kaur, H. , Interpenetrating polymer networks : 3.
Properties of the gelatin - sodium carboxymethylcellulose system, *Polymer*,
1992, Vol. 33, No. 11, 2388-2391
- 31 Bae, Y. H. , Okano, T. and Kim, S. W. , A new thermo - sensitive
hydrogel: Interpenetrating polymer networks from *N*-acryloylpyrrolidine
and poly(oxyethylene), *Makromol. Chem., Rapid Commun.* , 1988, Vol. 9,
185-189
- 32 Roha, M. and Wang, B. The effect of functional azo initiator on PMMA and
polyurethane IPN systems. I. synthesis, characterisation, and thermal
effects, *Journal of Applied Polymer Science*, 1992, Vol. 45, 1367-1382
- 33 Hourston, D. and Huson, M. , Semi- and fully-interpenetrating polymer
networks based on polyurethane-polyacrylate systems. XII. The influences
of polymerisation pressure on morphology and properties, *Journal of Applied
Polymer Science*, 1992, Vol. 46, 973-979
- 34 Braden, M. , Composition for use in making bone cement, US patent
4,791,150, December 1988
- 35 Patel, M. P. and Braden, M. , Heterocyclic methacrylates for clinical
applications (1), *Biomaterials*, 1991, Vol. 12, No. 7, 645-648
- 36 Patel, M. P. and Braden, M. , Heterocyclic methacrylates for clinical
applications (2), *Biomaterials*, 1991, Vol. 12, No. 7, 649-652
- 37 Cook, W. D. and Moopnar, M. , Influence of chemical structure on the
fracture behaviour of dimethacrylate composite resins, *Biomaterials*, 1990,
Vol. 11, 272-276
- 38 Davy, K. W. M. and Braden, M. , Mechanical properties of elastomeric
poly(alkyl methacrylates), *Biomaterials*, 1990, Vol. 8 No. 5, 393-396
- 39 Bowden, P. B. , The yield behaviour of glassy polymers, *The Physics of
Glassy Polymers*, Ed. Haward, R. N. , Applied Science, Barking, Great
Britain, 1973, 279-339
- 40 Ed.Brandrup, J. and Immergut, E. H. , *Polymer handbook*, Third edition,
Published by Wiley-Interscience, New York, 1989

- 41 Braden, M. , Polymeric materials in dentistry and related fields, Medical Engineering UK / Japan biomaterials symposium, October 1987
- 42 Clark, R. , Dynamic mechanical thermal analysis of dental polymers (1), Biomaterials, 1989, Vol. 10, No. 7, 494-498
- 43 Patel, M. P. and Braden, M. , Heterocyclic methacrylates for clinical applications (3), Biomaterials, 1991, Vol. 12, No. 7, 653-657
- 44 Patel, M. P. and Braden, M. , Cross-linking and ring opening polymerisation of heterocyclic methacrylates and acrylated, Biomaterials, 1989, Vol. 10, No. 7, 277-280
- 45 Braden, M. , Polymers for dental and other clinical use, Medical Engineering UK / Japan biomaterials symposium, Sept. 1989
- 46 Clarke, R. , Dynamic mechanical thermal analysis of dental polymers (3), Biomaterials, 1989, Vol. 10, No. 8, 630-633
- 47 Clarke, R. , Dynamic mechanical thermal analysis of dental polymers (2), Biomaterials, 1989, Vol. 10, 91-95
- 48 Parker, S. and Braden, M. , Water absorption of methacrylate soft lining materials, Biomaterials, 1989, Vol. 10, No. 8, 630-633
- 49 Atsuta, M. , Abell, A. , Turner, D. , Nakabayashi, N. and Takeyama, M. A new coupling agent for composite materials : 4-Methacryloxyethyl trimellitic anhydride, Journal of Biomedical Materials Research, 1982, Vol. 16, 619-628
- 50 Nakabayashi, N. , Biocompatibility and bonding to dentin, Medical Engineering UK / Japan Biomaterial Symposium, Oct 1987
- 51 Nakabayashi, N. and Kazuhiko, I. , Adhesive bone cement, Medical Engineering UK / Japan Biomaterial Symposium, Sept 1989
- 52 Nakabayashi, N. , Bonding of restorative materials to dentine: the present status in japan, International Dental Journal, Vol. 35, No.2, 145-154
- 53 Liu, Y. K. , Park, J. B. , Njus, G. O. and Stienstra, D. , Bone particle impregnated bone cement, Journal of Biomedical materials Research, Vol. 21, 1987, 247-261

- 54 Bundy, K. J. and Penn, R. W. , Effect of surface preparation on metal / bone cement interfacial strength, Journal of Biomedical materials Research, Vol. 21, 1987, 773-805
- 55 Pourdeyhimi, B, Wagner, H. D. and Schwartz, P. , A comparison of mechanical properties of discontinuous kevlar fibre reinforces bone and dental cements, Journal of materials science, 1986, Vol. 21, 4468-4474
- 56 Ishihara, K. and Nakabayashi, N. Adhesive bone cement both to bone and metals : 4-META in MMA initiated with tri-*n* -butyl borane, Journal of Biomedical Materials Research, 1989, Vol. 23, 1475-1482
- 57 Owens, D. K. , Estimation of the surface free energy of polymers, Journal of Applied Polymer Science, 1969, Vol. 13, 1741-1747
- 58 Moore, W. J. , Physical Chemistry, Chapter 11, Interfaces
- 59 Oxley, H. , Hydrogels containing cyclic and linear polyethers, PhD Thesis, Aston University, April 1991
- 60 Tighe, B. J. , States of matter lecture notes 1990
- 61 Panzer, P. , Components of solid surface free energy from wetting measurements, Journal of Colloid and Interfacial Science, 1973, Vol. 44, no. 1.
- 62 Modification of poly(ether urethane) for biomedical applications by radiation induced graftings, water sorption, surface properties and protein adsorption of grafted films, Journal of biomedical materials research, 1984, Vol. 18, 655-669
- 63 Fowkes, F. M. , Additivity of intermolecular forces at interfacial tensions of dispersion forces in various liquids, 1963, Journal of Physical Chemistry, Vol. 67, 2538-2541
- 64 Tighe, B. J. and Trevett, A. S. , The characterisation of mechanical properties of soft contact lenses, 1990, British Contact Lens Association Transactions, Annual Clinical Conference, Glasgow, 57-61
- 65 Yuanping, G. and Ogilby, P. R. , A new technique to quantify oxygen diffusion in polymer films, Macromolecules, 1992, Vol. 25, 4962-4966

- 66 Alexander, B. and Fleming, J. S. , Evaluation of a chemical technique for determining the oxygen permeability of synthetic membranes, *Journal of Biomedical Materials Research*, 1982, Vol. 16, 31-38
- 67 Compan, V. , Garrido, J. , Manzanares, J. A. , Andres, J. , Esteve, J. S. and Lopez, M., L. , True and apparent oxygen permeabilities of contact lenses, *Optometry and Vision science*, 1992, Vol. 69, No. 9, 685-690
- 68 Kumaki, T. , Sisido, M. and Imanishi, Y. , Antithrombogenicity and oxygen permeability of block and graft copolymers of polydimethylsiloxane and poly(α -amino acid), *Journal of Biomedical Materials Research*, 1985, Vol. 19, 785-811
- 69 Ulubayram, K and Hasirci, N. , Polyurethanes : effect of chemical composition on mechanical properties and oxygen permeability, *Polymer*, 1992, Vol. 33, No. 10, 2084-2088
- 70 Tsutsumi, N. , Nishikawa, Y. , Kiyotsukuri, T. and Nagata, M. , New copolymer of vinyl p-tert-butylbenzoate with 3-methacryloxy-propyltris (trimethylsiloxy) silane and oxygen permeability, *Polymer*, 1992, Vol. 33, No. 1, 209-211
- 71 Tighe, B. and Kishi, M. , GP materials - patents, products and properties, *Optician*, August 5th 1988, 21-28
- 72 Compan, V. , Garrido, J. , Manzanares, J. A. , Andres, J. , Esteve, J. S. and Lopez, M., L. , True and apparent oxygen permeabilities of contact lenses, *Optometry and Vision science*, 1992, Vol. 69, No. 9, 685-690
- 73 Matsumoto, K. and Ping, X. , Gas permeation properties of hexafluoro aromatic polyimides, *Journal of Applied Polymer Science*, 1993, Vol. 47, 1961-1972
- 74 Ishihara, K. , Hiroki, A. and Nakabayashi, N. Adhesive bone cement containing hydroxyapatite particle as bone filler, *Journal of Biomedical Materials Research*, 1992, Vol. 26, 937-945
- 75 Sperling, L. H. , Pure and applied research on interpenetrating polymer networks and related materials, *Polymer Blends and Mixtures*, 1985, Vol. 89, Edited by Walsh *et. al.*

- 76 Kiyotsukuri, T. , Mimaki, M. and Tsutsumi, N. , Oxygen permeability of silicon-containing network polyamide and copolyamide films, *Polymer*, 1991, Vol. 32, No. 14, 2605-2611
- 77 Dominguez, L. ,Novel Hydrogel Based Interpenetrating Polymer Networks, MSc Thesis, Aston University, 1979

APPENDIX 1

Tensile Data

Composition	EWC (%)	Initial Modulus (MPa)	Tensile Strength (MPa)	Elongation at Break (%)	Appearance Hydrated	Appearance Dehydrated
THFFMA:NVP 20:80	82	0.17 Std. Dev. 0.01	0.06 Std. Dev. 0.01	38 Std. Dev. 16	Clear	Clear
THFFMA:NVP 25:75	78	0.19 Std. Dev. 0.02	0.10 Std. Dev. 0.02	63 Std. Dev. 14	Clear	Clear
THFFMA:NVP 30:70	74	0.20 Std. Dev. 0.01	0.12 Std. Dev. 0.04	64 Std. Dev. 20	Clear	Clear
THFFMA:NVP 40:60	64	0.50 Std. Dev. 0.01	0.19 Std. Dev. 0.02	39 Std. Dev. 5	Clear	Clear
THFFMA:NVP :CAB 40:60:5	60	1.03 Std. Dev. 0.04	0.53 Std. Dev. 0.05	59 Std. Dev. 6	White	Clear
THFFMA:NVP :CAB 40:60:10	57	2.04 Std. Dev. 0.19	0.74 Std. Dev. 0.13	51 Std. Dev. 11	White	Clear
THFFMA:NVP :CAB 40:60:15	53	2.89 Std. Dev. 0.20	1.05 Std. Dev. 0.16	49 Std. Dev. 10	White	Clear

Composition	EWC (%)	Initial Modulus (MPa)	Tensile Strength(MPa)	Elongation at Break (%)	Appearance Hydrated	Appearance Dehydrated
THFFMA:NVP 60:40	49	0.51 Std. Dev. 0.03	0.97 Std. Dev. 0.11	190 Std. Dev. 15	Clear	Clear
THFFMA:NVP :CAB 60:40:5	45	2.51 Std. Dev. 0.12	3.39 Std. Dev. 0.21	170 Std. Dev. 12	White	Clear
THFFMA:NVP :CAB 60:40:10	41	7.74 Std. Dev. 0.48	5.57 Std. Dev. 0.29	168 Std. Dev. 16	White	Clear
THFFMA:NVP :CAB 60:40:15	40	15.19 Std. Dev. 2.95	6.19 Std. Dev. 0.53	128 Std. Dev. 17	White	Clear
THFFMA:NVP :CAB 60:40:20	36	39.70 Std. Dev. 4.50	8.02 Std. Dev. 1.05	115 22	White	Clear
THFFMA:NVP :PU1 40:60:5	60	0.60 Std. Dev. 0.60	0.41 Std. Dev. 0.41	72 Std. Dev. 10	Cloudy	Clear
THFFMA:NVP :PU1 40:60:10	57	0.58 Std. Dev. 0.05	0.73 Std. Dev. 0.17	112 Std. Dev. 20	Cloudy	Clear

Composition	EWC (%)	Initial Modulus (MPa)	Tensile Strength (MPa)	Elongation at Break (%)	Appearance Hydrated	Appearance Dehydrated
THFFMA:NVP :PU1 40:60:15	54	0.76 Std. Dev. 0.05	0.89 Std. Dev. 0.12	105 Std. Dev. 12	Cloudy	Clear
THFFMA:NVP :PU2 40:60:5	57	1.06 Std. Dev. 0.24	0.92 Std. Dev. 0.28	40 Std. Dev. 6	Clear	Clear
THFFMA:NVP :PU2 40:60:10	55	1.71 Std. Dev. 0.16	1.24 Std. Dev. 0.22	37 Std. Dev. 13	Clear	Clear
THFFMA:NVP :PU2 40:60:15	52	4.19 Std. Dev. 0.33	2.80 Std. Dev. 0.19	52 Std. Dev. 9	Clear	Clear
THFFA:NVP 20:80	86	0.12 Std. Dev. 0.01	0.11 Std. Dev. 0.03	85 Std. Dev. 17	Clear	Clear
THFFA:NVP 75:25	83	0.12 Std. Dev. 0.01	0.12 Std. Dev. 0.01	107 Std. Dev. 8	Clear	Clear
THFFA:NVP 30:70	82	0.22 Std. Dev. 0.01	0.13 Std. Dev. 0.03	60 Std. Dev. 14	Clear	Clear

Composition	EWC (%)	Initial Modulus (MPa)	Tensile Strength(MPa)	Elongation at Break (%)	Appearance Hydrated	Appearance Dehydrated
THFFA:NVP 40:60	81	0.14 St. Dev. 0.01	0.14 St. Dev. 0.02	104 St. Dev. 9	Clear	Clear
THFFA:NVP :CAB 40:60:5	74	0.49 St. Dev. 0.02	0.48 St. Dev. 0.04	135 St. Dev. 12	White	Cloudy
THFFA:NVP :CAB 40:60:10	68	1.73 St. Dev. 0.05	1.11 St. Dev. 0.05	191 St. Dev. 11	White	Cloudy
THFFA:NVP :CAB 40:60:15	62	2.36 St. Dev. 0.22	1.47 St. Dev. 0.07	147 St. Dev. 9	White	Cloudy
THFFA:NVP 60:40	72	0.11 St. Dev. 0.01	0.18 St. Dev. 0.04	176 St. Dev. 39	Clear	Clear
THFFA:NVP :CAB 60:40:5	64	0.27 St. Dev. 0.01	0.76 St. Dev. 0.17	251 St. Dev. 38	White	Cloudy
THFFA:NVP :CAB 60:40:10	58	0.49 St. Dev. 0.04	1.59 St. Dev. 0.32	329 St. Dev. 58	White	Cloudy

Composition	EWC (%)	Initial Modulus (MPa)	Tensile Strength(MPa)	Elongation at Break (%)	Appearance Hydrated	Appearance Dehydrated
THFFA:NVP :CAB 60:40:15	57	0.85 St. Dev. 0.21	2.81 St. Dev. 0.72	317 St. Dev. 69	White	Cloudy
THFFA:NVP :PU1 40:60:5	74	0.22 St. Dev. 0.02	0.20 St. Dev. 0.05	104 St. Dev. 23	Clear	Clear
THFFA:NVP :PU1 40:60:10	73	0.21 St. Dev. 0.01	0.21 St. Dev. 0.04	111 St. Dev. 22	Clear	Clear
THFFA:NVP :PU1 40:60:15	70	0.29 St. Dev. 0.01	0.26 St. Dev. 0.04	96 St. Dev. 15	Clear	Clear
THFFA:NVP :PU2 40:60:5	77	0.17 St. Dev. 0.01	0.22 St. Dev. 0.05	129 St. Dev. 22	Clear	Clear
THFFA:NVP :PU2 40:60:10	74	0.19 St. Dev. 0.01	0.25 St. Dev. 0.05	120 St. Dev. 17	Clear	Clear
THFFA:NVP :PU2 40:60:15	71	0.26 St. Dev. 0.01	0.37 St. Dev. 0.06	133 St. Dev. 18	Clear	Clear

Composition	EWC (%)	Initial Modulus (MPa)	Tensile Strength (MPa)	Elongation at Break (%)	Appearance Hydrated	Appearance Dehydrated
IBMA:NVP 40:60	31	118.50 St. Dev. 1.85	8.85 St. Dev. 0.95	9 St. Dev. 2	Cloudy	Clear
IBMA:NVP :CAB 40:60:5	30	120.65 St. Dev. 12.45	9.26 St. Dev. 0.90	9 St. Dev. 0.1	White	Cloudy
IBMA:NVP :CAB 40:60:10	28	135.40 St. Dev. 9.5	9.75 St. Dev. 0.22	8 St. Dev. 0.3	White	Cloudy
IBMA:NVP :CAB 40:60:15	27.80	154.10 St. Dev. 13.50	9.90 St. Dev. 0.70	7 St. Dev. 1	White	Cloudy
IBMA:NVP :PU1 40:60:5	28	115.80 St. Dev. 11.20	13.65 St. Dev. 0.31	24 St. Dev. 2	White	Cloudy
IBMA:NVP :PU1 40:60:10	28	100.70 St. Dev. 9.50	14.47 St. Dev. 0.62	33 St. Dev. 4	White	Cloudy
IBMA:NVP :PU1 40:60:15	27	91.50 St. Dev. 6.20	15.21 St. Dev. 1.52	31 St. Dev. 19	White	Cloudy

Composition	EWC (%)	Initial Modulus (MPa)	Tensile Strength(MPa)	Elongation at Break (%)	Appearance Hydrated	Appearance Dehydrated
IBMA:NVP :PU2 40:60:5	27	128.40 St. Dev. 24.30	15.25 St. Dev. 1.47	13 St. Dev. 1	White	Cloudy
IBMA:NVP :PU2 40:60:10	27	143.90 St. Dev. 4.70	16.52 St. Dev. 0.76	17 St. Dev. 3	White	Cloudy
IBMA:NVP :PU2 40:60:15	24	157.70 St. Dev. 5.60	17.12 St. Dev. 3.68	18 St. Dev. 8	White	Cloudy
IBUTMA:NVP 40:60	43	97.90 St. Dev. 7.50	7.91 St. Dev. 0.32	61 St. Dev. 6	Clear	Clear
IBUTMA:NVP :CAB 40:60:5	39	117.24 St. Dev. 10.50	9.15 St. Dev. 0.31	59 St. Dev. 7	Cloudy	Clear
IBUTMA:NVP :CAB 40:60:10	38	122.51 St. Dev. 5.70	9.70 St. Dev. 0.18	53 St. Dev. 1	Cloudy	Clear
IBUTMA:NVP :CAB 40:60:15	36	125.74 St. Dev. 20.80	10.69 St. Dev. 0.17	45 St. Dev. 8	Cloudy	Clear

Composition	EWC (%)	Initial Modulus (MPa)	Tensile Strength(MPa)	Elongation at Break (%)	Appearance Hydrated	Appearance Dehydrated
IBUTMA:NVP 60:40	22	192.10 St. Dev. 17.00	21.10 St. Dev. 0.50	51 St. Dev. 11	Clear	Clear
IBUTMA:NVP :CAB 60:40:5	21	193.03 St. Dev. 17.50	21.40 St. Dev. 0.80	68 St. Dev. 21	Cloudy	Clear
IBUTMA:NVP :CAB 60:40:10	19	194.11 St. Dev. 14.50	21.81 St. Dev. 1.00	60 St. Dev. 11	Cloudy	Clear
IBUTMA:NVP :CAB 60:40:15	18	195.04 St. Dev. 16.50	22.40 St. Dev. 0.80	57 St. Dev. 9	Cloudy	Clear
IBUTMA:NVP :PU1 40:60:5	40	59.40 St. Dev. 9.00	9.81 St. Dev. 0.45	84 St. Dev. 12	Cloudy	Clear
IBUTMA:NVP :PU1 40:60:10	39	42.10 St. Dev. 3.50	10.60 St. Dev. 0.85	123 St. Dev. 25	Cloudy	Clear
IBUTMA:NVP :PU1 40:60:15	38	28.10 St. Dev. 1.40	11.19 St. Dev. 1.02	161 St. Dev. 26	Cloudy	Clear

Composition	EWC (%)	Initial Modulus (MPa)	Tensile Strength(MPa)	Elongation at Break (%)	Appearance Hydrated	Appearance Dehydrated
IBUTMA:NVP :PU2 40:60:5	38	102.90 St. Dev. 9.20	10.34 St. Dev. 0.66	39 St. Dev. 2	Cloudy	Clear
IBUTMA:NVP :PU2 40:60:10	35	110.50 St. Dev. 17.80	12.41 St. Dev. 0.60	56 St. Dev. 12	Cloudy	Clear
IBUTMA:NVP :PU2 40:60:15	33	127.20 St. Dev. 20.00	13.71 St. Dev. 0.58	74 St. Dev. 24	Cloudy	Clear
TBMA:NVP 40:60	36	184.10 St. Dev. 10.90	11.24 St. Dev. 0.65	42 St. Dev. 3	Clear	Clear
TBMA:NVP :CAB 40:60:5	33	180.83 St. Dev. 9.95	12.46 St. Dev. 0.15	44 St. Dev. 4	Cloudy	Cloudy
TBMA:NVP :CAB 40:60:10	31	177.86 St. Dev. 10.50	11.19 St. Dev. 0.82	15 St. Dev. 3	Cloudy	Cloudy
TBMA:NVP :CAB 40:60:15	30	142.89 St. Dev. 6.75	11.75 St. Dev. 0.44	18 St. Dev. 0.3	Cloudy	Cloudy

Composition	EWC (%)	Initial Modulus (MPa)	Tensile Strength (MPa)	Elongation at Break (%)	Appearance Hydrated	Appearance Dehydrated
TBMA:NVP 60:40	18	312.00 St. Dev. 20.50	19.83 St. Dev. 0.95	6 St. Dev. 1.2	Clear	Clear
TBMA:NVP :CAB 60:40:5	17	320.50 St. Dev. 15.60	20.20 St. Dev. 1.00	6.5 St. Dev. 0.6	Cloudy	Cloudy
TBMA:NVP :CAB 60:40:10	14	332.30 St. Dev. 20.45	21.50 St. Dev. 0.75	6.7 St. Dev. 0.8	Cloudy	Cloudy
TBMA:NVP :CAB 60:40:15	12	347.50 St. Dev. 21.00	22.10 St. Dev. 1.05	6.9 St. Dev. 0.4	Cloudy	Cloudy
TBMA:NVP :PU1 40:60:5	38	74.30 St. Dev. 12.60	11.76 St. Dev. 0.89	55 St. Dev. 10	White	Cloudy
TBMA:NVP :PU1 40:60:10	38	48.10 St. Dev. 4.40	11.92 St. Dev. 0.98	85 St. Dev. 17	White	Cloudy
TBMA:NVP :PU1 40:60:15	39	20.9 St. Dev. 4.1	12.0 St. Dev. 1.0	130 St. Dev. 10	White	Cloudy

Composition	EWC (%)	Initial Modulus (MPa)	Tensile Strength(MPa)	Elongation at Break (%)	Appearance Hydrated	Appearance Dehydrated
TBMA:NVP	34	151.3	13.6	40	White	Cloudy
:PU2 40:60:5		St. Dev. 33.8	St. Dev. 0.8	St. Dev. 11		
TBMA:NVP	32	141.0	16.8	47	White	Cloudy
:PU2 40:60:10		St. Dev. 6.80	St. Dev. 0.4	St. Dev. 7		
TBMA:NVP	30	132.9	16.9	52	White	Cloudy
:PU2 40:60:15		St. Dev. 16.1	St. Dev. 0.7	St. Dev. 5		
IBMA:NVP	56	28.6	5.0	35	Cloudy	Clear
20:80		St. Dev.2.4	St. Dev. 0.9	St. Dev. 6		
IBMA:NVP	46	35.4	6.8	29	Cloudy	Clear
75:25		St. Dev.3.5	St. Dev. 1.5	St. Dev. 4		
IBMA:NVP	40	59.5	9.7	25	Cloudy	Clear
30:70		St. Dev.4.0	St. Dev. 1.0	St. Dev. 3		
LMA:NVP	68	0.141	0.162	115	Clear	Clear
20:80		St. Dev. 0.05	St. Dev. 0.035	St. Dev. 20		

Composition	EWC (%)	Initial Modulus (MPa)	Tensile Strength(MPa)	Elongation at Break (%)	Appearance Hydrated	Appearance Dehydrated
LMA:NVP 30:70	58	0.367 St. Dev. 0.09	0.341 St. Dev. 0.08	93 St. Dev. 10	Clear	Clear
LMA:NVP 40:60	51	0.277 St. Dev. 0.07	0.324 St. Dev. 0.06	117 St. Dev. 12	Clear	Clear
MMA:NVP 20:80	77	0.117 St. Dev. 0.08	0.129 St. Dev. 0.04	110 St. Dev. 15	Clear	Clear
MMA:NVP 30:70	68	0.557 St. Dev. 0.08	0.807 St. Dev. 0.09	145 St. Dev. 16	Clear	Clear
MMA:NVP 40:60	56	1.689 St. Dev. 0.1	2.651 St. Dev. 0.95	157 St. Dev. 21	Clear	Clear
MMA:NVP 50:50	39	7.21 St. Dev. 0.7	4.746 St. Dev. 1.0	72 St. Dev. 17	Clear	Clear

APPENDIX 2

Water Binding Data

Composition	EWC (%)	Freezing Water (%)	Non-freezing Water (%)
THFFMA:NVP 20:80	82	62	20
THFFMA:NVP 25:75	78	60	18
THFFMA:NVP 30:70	74	56	18
THFFMA:NVP 60:40	49	21	28
THFFMA:VP:CAB 60:40:5	45	16	29
THFFMA:VP:CAB 60:40:10	43	12	29
THFFMA:VP:CAB 60:40:15	41	13	28
THFFA:NVP 20:80	86	75	11
THFFA:NVP 25:75	83	70	13
THFFA:NVP 30:70	82	67	16
THFFA:VP 60:40	72	53	19
THFFA:NVP:CAB 60:40:5	64	44	20
THFFA:NVP:CAB 60:40:10	58	34	24

Composition	EWC (%)	Freezing Water (%)	Non-freezing Water (%)
THFFA:NVP:CAB 60:40:15	57	31	26
IBUTMA:NVP 60:40	22	0	22
IBUTMA:VP:CAB 60:40:5	20	0	20
IBUTMA:VP:CAB 60:40:10	19	0	19
IBUTMA:VP:CAB 60:40:15	18	0	18
TBMA:NVP 60:40	18	0	18
TBMA:NVP:CAB 60:40:5	16	0	16
TBMA:NVP:CAB 60:40:10	14	0	14
TBMA:NVP:CAB 60:40:15	12	0	12
IBMA:NVP 20:80	56	29	27
IBMA:NVP [*] 25:75	46	16	31
IBMA:NVP 30:70	40	8	32

APPENDIX 3

Dehydrated Surface Properties

COMPOSITION	POLAR COMPONENT mN/m	DISPERSIVE COMPONENT mN/m	TOTAL SURFACE ENERGY mN/m
THFFMA:NVP 20:80	10.5	38.5	49.0
THFFMA:NVP 25:75	8.7	40.2	48.9
THFFMA:NVP 30:70	6.8	42.1	48.9
THFFMA:NVP 40:60	11.0	36.3	47.3
THFFMA:NVP :CAB 40:60:5	11.4	37.9	49.3
THFFMA:NVP :CAB 40:60:10	10.4	37.9	48.3
THFFMA:NVP :CAB 40:60:15	7.5	39.3	46.8
THFFMA:NVP 60:40	8.7	35.5	44.2
THFFMA:NVP :CAB 60:40:5	11.4	28.2	39.6
THFFMA:NVP :CAB 60:40:10	9.1	29.7	38.8
THFFMA:NVP :CAB 60:40:15	3.6	31.1	34.7
THFFMA:NVP :CAB 60:40:20	3.3	30.2	33.5

COMPOSITION	POLAR COMPONENT mN/m	DISPERSIVE COMPONENT mN/m	TOTAL SURFACE ENERGY mN/m
THFFMA:NVP :PU1 40:60:5	11.8	37.0	48.8
THFFMA:NVP :PU1 40:60:10	7.6	37.4	45.0
THFFMA:NVP :PU1 40:60:15	7.2	36.1	43.3
THFFMA:NVP :PU2 40:60:5	3.3	38.3	41.6
THFFMA:NVP :PU2 40:60:10	5.8	40.0	45.8
THFFMA:NVP :PU2 40:60:15	4.4	39.7	44.1
THFFA:NVP 20:80	9.3	38.1	47.4
THFFA:NVP 75:25	6.9	40.0	46.9
THFFA:NVP 30:70	7.1	39.1	46.2
THFFA:NVP 40:60	5.6	38.3	43.9
THFFA:NVP :CAB 40:60:5	4.5	36.6	41.1
THFFA:NVP :CAB 40:60:10	3.7	38.7	42.4

COMPOSITION	POLAR COMPONENT mN/m	DISPERSIVE COMPONENT mN/m	TOTAL SURFACE ENERGY mN/m
THFFA:NVP :CAB 40:60:15	2.1	40.0	42.1
THFFA:NVP 60:40	2.0	39.5	41.5
THFFA:NVP :CAB 60:40:5	0.9	36.8	37.7
THFFA:NVP :CAB 60:40:10	0.7	38.6	39.3
THFFA:NVP :CAB 60:40:15	6.1	30.3	36.4
THFFA:NVP :PU1 40:60:5	4.0	40.6	44.6
THFFA:NVP :PU1 40:60:10	4.0	42.1	46.1
THFFA:NVP :PU1 40:60:15	2.0	40.1	42.1
THFFA:NVP :PU2 40:60:5	8.2	34.9	43.1
THFFA:NVP :PU2 40:60:10	5.2	39.6	44.8
THFFA:NVP :PU2 40:60:15	4.0	40.4	44.4
IBMA:NVP 40:60	7.2	34.3	41.5

COMPOSITION	POLAR COMPONENT mN/m	DISPERSIVE COMPONENT mN/m	TOTAL SURFACE ENERGY mN/m
IBMA:NVP :CAB 40:60:5	5.3	38.9	44.2
IBMA:NVP :CAB 40:60:10	4.3	35.3	39.6
IBMA:NVP :CAB 40:60:15	3.9	36.2	40.1
IBMA:NVP :PU1 40:60:5	7.8	36.8	44.6
IBMA:NVP :PU1 40:60:10	3.7	40.8	44.5
IBMA:NVP :PU1 40:60:15	2.3	40.3	42.6
IBMA:NVP :PU2 40:60:5	7.1	37.2	44.3
IBMA:NVP :PU2 40:60:10	5.6	34.2	39.8
IBMA:NVP :PU2 40:60:15	3.4	36.9	40.3
IBUTMA:NVP 40:60	8.5	35.5	44.0
IBUTMA:NVP :CAB 40:60:5	8.8	36.0	44.4
IBUTMA:NVP :CAB 40:60:10	6.8	34.0	40.8

COMPOSITION	POLAR COMPONENT mN/m	DISPERSIVE COMPONENT mN/m	TOTAL SURFACE ENERGY mN/m
IBUTMA:NVP :CAB 40:60:15	2.4	38.7	41.1
IBUTMA:NVP 60:40	11.9	32.4	44.3
IBUTMA:NVP :CAB 60:40:5	10.4	32.0	42.4
IBUTMA:NVP :CAB 60:40:10	9.6	31.3	40.9
IBUTMA:NVP :CAB 60:40:15	9.0	31.6	40.6
IBUTMA:NVP :PU1 40:60:5	5.1	36.1	41.2
IBUTMA:NVP :PU1 40:60:10	3.4	40.2	43.6
IBUTMA:NVP :PU1 40:60:15	3.3	37.0	40.3
IBUTMA:NVP :PU2 40:60:5	8.2	33.8	42.0
IBUTMA:NVP :PU2 40:60:10	7.2	35.7	42.9
IBUTMA:NVP :PU2 40:60:15	4.9	38.1	44.3
IBMA:NVP 20:80	28.4	29.6	58.0

COMPOSITION	POLAR COMPONENT mN/m	DISPERSIVE COMPONENT mN/m	TOTAL SURFACE ENERGY mN/m
IBMA:NVP 75:25	22.4	32.2	54.6
IBMA:NVP 30:70	13.6	35.3	48.9
TBMA:NVP 40:60	17.8	28.6	46.4
TBMA:NVP :CAB 40:60:5	13.8	29.4	43.2
TBMA:NVP :CAB 40:60:10	12.6	29.2	41.8
TBMA:NVP :CAB 40:60:15	12.0	29.5	41.5
TBMA:NVP 60:40	3.9	40.3	44.2
TBMA:NVP :CAB 60:40:5	4.9	38.2	41.1
TBMA:NVP :CAB 60:40:10	4.8	33.6	38.4
TBMA:NVP :CAB 60:40:15	4.4	33.8	38.2
TBMA:NVP :PU1 40:60:5	3.9	36.8	40.7
TBMA:NVP :PU1 40:60:10	3.7	38.4	42.1

COMPOSITION	POLAR COMPONENT mN/m	DISPERSIVE COMPONENT mN/m	TOTAL SURFACE ENERGY mN/m
TBMA:NVP :PU1 40:60:15	5.3	36.6	41.9
TBMA:NVP :PU2 40:60:5	5.6	33.6	39.2
TBMA:NVP :PU2 40:60:10	5.0	34.5	39.5
TBMA:NVP :PU2 40:60:15	3.7	39.6	43.3
THFFA	4.8	33.6	38.4
THFFA:CAB 95:5	9.3	27.9	37.2
THFFA:CAB 90:10	7.0	30.4	37.4
THFFA:CAB 85:15	6.6	31.6	38.2
THFFMA	27.1	28.6	55.7
THFFMA:CAB 95:5	17.5	30.6	48.1
THFFMA:CAB 90:10	13.9	30.3	44.2
THFFMA:CAB 85:15	13.3	30.5	43.8

COMPOSITION	POLAR COMPONENT mN/m	DISPERSIVE COMPONENT mN/m	TOTAL SURFACE ENERGY mN/m
IBUTMA	12.2	28.9	41.1
IBUTMA:CAB 95:5	10.0	31.7	41.7
IBUTMA:CAB 90:10	9.6	32.8	42.4
IBUTMA:CAB 85:15	8.8	33.6	42.4
TBMA	12.6	29.2	41.8
TBMA:CAB 95:5	9.9	29.2	39.1
TBMA:CAB 90:10	7.7	31.1	38.8
TBMA:CAB 85:15	7.1	31.4	38.51
THFFMA:PC 95:5	19.7	31.3	51.0
TRIS:HFIPMA 50:50	6.0	17.5	23.5
TRIS:HFIPMA: THFFMA 47.5:47.5:5	6.3	21.6	27.9
TRIS:HFIPMA: THFFMA 45:45:10	8.9	22.2	31.1

COMPOSITION	POLAR COMPONENT mN/m	DISPERSIVE COMPONENT mN/m	TOTAL SURFACE ENERGY mN/m
TRIS:HFIPMA: THFFMA 42.5:42.5:15	11.1	20.9	32.0
TRIS:HFIPMA - Lens 50:50	5.8	17.6	23.4
TRIS:THFFMA 50:50	15.1	26.5	41.6
TRIS:THFFMA: NVP 50:50:5	10.9	29.3	40.2
TRIS:THFFMA: 4-META 50:50:2.5	23.2	27.5	50.7
TRIS:THFFMA: 4-META 50:50:5	24.6	27.8	52.4
TRIS:THFFMA: 4-META 50:50:7.5	29.0	29.0	57.2
TRIS:THFFA 50:50	0.6	34.0	34.6
TRIS:THFFA: NVP 50:50:2	2.9	16.8	19.7
TRIS:THFFA: 4-META 50:50:2.5	16.1	33.6	49.7

COMPOSITION	POLAR COMPONENT mN/m	DISPERSIVE COMPONENT mN/m	TOTAL SURFACE ENERGY mN/m
TRIS:THFFA: 4-META 50:50:5	17.0	34.2	51.2
TRIS:THFFA: 4-META 50:50:7.5	17.5	34.4	51.9
TRIS:IBUTMA 50:50	14.9	29.5	44.4
TRIS:IBUTMA: 4-META 50:50:2.5	19.1	27.2	46.3
TRIS:IBUTMA: 4-META 50:50:5	24.6	30.0	54.6
TRIS:IBUTMA:4- META 50:50:7.5	26.3	26.7	53.0
TRIS:TBMA 50:50	8.6	27.1	35.7
TRIS:TBMA: 4-META 50:50:2.5	10.7	37.1	47.8
TRIS:TBMA: 4-META 50:50:5	24.7	29.5	54.2
TRIS:TBMA: 4-META 50:50:7.5	26.5	30.9	57.4
TRIS:IBMA 50:50	11.8	28.5	40.3

COMPOSITION	POLAR COMPONENT mN/m	DISPERSIVE COMPONENT mN/m	TOTAL SURFACE ENERGY mN/m
TRIS:IBMA: 4-META 50:50:2.5	16.3	28.3	44.6
TRIS:IBMA: 4-META 50:50:5	24.0	28.5	52.5
TRIS:IBMA: 4-META 50:50:7.5	27.0	28.3	55.3
4-META:TRIS: THFFMA:TBMA 5:35:25:35	18.3	29.0	47.3
MMA:TRIS:IBMA 10:10:80	11.7	31.5	43.2
4-META:THFFMA :TRIS:IBUTMA 5:20:15:60	15.6	33.4	49.0
4-META:THFFMA :TRIS:TBMA 5:10:60:25	8.2	30.9	39.1
TRIS	4.7	20.1	24.8
CAB	6.4	40.3	46.7
PU 1	7.1	37.5	44.6
THFFMA: PU 1 95:5	1.1	36.5	37.6

COMPOSITION	POLAR COMPONENT mN/m	DISPERSIVE COMPONENT mN/m	TOTAL SURFACE ENERGY mN/m
THFFA: PU 1 95:5	1.2	32.5	33.7

APPENDIX 4

Hydrated Surface Properties

COMPOSITION	POLAR COMPONENT mN/m	DISPERSIVE COMPONENT mN/m	TOTAL SURFACE ENERGY mN/m
THFFMA:NVP 20:80	45.6	23.6	69.1
THFFMA:NVP 25:75	43.8	24.5	68.3
THFFMA:NVP 30:70	43.5	23.5	66.9
THFFMA:NVP 60:40	43.1	20.4	63.5
THFFMA:NVP :CAB 60:40:5	40.8	22.3	63.1
THFFMA:NVP :CAB 60:40:10	39.8	23.4	63.2
THFFMA:NVP :CAB 60:40:15	39.3	23.4	62.6
THFFA:NVP 20:80	43.6	12.3	55.9
THFFA:NVP 25:75	43.6	15.5	59.1
THFFA:NVP 30:70	44.0	15.2	59.1
THFFA:NVP 60:40	42.7	17.0	59.7
THFFA:NVP :CAB 60:40:5	41.8	17.2	59.0

COMPOSITION	POLAR COMPONENT mN/m	DISPERSIVE COMPONENT mN/m	TOTAL SURFACE ENERGY mN/m
THFFA:NVP :CAB 60:40:10	40.8	18.2	59.0
THFFA:NVP :CAB 60:40:15	38.2	20.2	58.4
IBMA:NVP 20:80	45.4	22.2	67.6
IBMA:NVP 25:75	44.2	23.4	67.6
IBMA:NVP 30:70	44.1	22.3	66.5
IBUTMA:NVP 60:40	42.2	20.1	62.3
IBUTMA:NVP :CAB 60:40:5	41.2	19.8	61.0
IBUTMA:NVP :CAB 60:40:10	38.9	19.2	59.0
IBUTMA:NVP :CAB 60:40:15	36.6	18.9	55.5
TBMA:NVP 60:40	41.8	15.2	56.9
TBMA:NVP :CAB 60:40:5	39.3	16.9	56.1
TBMA:NVP :CAB 60:40:10	38.7	17.4	56.1

COMPOSITION	POLAR COMPONENT mN/m	DISPERSIVE COMPONENT mN/m	TOTAL SURFACE ENERGY mN/m
TBMA:NVP :CAB 60:40:15	38.2	17.2	55.4
THFFA	40.2	20.9	61.1
THFFA:CAB 95:5	44.8	17.5	62.3
THFFA:CAB 90:10	41.8	18.6	60.3
THFFA:CAB 85:15	35.5	25.8	61.3
TRIS:THFFMA: NVP 50:50:5	32.2	20.7	52.8
TRIS:THFFA 50:50	44.0	10.1	54.1
THFFA:PU1 90:10	35.5	20.1	55.6

APPENDIX 5

Oxygen Permeabilities

Composition	Dk (cc cm/ cm ² S cm Hg)
THFFMA:NVP 20:80	9.96 X 10 ⁻¹⁰
THFFMA:NVP 25:75	9.57 X 10 ⁻¹⁰
THFFMA:NVP 30:70	9.02 X 10 ⁻¹⁰
THFFMA:NVP 60:40	4.98 X 10 ⁻¹⁰
THFFMA:NVP:CAB 60:40:5	4.59 X 10 ⁻¹⁰
THFFMA:NVP:CAB 60:40:10	4.48 X 10 ⁻¹⁰
THFFMA:NVP:CAB 60:40:15	4.10X 10 ⁻¹⁰
THFFA:NVP 20:80	10.57 X 10 ⁻¹⁰
THFFA:NVP 25:75	9.87 X 10 ⁻¹⁰
THFFA:NVP 30:70	9.76 X 10 ⁻¹⁰
THFFA:NVP 60:40	9.88 X 10 ⁻¹⁰
THFFA:NVP:CAB 60:40:5	8.88 X 10 ⁻¹⁰

Composition	Dk (cc cm/ cm ² S cm Hg)
THFFA:NVP:CAB 60:40:10	8.52 X 10 ⁻¹⁰
THFFA:NVP:CAB 60:40:15	8.04 X 10 ⁻¹⁰
IBUTMA:NVP 60:40	3.83 X 10 ⁻¹⁰
IBUTMA:NVP:CAB 60:40:5	3.43 X 10 ⁻¹⁰
IBUTMA:NVP:CAB 60:40:10	2.72 X 10 ⁻¹⁰
IBUTMA:NVP:CAB 60:40:15	2.65 X 10 ⁻¹⁰
TBMA:NVP 60:40	2.97 X 10 ⁻¹⁰
TBMA:NVP:CAB 60:40:5	2.44 X 10 ⁻¹⁰
TBMA:NVP:CAB 60:40:10	2.37 X 10 ⁻¹⁰
TBMA:NVP:CAB 60:40:15	2.27 X 10 ⁻¹⁰
IBMA:NVP 20:80	4.19 X 10 ⁻¹⁰
IBMA:NVP 25:75	3.93 X 10 ⁻¹⁰

Composition	Dk (cc cm/ cm ² S cm Hg)
IBMA:NVP 30:70	3.89 X 10 ⁻¹⁰
IBMA:NVP 60:40	2.46 X 10 ⁻¹⁰
IBMA:NVP:CAB 60:40:5	2.15 X 10 ⁻¹⁰
IBMA:NVP:CAB 60:40:10	1.93 X 10 ⁻¹⁰
IBMA:NVP:CAB 60:40:15	3.50 X 10 ⁻¹⁰
THFFMA	0.60 X 10 ⁻¹⁰
THFFMA:CAB 95:5	0.85 X 10 ⁻¹⁰
THFFMA:CAB 90:10	0.91 X 10 ⁻¹⁰
THFFMA:CAB 85:15	0.97 X 10 ⁻¹⁰
THFFA	4.39 X 10 ⁻¹⁰
THFFA:CAB 95:5	1.87 X 10 ⁻¹⁰
THFFA:CAB 90:10	1.72 X 10 ⁻¹⁰

Composition	Dk (cc cm/ cm ² S cm Hg)
THFFA:CAB 85:15	1.63 X 10 ⁻¹⁰
IBUTMA	4.02 X 10 ⁻¹⁰
IBUTMA:CAB 95:5	5.67 X 10 ⁻¹⁰
IBUTMA:CAB 90:10	5.91 X 10 ⁻¹⁰
IBUTMA:CAB 85:15	6.13 X 10 ⁻¹⁰
TBMA	5.89 X 10 ⁻¹⁰
TBMA:CAB 95:5	6.94 X 10 ⁻¹⁰
TBMA:CAB 90:10	7.23 X 10 ⁻¹⁰
TBMA:CAB 85:15	7.50 X 10 ⁻¹⁰
THFFMA:PC 95:5	0.22 X 10 ⁻¹⁰
TRIS:HFIPMA 50:50	49.88 X 10 ⁻¹⁰
TRIS:HFIPMA:THFFMA 47.5:47.5:5	45.56 X 10 ⁻¹⁰

Composition	Dk (cc cm/ cm ² S cm Hg)
TRIS:HFIPMA:THFFMA 45:45:10	42.33 X 10 ⁻¹⁰
TRIS:HFIPMA:THFFMA 42.5:42.5:15	40.18 X 10 ⁻¹⁰
TRIS:HFIPMA - Lens 50:50	42.23 X 10 ⁻¹⁰
TRIS:THFFMA 50:50	19.31 X 10 ⁻¹⁰
TRIS:THFFMA:NVP 50:50:5	18.18 X 10 ⁻¹⁰
TRIS:THFFMA:4-META 50:50:2.5	18.83 X 10 ⁻¹⁰
TRIS:THFFMA:4-META 50:50:5	18.12 X 10 ⁻¹⁰
TRIS:THFFMA:4-META 50:50:7.5	17.98 X 10 ⁻¹⁰
TRIS:THFFA 50:50	30.04 X 10 ⁻¹⁰
TRIS:THFFA:NVP 50:50:2	24.66 X 10 ⁻¹⁰
TRIS:THFFA:4-META 50:50:2.5	28.55 X 10 ⁻¹⁰
TRIS:THFFA:4-META 50:50:5	27.36 X 10 ⁻¹⁰

Composition	Dk (cc cm/ cm ² S cm Hg)
TRIS:THFFA:4-META 50:50:7.5	26.88 X 10 ⁻¹⁰
TRIS:IBUTMA 50:50	28.26 X 10 ⁻¹⁰
TRIS:IBUTMA:4-META 50:50:2.5	28.13 X 10 ⁻¹⁰
TRIS:IBUTMA:4-META 50:50:5	25.95 X 10 ⁻¹⁰
TRIS:IBUTMA:4-META 50:50:7.5	25.58 X 10 ⁻¹⁰
TRIS:TBMA 50:50	27.82 X 10 ⁻¹⁰
TRIS:TBMA:4-META 50:50:2.5	26.84 X 10 ⁻¹⁰
TRIS:TBMA:4-META 50:50:5	26.02 X 10 ⁻¹⁰
TRIS:TBMA:4-META 50:50:7.5	25.82 X 10 ⁻¹⁰
TRIS:IBMA 50:50	25.91 X 10 ⁻¹⁰
TRIS:IBMA:4-META 50:50:2.5	25.45 X 10 ⁻¹⁰
TRIS:IBMA:4-META 50:50:5	23.99 X 10 ⁻¹⁰

Composition	Dk (cc cm/ cm ² S cm Hg)
TRIS:IBMA:4-META 50:50:7.5	23.34 X 10 ⁻¹⁰
4-META:TRIS:THFFMA :TBMA 5:35:25:35	12.39 X 10 ⁻¹⁰
MMA:TRIS:IBMA 10:10:80	6.02 X 10 ⁻¹⁰
4-META:THFFMA:TRIS :IBUTMA 5:20:15:60	6.31 X 10 ⁻¹⁰
4-META:THFFMA:TRIS :TBMA 5:10:60:25	19.01 X 10 ⁻¹⁰

APPENDIX 6

'Onset' of Glass Transition Temperatures using Thermal Mechanical Analysis

Composition	Onset Temperature °C
THFFMA	51.64
THFFMA:CAB 95:5	51.93
THFFMA:CAB 90:10	54.25
THFFMA:CAB 85:15	56.08
IBUTMA	55.71
IBUTMA:CAB 95:5	63.65
IBUTMA:CAB 90:10	66.32
IBUTMA:CAB 85:15	69.42
TBMA	74.25
TBMA:CAB 95:5	84.25
TBMA:CAB 90:10	91.97
TBMA:CAB 85:15	98.05
TRIS : THFFMA 50:50	34.79
TRIS : Isobutyl MA 50:50	43.12
TRIS : HFIPMA 50:50	50.42
TRIS : TBMA 50:50	69.28
TRIS : Isobornyl MA 50:50	73.54
TRIS : HFIPMA 50 : 50	50.42
TRIS: :HFIPMA: THFFMA 47.5:47.5:5	68.63
TRIS : HFIPMA: THFFMA 45:45:10	55.84
TRIS:HFIPMA:THFFMA 42.5:42.5:15	51.36
TRIS:HFIPMA:THFFMA 47.5:47.5:5	68.63

Composition	Onset Temperature °C
MAA:TRIS:IBUTMA 10:10:80	82.88
4-META:TRIS:THFFMA: TBMA 5:20:15:60	73.48
THFFMA:PC 95:5	47.27
NVP:THFFA 70:30	69.62
TBMA:NVP:CAB 60:40:5	60.62

APPENDIX 7

Approximate Glass Transition Temperatures
Obtained using Differential Scanning Calorimetry

Composition	Transition Temperature
	°C
THFFMA:NVP 20:80	94
THFFMA:NVP 25:75	73
THFFMA:NVP 30:70	61
THFFA:NVP 20:80	74
THFFA:NVP 25:75	72
THFFA:NVP 30:70	70
IBMA:NVP 20:80	66
IBMA:NVP 25:75	62
IBMA:NVP 30:70	57